0008-7114

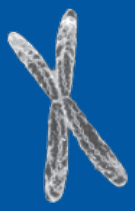

Caryologia

2023
Vol. 76 - n. 3

International Journal of Cytology,
Cytosystematics and Cytogenetics

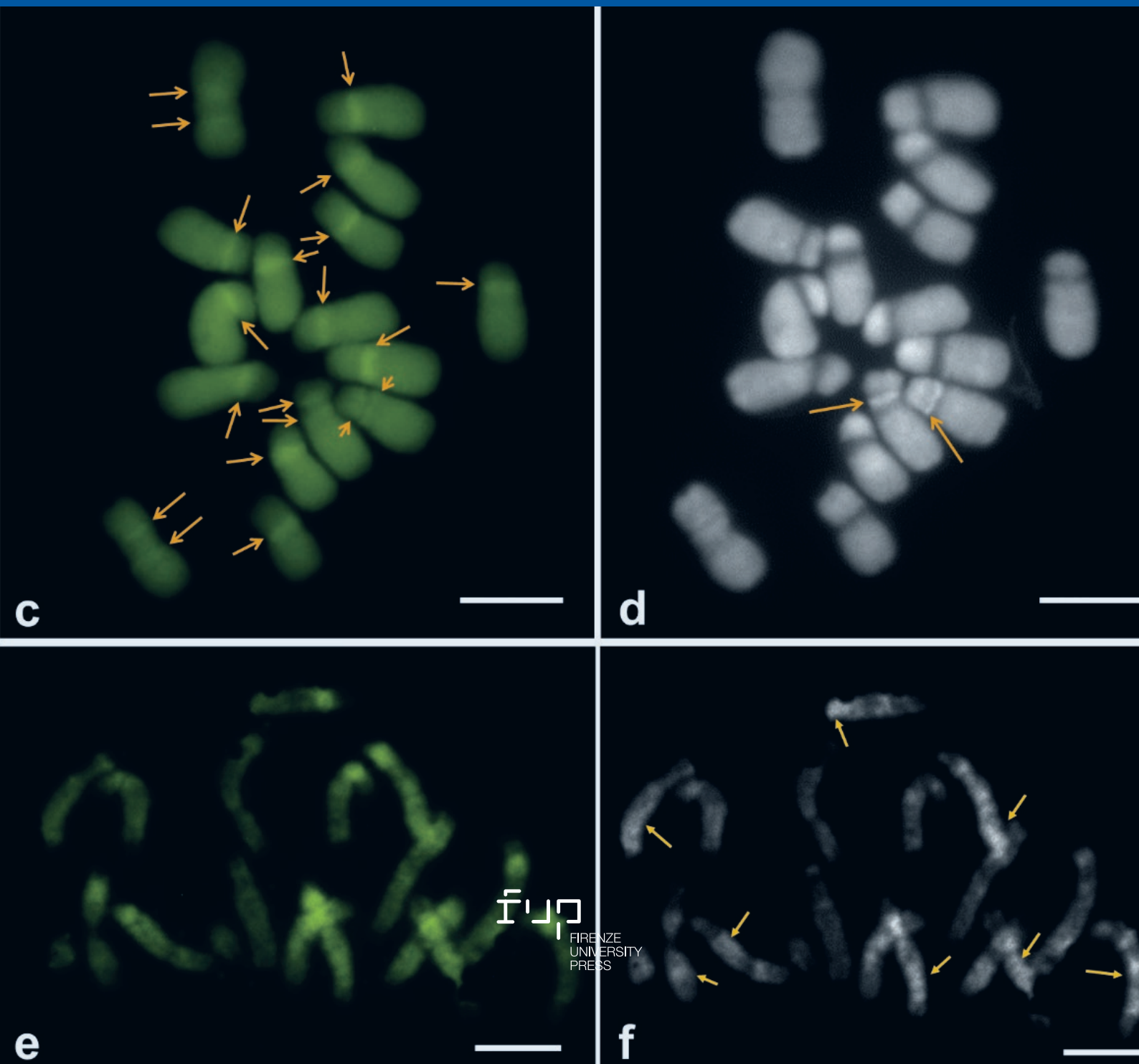

FIRENZE
UNIVERSITY
PRESS

Caryologia. International Journal of Cytology, Cytosystematics and Cytogenetics
Caryologia is devoted to the publication of original papers, and occasionally of reviews, about plant, animal and human karyological, cytological, cytogenetic, embryological and ultrastructural studies. Articles about the structure, the organization and the biological events relating to DNA and chromatin organization in eukaryotic cells are considered. *Caryologia* has a strong tradition in plant and animal cytosystematics and in cytotoxicology. Bioinformatics articles may be considered, but only if they have an emphasis on the relationship between the nucleus and cytoplasm and/or the structural organization of the eukaryotic cell.

Cover: figure from the article inside by Indranil Santra, Diptesh Biswas, Biswajit Ghosh. Chromosomal characterization mediated by karyomorphological analysis and differential banding pattern in fenugreek (*Trigonella foenum-graecum* L.): a neglected legume.

Caryologia

International Journal of Cytology, Cytosystematics and Cytogenetics

Volume 76, Issue 3 - 2023

Firenze University Press

***Caryologia*. International Journal of Cytology, Cytosystematics and Cytogenetics**
Published by
Firenze University Press – University of Florence, Italy
Via Cittadella, 7 - 50144 Florence - Italy
http://www.fupress.com/caryologia

Caryologia
International Journal of Cytology, Cytosystematics and Cytogenetics

Firenze University Press
www.fupress.com/caryologia

Citation: Lima-De-Faria, A. (2023). The chromosome resembles more a crystal than other cell organelles. *Caryologia* 76(3): 3-7. doi: 10.36253/caryologia-2332

Received: October 13, 2023

Accepted: December 14, 2023

Published: February 29, 2024

Data Availability Statement: All relevant data are within the paper and its Supporting Information files.

Competing Interests: The Author(s) declare(s) no conflict of interest.

The chromosome resembles more a crystal than other cell organelles

Antonio Lima-De-Faria

Professor Emeritus of Molecular Cytogenetics, Lund University, Lund, Sweden
E-mail: tatyana.turova@matstat.lu.se; stefanonikolaevic@gmail.com

Abstract. Several organelles in the cell, such as mitochondria and chloroplasts, are limited by one or several membranes, whereas others, like ribosomes and nucleoli have no membranes. Their shape is decided by their inner atomic coherence. The mineral crystal has no delimiting membranes built by separate atoms. Atomic self-assembly determines its pattern. Remarkable is that the chromosome has no outer membrane limiting its pattern as seen in the light and electronic microscopes. Its pattern is also decided by the inner coherence of the atomic configuration of its DNA, RNA, and proteins. The chromosome appears to occupy an intermediate position between a mineral crystal and a cell organelle when its atomic configuration is considered.

Keywords: chromosome, crystal structure, DNA.

MOLECULAR BIOLOGY DID NOT ORIGINATE FROM NATURAL SCIENCE BUT WAS A RESULT OF THE INTERACTION BETWEEN CRYSTALLOGRAPHY AND PHYSICS

It is usually not realized that the field of Molecular Biology had not its origin in Natural Sciences but resulted from the interaction of crystallography with physics. Cell biologists lacked many times knowledge of these two fields of science or these were mainly foreign to their minds.

The pioneers were Max von Laue (1879-1969), William Bragg (1862-1942) and Lawrence Bragg (1890-1971). All three were physicists. von Laue demonstrated that X rays were electromagnetic waves. He then realized that the atoms in a crystal were in an ordered array, in accord with their external regularity. He passed a narrow beam of X-rays through a crystal of a copper compound and obtained a diffraction pattern of spots on a photographic film.

This experiment became the basis of future X-ray crystallography. It allowed to measure the interatomic distance in crystals of diamond, copper, and salts such as KCI. The ordered atomic interior of crystals became a reality.

A PHYSICIST INROAD INTO GENETICS. SCHRÖDINGER WAS LOOKING FOR THE SIZE OF THE GENE BEFORE THE STRUCTURE OF DNA WAS ELUCIDATED

Several years before the chemical structure of DNA was revealed, the structure of genes and their size, was already a preoccupation. Geneticists, like most biologists tend to be conservative, and for them to venture into the molecular organization of the chromosome was foreign to their minds. But physicists, who at that time were already dealing with the extremely small elementary particles, such as the neutrino, felt obliged to inquire into the physics of living matter. Besides, by that time, geneticists asserted that the gene was to be built of proteins, because they were complex structures that demanded complex molecules. Nucleic acids, such as DNA, were too simple atomic combinations to carry the genetic material.

The leading physicist Schrödinger (1944) (Nobel Laureate 1933) was a professor in Berlin but had left Germany when Hitler assured power in 1933. He gave a series of lectures in 1943, in Dublin, Ireland, that were written down in his classic work "What is Life. The Physical Aspect of the Living Cell" (1944). By that time DNA had been demonstrated as being the genetic material in bacteria (Avery et al. 1943) but their experiment was regarded by geneticists to be of marginal value because at that time it was not known whether bacteria had chromosomes.

ASSERTING THAT ORDER IS TO BE SEARCHED IN LIVING PROCESSES

Schrödinger's main contribution was to emphasize the cell's physical construction and function:

1 Where others saw disorder, in the construction of the cell, he looked for order and stated: "We have inherited from our forefathers the keen longing for unified, all-embracing knowledge".
2 For the first time he called the chromosome "an aperiodic crystal" and added that "in physics we have dealt hitherto only with periodic crystals". And expressed clearly: "The difference in structure is of the same kind as that between an ordinary wallpaper in which the same pattern is repeated again and again in regular periodicity and a masterpiece of embroidery, say a Raphael tapestry, which shows no dull repetition, but an elaborate, coherent, meaningful design traced by the great master".
3 He calculated the size of atoms, but as he pointed out, we could not see them at that time. They ought to be "between about 1/5000 and 1/2000 of the wave-length of yellow light". Atomic diameters would range between 1 and 2 angstrom.
4 Schrödinger emphasized as well that physical laws are only approximate since they rest on atomic statistics. "As we shall presently see, incredibly small groups or atoms, much too small to display exact statistical laws, do play a dominating role in the very orderly and lawful events within a living organism".
5 He calculated the size of a gene as being "the volume of a gene equal to a cube of side 300 angstrom, being probably a large protein molecule".
6 "The gene has been kept at a temperature of 98° F, during all that time. How are we to understand that it has remained unperturbed by the disordering tendency of the heat motion for centuries?". Actually we know today that this period extended for millions of years, since the ribosomal RNA genes present in bacteria are the same as those found in plants and humans, only with minor modifications of the molecular edifice.
7 "Life seems to be orderly and lawful behavior of matter, not based exclusively on its tendency to go over from order to disorder, but based partly on existing order that is kept up". He calls it a new principle, "the order from order principle".

THE CHROMOSOME'S DNA TURNS OUT TO BE MORE PERIODIC THAN SCHRÖDINGER COULD HAVE ENVISAGED. THE EUKARYOTIC CHROMOSOME ARCHITECTURE IS BASED ON HIGHLY REPETITIVE DNA

Already at the prokaryotic level the DNA shows repeated sequences at precise positions. Examples are the IS elements and transposons of these genomes. In eukaryotes, the relative amounts of single copy and repetitive DNAs of many genomes are known, and certain classes of satellite DNA occur in the centromere and telomere regions.

In plant chromosomes the bulk of their DNA is made up of about 30 different repeat sequences. These are the tandemly repeated satellite DNA sequences of the centromere, telomeres and elsewhere. There are also long swathes of retrotransposon sequences. In maize they are of such high copy number that they form clusters that stretch for megabases along the DNA (Brown 2017).

Half of the human genome consists of repetitive DNA. Sequences consisting of 150 to 300 base pairs in length are repeated many thousands of times, and so called *Alu* sequences (circa 300 base pairs) They are present more than a million times.

Table 1. Reproduction of DNA can be compared to minerals.

REPRODUCTION	
Without DNA	With DNA
Centrioles	Chromosomes
Minerals	Cells
CELL ORGANELLES	
With membrane	Without membrane
	Centrioles
Chloroplasts	Chromosomes
Mithocondria	Nucleolus
CELL AND CELL ORGANELLE	
Membrane	No membrane
Cell	
Cell membrane	
(By self-assembly)	Ribosome
Endoplasmic	
Reticulum	Chromosome
Nuclear	
Envelope	
Mitochondrion	
Chloroplast	

Hence, the problem is not one of periodicity but mainly of the ability to be a self-sustained entity maintained by its atomic coherence.

This obliges to consider the role of membranes in the establishment of order in chemical reactions as well as their role in the establishment of well defined order in their construction.

THE CELL IS A WORLD OF MEMBRANES

The cell started, by being enveloped in a thick layer that separates it sharply from the environment. Besides it harbors a series of different membrane types.

But life creates many side solutions that led the cell to produce organelles that are not enclosed in membranes. The *membranous* part of the. cell consists of: (1) cell or plasma membrane, (2) nuclear membrane, (3) rough endoplasmic reticulum, (4) smooth endoplasmic reticulum, (5) Golgi apparatus, (6) mitochondria, (7) chloroplasts (in plants), (8) lysosomes, (9) centrosomes. But there are also *non-membranous* cell organelle: (1) chromosomes, (2) ribosomes, (3) nucleoli.

1 The *cell membrane* has long been known to consist of two protein layers separated by a phospholipid bilayer which regulates substance transport in and out of the cell.
2 *The nuclear envelope* consists of two lipid bilayer membranes an inner and outer membrane building a perinuclear space. The outer nuclear membrane is continuous with the endoplasmic reticulum. This is a connection between membranes that puts in evidence the ability to extend their range to other non-membranous organelles. One of its characteristics is its many nuclear pores. Filament proteins, called lamins give structural support to the nucleus.
3 The *endoplasmic reticulum* is a network of flattened membrane-enclosed sacs (*cisternae*) and tubular structures. These are continuous with the outer nuclear membrane. Both the rough and smooth reticulum are found in most eukaryotic cells but not in red blood cells or spermatozoa.
4 *Mitochondria* have two membranes: outer membrane and inner membrane. The two membranes have distinct properties. Infoldings of the inner membrane build cristae and there is a fluid internal matrix.
5 The *chloroplast* is even more complex. It is limited by a double layer with an intermediate space. Following secondary endosymbiosis chloroplasts may possess three or four membranes.

THE NON-MEMBRANOUS ORGANELLES OF THE CELL

(1) CHROMOSOME: As late as the 1960s there was a debate among cytologists of wether the chromosome had a surrounding membrane, called matrix, or this supposed pellicle was only an artifact. Soon more accurate studies and the electron microscope disposed of this artifact. The chromosome has no membrane surrounding its structure.

This situation is not unique, other organelles too do not have membranes limiting their bodies. These are the ribosomes and the nucleoli.

(2) RIBOSOME: Ribosomes in bacteria and eukaryotes are macromolecular "machines" found within all living cells that perform protein synthesis by messenger RNA translation. They link amino acids together to form polypeptide chains following an order specified by the codons of messenger RNA.

Ribosomes consist of two major components: the small and large ribosomal subunits (30S and 50S). Each subunit consists of one or more ribosomal RNA molecules and many ribosomal proteins. Together with other molecules they build the translational apparatus. Amino acids are selected and carried to the ribosome by transfer RNA. The 30S component has mainly a decoding function, the 50S has a mainly catalytic function. Ribosomes are often associated with the intracellular membrane that make up the rough endoplasmic reticulum,

but are an independent non-membranous edifice built by dozens of distinct proteins of variable number.

(3) NUCLEOLUS: Nucleoli have been studied in over 500 species of eukaryotes from algae to humans and they were found to be a very well defined spherical body containing vacuoles (Lima-de-Faria, 1973, 1979).

The chemical composition of the nucleolus has been well established.

The nucleolus is the largest structure in the nucleus of eukaryotic cells and is known as the site of ribosome biogenesis. It also has other functions participating in the formation of signal recognition particles and in the cell's response to stress.

Nucleoli are a large structural edifice made of proteins, DNA and RNA. They are formed at a specific site called the nucleolar organizing region and are formed only in specific chromosomes.

Nucleoli have vacuoles that are clear areas in their center. The nucleolus consists of three major components: a fibrillar center, a dense fibrillar component and a granular component. In plants, some species have high concentrations of iron in this organelle.

To generate the 18S RNA, 5.8S and 28S RNA, RNA modifying enzymes are brought to recognition sites by interaction with guide RNAs showing a most ordered process. An additional RNA molecule is the 5SRNA which is also necessary. The DNA sequence responsible for its formation lies outside the nucleolus organizer region being transcribed in the nucleoplasm.

Significant is that this spherical cell organelle maintains this most regular configuration in hundreds of different species as an independent edifice without membrane.

THE CHROMOSOME IS MORE SIMILAR TO A MINERAL CRYSTAL THAN TO OTHER CELL ORGANELLES. IT IS NOT LIMITED BY A MEMBRANE

A cell, a nucleus, a chloroplast, a mitochondrion, all are limited by well defined membranes that show a complex structure when analysed with the electron microscope. Membranes are in abundance all over the cell. The endoplasmic reticulum that fills the cytoplasm consists of a long series of membranes tightly stapled on each other that could have been used as well to put definite limits on the chromosome.

But this is not the case. In this respect the chromosome is like the nucleolus, which has its limits determined by its molecular structure. The nucleolus may in exceptional cases have a radial shape but in the most studied species it has a regular spherical structure.

Hence both the chromosome, the ribosome and the nucleolus are in this respect closer to mineral crystals, which have natural faces determined solely by their molecular configurations.

A crystal of quartz, or any other mineral has facets that are not covered by any limiting structure, they emerge solely as a result of the atomic interactions of their constituent molecules.

Hence, the chromosome's atomic construction is closer to that of a mineral crystal than to a cell organelle.

DNA ASSOCIATED PROTEIN ALSO CRYSTALLIZE

It may be recalled that DNA, and its associate proteins, could not have been identified as macromolecules, atom by atom, if they were not crystallized. It is only by reducing them to this ordered condition that their atomic structure and their special organization could be defined.

Their crystallization was possible for the simple reason that their atomic configurations are highly ordered.

DEFINITION OF A CRYSTAL

"A solidified form of substance in which the atoms or molecules are arranged in a definite repeating pattern so that the external shape of a particle or mass of the substance is made up of planed faces in a symmetrical arrangement" (Webster 1976). The definition of Klein and Hurlbut (1985) is: "any solid with an ordered internal structure regardless of whether it possesses external faces". And in a broader definition: "a homogenous solid possessing long-range, three dimensional internal order".

MINERALOGISTS POINT OUT THAT DNA IS ALSO A CRYSTAL

The definition of a crystal by Wenk and Bulakh states clearly that DNA is a crystal: "is a homogenous chemical compound with a regular and periodic arrangement of atoms. But crystals are not restricted to minerals: they comprise most solid matter such as sugar, cellulose, metals, bones and even DNA".

RIBOSOMES ALSO ASSUME A CRYSTAL FORM AS A RESULT OF THEIR ORDERED ATOMIC STRUCTURE

Viruses, which consist of nucleic acids and proteins, can become crystal structures but abandon this ordered

configuration when they reproduce in the cell. Ribosomes can form crystalline structures as is the case in chicken, mouse, and other types of tissues (Morimoto et al. 1972). Ribosomes become crystalline when the cells are chilled to 5-15°. Chromosomes follow the same condition. They also become crystallized when their activity becomes minimal and are obliged to occupy a minimum of space.

ACTUALLY, THE CHROMOSOME BECOMES A CRYSTAL IN THE ANIMAL SPERM

The evidence just described is corroborated by a key observation that is usually not cited. The arrangement of DNA in sperm nuclei has been studied by X-ray diffraction and polarizing microscopy. During spermiogenesis the proteins gradually condense. They also acquire specific patterns which are typical of the arrangement.

The crystalline organization of the chromosomes is particularly evident in the spermatids of two grasshopper species, *Dissosteira carolina* and *Melanoplus femur rubrum*. During development the nuclear fibers form plates which are oriented longitudinally to the major axis of the nucleus. Later these lamellae coalesce into a "crystalline body" (Gall and Björk,1958) as described by the antlion. As the electron microscope sections show the pattern is most similar to that of ribosome crystals.

REFERENCES

1 Brown, T. A. 2017. Genome IV. CRC Press inc., USA.
2 Lima-de-faria, A. 1973. Equations Defining the Position of Ribosomal Cistrons in the Eukaryotic Chromosome. Nature New Biology 241:136-139.
3 Lima-de-Faria, A. 1979. Prediction of gene location and clarification of genes according to the chromosome field. Alfred Benzon Symposium No. 13. *Specific Eukaryotic Genes. Structural Organization and Function*. Munksgaard, Copenhagen, 25-38.
4 Comings, D. E. 1972. Replication heterogeneity in uremammalian DNA. Exp. Cell Res. 71:106-112.
5 Gall, J. and Björk, L. B. 1958. The Spermatid Nucleus in Two Species of Grasshopper. J. Biophys. and Biochem. Cytol. 4:479-484.
6 Byers, B. 1967. Structure and formation of ribosome crystals in hypothermic chick embryo cells. J. Mol. Biol. 26:155-167.

Caryologia
International Journal of Cytology, Cytosystematics and Cytogenetics

Firenze University Press
www.fupress.com/caryologia

OPEN ACCESS

Citation: Nassar, M., Sakhraoui, N., & Domina, G. (2023). Karyotype asymmetry in some Scilloideae (Hyacinthaceae) members from Algeria. *Caryologia* 76(3): 9-18. doi: 10.36253/caryologia-2238

Received: July 7, 2023

Accepted: January 18, 2024

Published: February 29, 2024

Data Availability Statement: All relevant data are within the paper and its Supporting Information files.

Competing Interests: The Author(s) declare(s) no conflict of interest.

ORCID

MN: 0000-0002-1161-6957
NS: 0000-0002-9853-5702
GD: 0000-0002-9125-764X

Karyotype asymmetry in some Scilloideae (Hyacinthaceae) members from Algeria

Meryem Nassar[1,4,*], Nora Sakhraoui[2,4], Gianniantonio Domina[3]

[1] *Department of Natural Sciences and Life BP 26, University of 20 August 1955, El Hadaiek Road-Skikda 21000, Algeria*
[2] *Department of Ecology and Environment BP 26, University of 20 August 1955, El Hadaiek Road-Skikda 21000, Algeria*
[3] *Department of Agricultural, Food and Forest Sciences University of Palermo, Viale delle Scienze, Bldg 4, 90128, Palermo, Italy*
[4] *Laboratory of Research in Biodiversity Interaction, Ecosystem and Biotechnology 'LRIBEB', University of 20 August 1955 BP 26, El Hadaiek Road-Skikda 21000, Algeria*
*Corresponding author E-mail: meryem4321@yahoo.fr, m.nassar@univ-skikda.dz

Abstract. This cytogenetic study attempts to shed light on the karyomorphological and asymmetry data of species in the subfamily Scilloideae previously included in *Scilla,* namely *Hyacinthoides lingulata* (Poir.) Rothm., *Prospero autumnale* (L.) Speta, *Prospero obtusifolium* (Poir.) Speta, *Barnardia numidica* (Poir.) Speta, and *Oncostema elongata* (Parl.) Speta. These taxa are predominantly from the Skikda region (northeastern Algeria). *H. lingulata* had a somatic chromosome number $2n=2x=16$, *P. autumnale* $2n=2x=14$, *P. obtusifolium* $2n=2x=8$, *B. numidica* $2n=2x=18$, and *O. elongata* $2n=2x=16$. The indices of intrachromosomal (M_{CA}, A_1, and AsI) and interchromosomal (CV_{CL}, CV_{CI}, and A_2) asymmetry revealed that *H. lingulata* has the most asymmetrical karyotype (1C), while *P. autumnale* has the most symmetrical karyotype (3A). *P. obtusifolium* has a relatively symmetrical karyotype (4A), while *B. numidica* and *O. elongata* have both an asymmetrical karyotype (1B). These findings differ from those previously reported for the same taxa in Algeria, hence indicating the substantial genetic variation that exists within the country.

Keywords: chromosomes, bulbous, plants, genetic diversity, *Scilla.*

INTRODUCTION

The Hyacinthaceae family comprises exclusively herbaceous species, most of which are bulbous. In phylogenetic classification, this family is now included in the Asparagaceae (APG IV 2016), and its genera fall under the subfamily Scilloideae. However, the nomenclature of its genera is still widely controversial. The species that belong to the former genus *Scilla* have also been split among several genera (Pfosser and Speta 1999). Three of them are related to the autumn squills of the North African flora, namely *Prospero*, *Hyacinthoides*, and *Barnardia*. The Hyacinthaceae family has a wide distribution in Algeria, where it occurs with a certain concentration in the Tell Atlas

region (Maire 1958; Quézel and Santa 1962). However, this family also includes endemic species shared between Algeria and neighboring countries, such as *Albuca amoena* (Batt.) J.C.Manning & Goldblatt, *Ornithogalum sessiliflorum* Desf. (both endemic to Morocco and Algeria), *Hyacinthoides aristidis* (Coss.) Rothm. (endemic to Algeria and Tunisia), and *H. lingulata* (Poir.) Rothm. (endemic to Morocco, Algeria, and Tunisia).

The cytogenetic research carried out by Hamouche *et al.*(2010), Véla and de Bélair (2016), and Azizi *et al.* (2016a), has shed light on the karyotypes of various species that are proliferating in Algeria. However, taking into account the variety of Algeria's ecosystems, it's possible that the genetic diversity found within Algeria's populations is much greater than what was earlier thought. Previous research has shown that the genus *Prospero* has a significant amount of polymorphism, both in terms of the ploidy level and the fundamental chromosomal number ($2n$=14, $2n$=28, and $2n$=42) (Hamouche *et al.* 2006; Hamouche *et al.* 2010; Jang *et al.* 2013; Jang *et al.* 2018). Two cytotypes, $2n$=8 and $2n$=16, have been found for *H. lingulata*, which primarily proliferates in diverse biotopes in the northwestern coastal region of Algeria (Hamouche *et al.* 2006; Hamouche *et al.* 2010). This underscores the necessity to extend and vary the sample regions in order to cover the widest possible range of ecosystems.

In light of this, we carried out cytogenetic research on some species of the Hyacinthaceae that are thriving in the Skikda area (northeastern Algeria), which have not been previously investigated. The following species were considered for the cytogenetic analyses: *H. lingulata* (Poir.) Rothm., *P. autumnale* (L.) Speta, *P. obtusifolium* (Poir.) Speta, *B. numidica* (Poir.) Speta, and *O. elongata* (Parl.) Speta. This study will allow us, on the one hand, to learn about the chromosomal composition of the studied taxa, and on the other hand, to shed light on the genetic diversity and karyological variation that may exist within Algeria's populations.

MATERIAL AND METHODS

The plants selected for cytogenetic analysis were collected from their natural habitat (Figure 1) and identified using the flora of North Africa (Maire, 1958), the GDB herbarium (https://gdebelair.com/), and confirmed Algerian occurrences documented on iNaturalist (https://www.inaturalist.org/observations?place_id=7300). The root tips were obtained from plants collected in nature (Table 1). Seed germination was not successful. After receiving a pretreatment with 0.05% colchicine, the roots were subsequently fixed in a combination of ethanol and acetic acid (3:1). Roots were then placed in a solution of hydrochloric acid (HCl 1N) and heated to 60 °C. This step lasted for 10 min. Following that, they were stained for at least 1h with Schiff's reagent, and lastly, they were crushed in a drop of 3% acetic carmine. At least 10 plates per each population were studied. A series of photographs were taken of the best plates, and then different measures were carried out to determine the karyotype of each species.

The chromosomal type was determined based on the terminology used by Levan *et al.* (1964). The karyotypes were accurately categorized using the Stebbins (1971) method. Different approaches were used to estimate additional parameters of karyotype asymmetry. HCL: Haploid total length, TF: Total form percentage (Huziwara 1962), AsI: Karyotype asymmetry index (Arano and Saito 1980), Syi: Karyotype asymmetry index, Rec: Chromosome size similarity index (Greihuber and Speta 1976), CV_{CL}: Coefficient of variation in chromosome length, CV_{CI}: Coefficient of variation in centromeric index, AI: Asymmetry index (Paszko 2006), A_1: Intrachromosomal asymmetry, A_2: Interchromosomal asymmetry (Romero Zarco 1986), M_{CA}: Mean centromeric asymmetry (Peruzzi and Eroğlu 2013). The Pearson correlation between several asymmetry indices was calculated using IBM SPSS Statistics 24 software. Additionally, the ideogram for each species was determined depending on their chromosomal size.

RESULTS

The karyotypes of five species from the subfamily Scilloideae have been thoroughly examined. Originally classified as *Scilla* by Maire (1958), these species have recently been reassigned to four distinct genera. Table 2 provides details on chromosomal numbers, total chromosome length, the ratio of long to short arms, and the total size of the haploid complement. *H. lingulata*, *P. autumnale*, *P. obtusifolium*, *B. numidica*, and *O. elongata* are all diploids with respective chromosome counts of 16, 14, 8, 18, and 16.

The specific karyotypic formulas for each species are further documented in Table 2. The karyotypes of these species consist mostly of metacentric, submetacentric, subtelocentric, and even telocentric chromosomes, particularly in the case of *H. lingulata* and *B. numidica*. The size of the chromosomes in *B. numidica* and *H. lingulata* varied from 1.27 μm to 6.49 μm depending on the species. *H. lingulata* stands out for having the largest haploid complement, which has an average size of 29.80

Figure 1. Illustration of the studied taxa showing differents parts of each plant: bulbs, flowers, and capsules,A: *Hyacinthoides lingulata*, B: *Prospero autumnale*, C: *P. obtusifolium*, D: *Barnardia numidica*, E: *Oncostema elongata*.

Table 1. Localities of the studied taxa.

Taxa	Locality	Habitat	Latitudes	Longitudes	Altitude	Month of collection
Hyacinthoides lingulata	Larbi Ben M'Hidi	Coastal dune	36°53'08"N	7°00'55"E	40 m	September
Prospero autumnale	Larbi Ben M'Hidi	Coastal dune	36°53'08"N	7°08'01"E	40 m	September
Prospero obtusifolium	Ramdan Djamel	Olive grove	36°45'18"N	6°54'40"E	90 m	December
Barnardia numidica	Filfilla	Rocky cliffs	36°53'01"N	7°00'55"E	340 m	November
Oncostema elongata	Ramdan Djamel	Olive grove	36°45'18"N	6°54'40"E	90 m	January

μm. This size exceeds that of the other species. Following closely is *O. elongata*, which possesses a total haploid complement size of 28.28 μm. *B. numidica* possesses chromosomes that are very tiny in size. However, its haploid complement measures 21.64 μm, which is larger than that of *P. obtusifolium* (16.60 μm) and *P. autumnale* (14.85 μm), as shown in Table 2.

In order to assess the level of asymmetry in the karyotypes of the studied species, we used Stebbins' categorization together with the CV_{CL} and M_{CA} values. The specific asymmetry indexes used are outlined in Table 3. *H. lingulata* has much more prominent asymmetry characteristics compared to other species. The karyotype of this species is categorized as 1C according to Stebbins'

Table 2. Karyotype features of the studied taxa.

Taxa	2n	SC-LC (µm)	LC/SC	p (µm)	q (µm)	CL (µm)	HCL	CI (min-max)	KF
Hyacinthoides lingulata	16	1.54-6.49	4.21	0.75±0.1	2.97±0.17	3.72±0.26	29.80	0.05-0.44	1m+2sm+3st+2t
Prospero autumnale	14	1.52-2.66	1.75	0.61±0.1	1.5±0.10	2.11±0.12	14.85	0.16-0.41	$1m+m^{sat}$+3sm+2st
Prospero obtusifolium	8	3.17-4.82	1.52	1.08±0.2	3.04±0.1	4.14±0.22	16.16	0.21-0.32	2sm+2st
Barnardia numidica	18	1.27-3.97	3.12	0.56±0.1	1.83±0.11	2.39±0.17	21.64	0.05-0.46	3m+2sm+3st+1t
Oncostema elongata	16	1.79-5.38	3.00	0.85±0.06	2.66±0.12	3.51±0.17	28.28	0.13-0.40	2m+1sm+5st

SC: shortest chromosome, LC: longest chromosome, p: mean short arm, q: mean long arm, CL: mean total chromosome length, HCL: total haploid chromosome length, CI: centromeric index, KF: karyotype formula, m: metacentric, sm: submetacentric, st: subtelocentric, t: telocentric.

Table 3. Asymmetry indices of the studies taxa.

Taxa	TF	AsI	Syi	Rec	CV_{CL}	CV_{CI}	AI	A_1	A_2	M_{CA}	S
Hyacinthoides lingulata	20.27	79.72	25.33	4.58	48.40	59.23	28.65	0.66	0.48	59.40	1C
Prospero autumnale	28.98	71.01	37.33	5.57	18.53	29.23	5.40	0.56	0.18	44.54	3A
Prospero obtusifolium	26.50	73.49	35.85	3.44	17.14	20.12	3.43	0.64	0.17	47.10	4A
Barnardia numidica	23.77	76.22	30.76	5.43	42.01	51.89	21.79	0.57	0.42	52.57	1B
Oncostema elongata	24.44	75.55	31.95	5.24	45.69	42.20	19.28	0.60	0.42	51.45	1B

classification, with intrachromosomal asymmetry index M_{CA} values of 59.4 and interchromosomal asymmetry index CV_{CL} values of 48.4.

In contrast, *P. autumnale* and *P. obtusifolium*, have significantly reduced asymmetry values. The intrachromosomal asymmetry indices (M_{CA}) for *P. autumnale* and *P. obtusifolium* are 44.54 and 47.10, respectively. Similarly, their interchromosomal asymmetry indices (CV_{CL}) are 18.53 and 17.14, respectively. The karyotypes of these two species are categorized as 3A and 4A, respectively. Although belonging to different genera, *B. numidica* and *O. elongata* exhibit very comparable asymmetry indices, which are characterized by rather high values. The intrachromosomal asymmetry indices M_{CA} for *B. numidica* and *O. elongata* are recorded as 52.57 and 51.45, respectively. The interchromosomal asymmetry index CV_{CL} for *B. numidica* is determined as 42.01, whereas for *O. elongata* it is calculated as 45.69. Both karyotypes are classified as 1B according to Stebbins' classification (1971).

DISCUSSION

Hyacinthoides lingulata

The earlier research carried out by Hamouche *et al.* (2006) and (2010) on populations from western Algeria assigned two different chromosomal numbers to this endemic taxon of North Africa. They were $2n$=8 and $2n$=16. This holds true when compared to the findings of the current investigation, which indicated that $2n$=16. Furthermore, certain similarities in caryotype descriptions have been observed between the two populations. The main difference is that the Skikda population has two telocentric chromosomes but no satellite chromosomes. According to Weiss Schneeweiss and Schneeweiss (2013), variation in caryotypical configuration between populations is indicative of chromosomal rearrangements, particularly those involving subtelocentric or telocentric chromosomes that appear to result from chromosomal deletion or translocation. Previous research (Sato 1936) showed that members of the Scilloideae subfamily had various caryotypes even within the same species. It is worth noting that the presence of such variability in karyotype organization does not always imply a significant morphological difference (Thompson 2005; Thompson 2020).

Prospero autumnale

The research conducted by Hamouche *et al.* (2010) on multiple populations from various locations in central Algeria revealed a high level of diversity within the species, which is closely associated with the altitude and environment in which they grow. Diploid ($2n$=$2x$=14),

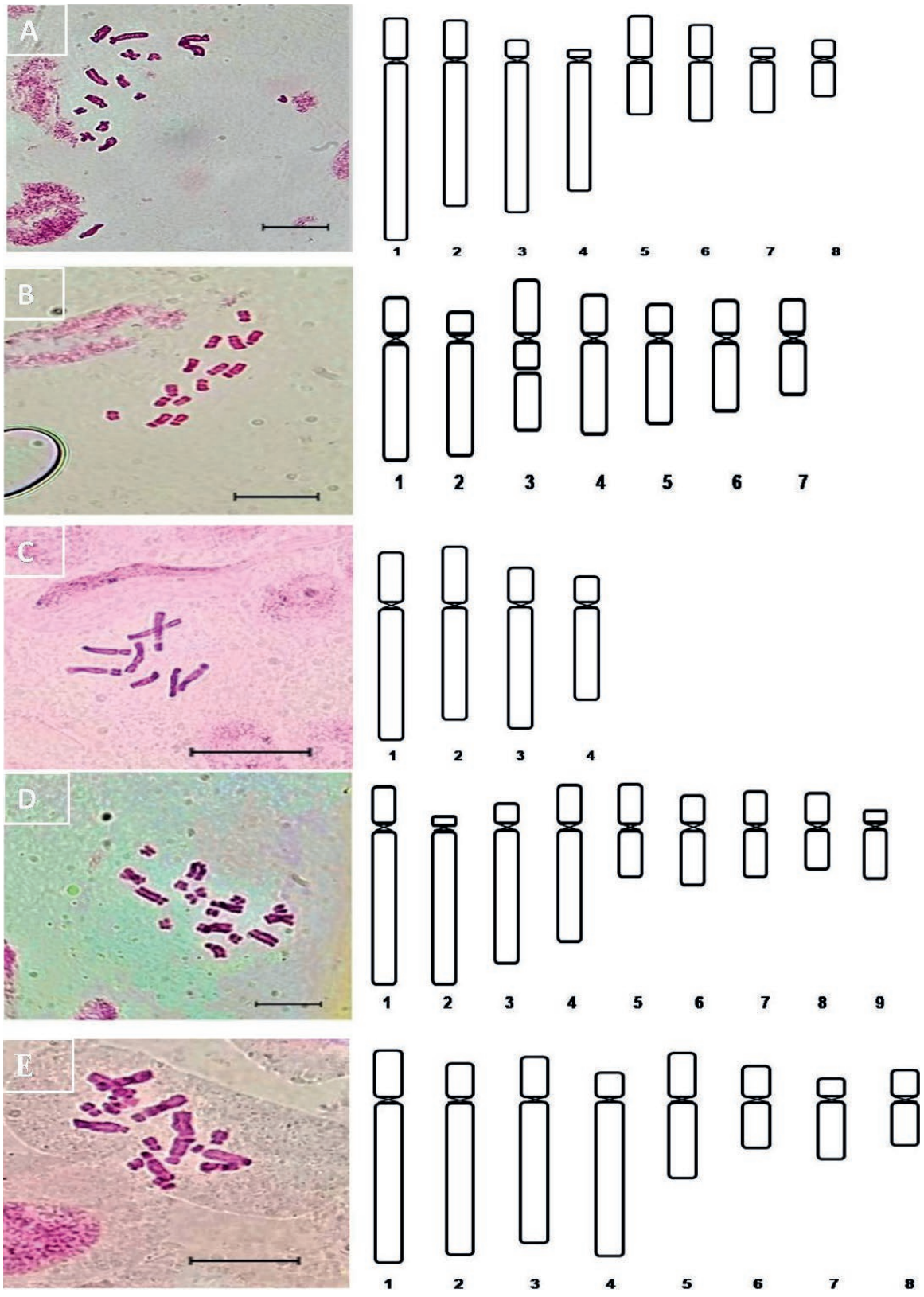

Figure 2. Mitotic metaphase and idiograms of the studied taxa. A: *Hyacinthoides lingulata* 2*n*=16, B: *Prospero autumnale* 2*n*=14, C: *P. obtusifolium* 2*n*=8, D: *Barnardia numidica* 2*n*=18, E: *O. elongata* 2*n*=16, scale bars=10 μm

tetraploid (2*n*=4*x*=24), and hexaploid (2*n*=6*x*=42) cytotypes were identified. The population of Skikda, which is located in northeastern Algeria, differs from the populations of Algiers, especially in terms of karyological description. It is distinguished by the presence of a metacentric chromosome (7) in addition to submetacentric and telocentric chromosomes, as well as a secondary constriction on the long arm of chromosome 3. In contrast, the diploid population (2*n*=2*x*=14) from Algiers exhibits only submetacentric and subtelocentric chromosomes, in addition to a satellite on the short arm of chromosome 5.

This implies that there is considerable variation even among diploid cytotypes (2*n*=2*x*=14) in Algeria, which might be due to chromosomal rearrangements such as inversions and translocations. Jang *et al.* (2013) and Jang *et al.* (2018) investigations both validated the existence of chromosomal rearrangements in the *P. autumnale* complex. In the *P. autumnale* complex, supernumerary forms such as B chromosomes and forms of aneuploidy, particularly in diploid cytotypes (2*n*=*2x*=14+1) and hexaploid cytotypes (2*n*=6*x*=42+1), have been documented (Rejoin *et al.* 1980; Hamouche *et al.* 2010; Jang *et al.* 2018). In addition, Jang *et al.* (2013) showed the existence of four diploid cytotypes with three distinct fundamental numbers, *x*=5, *x*=6, and *x*=7, based on their study of seventeen individuals from various countries bordering the Mediterranean Sea. Individuals with the cytotype 2*n*=2*x*=14 were assigned two chromosomal descriptions, including one with submetacentric chromosomes (secondary constriction on chromosome 3), a subtelocentric chromosomes and a small metacentric chromosome. This is an exact match to the chromosomal description discovered in this investigation. The possibility cannot be ruled out for the presence of other *P. autumnale* complex cytotypes in Algeria, given the country's vast size and the vast diversity of its habitats and climates.

Prospero obtusifolium

Our findings regarding chromosomal number and formula are consistent with the studies conducted by Ebert *et al.* (1996), Hamouche *et al.* (2010), and Jang *et al.* (2013). These studies all identified a single cytotype (2*n*=8) in populations throughout the Mediterranean basin. Overall, this indicates that the species has successfully maintained significant stability in its karyotype composition, even when dispersed over different habitats and a wide geographic area.

Barnardia numidica

Our population exhibits a chromosomal formula distinct from that of the central Algerian population (2*n*=2*x*=18=4m+2sm-sat+3st) by possessing a telocentric pair but lacking a satellite. Both populations share metacentric and subtelo-centric chromosomes. The karyotype consists of two distinct sets of chromosomes, one containing small metacentric or submetacentric chromosomes and the other containing big subtelo-centric chromosomes (bimodal karyotype). The variation in size that was found might be attributed to hybridization, as shown by previous research (Speta 1979; Ebert *et al.* 1996; Hamouche *et al.* 2010). Other studies have indicated that this heterogeneity is linked to higher amplification of distinct forms of heterochromatin within specific chromosomal sets (De la Herrán *et al.* 2001). Indeed, the existence of a bimodal karyotype has already been observed in Hyacinthaceae species such as *Ornithogalum* (Stedje 1989) and *Galtonia* (Forrest and Jong 2004).

Oncostema elongata

There is still no taxonomic consensus on the specific delimitation within *O. peruviana* (*Scilla peruviana*). Some authors attribute the variability observed in the CW Mediterranean to a single species (Almeida da Silva and Crespí 2013; Almeida da Silva *et al.* 2014), others prefer to consider different species (Dobignard and Chatelain 2010; APD 2023). Previous research has pointed to the presence of different chromosomal counts of 2*n*=16, 2*n*=15, and 2*n*=14 have been seen in different individuals of *O. peruviana* (Sato 1936).

The same is true for *O. hughii* (Tineo ex Guss.) Speta, which has four distinct numbers (2*n*=17, 2*n*=19, 2*n*=20, and 2*n*=22). It is worth noting that these chromosomal count differences were discovered in plants that shared the same habitat (Sato 1936). In addition, the same author has shown that *O. peruviana* (L.) Speta has a stable karyotype with 2*n*=16=1M+4stSat+2m+1st. Although 2*n*=16 is thought to be the fundamental chromosome number in *O. peruviana* (Sato 1936; Battaglia 1950, Barone *et al.* 2021).

Several asymmetry indices have been established since the work of Stebbins to evaluate karyotype asymmetry in its evolutionary state (Romero Zarco 1986). These are the first data on karyotype asymmetry for the several species included in this study. According to Peruzzi and Eroglu (2013), the intrachromosomal asymmetry index M_{CA} and the interchromosomal asymmetry index CV_{CL} are extensively utilized due to their abil-

ity to detect even the most subtle chromosomal variations. Various asymmetry parameters have disclosed karyotype diversity among the studied species. Species in the genus *Prospero*, such as *P. autumnale* and *P. obtusifolium*, classified as types 3A and 4A, respectively, appear to have the most symmetrical karyotypes, indicating relatively stable karyotypes, according to Stebbins' classification. The karyotypes of *B. numidica, O. elongata* and *H. lingulata,* on the other hand, belong to categories 1B, 1B and 1C, respectively, indicating asymmetrical karyotypes. High CV_{CL} and M_{CA} values for all three species, especially *H. lingulata*, support this result (Table 3). The intrachromosomal asymmetry index M_{CA} had a significant negative connection with Syi (-0.997**) and TF (-0.996**) and a positive correlation with AsI (0.996**) and HCL (0.917**) according to Pearson correlation. It also correlated positively with CV_{CL} (0.093) and CV_{CI} (0.516), although not significantly. The interchromosomal asymmetry index CV_{CL}, on the other hand, had a strong and positive relationship with CV_{CI} (0.83*), AI (0.99**), A_2 (0.99**), and HCL (0.91**). Therefore, differences in asymmetry between chromosomes in the same set are associated with differences in size, which may result from changes in structure as well as differences in shape, particularly the location of the chromosomal centromere.

The karyotypes of *P. autumnale* and *P. obtusifolium* are notable for their symmetrical structure, but those of *B. numidica*, *O. elongata*, and *H. lingulata* have significant asymmetry. According to Stebbins (1971), asymmetric karyotypes are seen as derived traits that have emerged more recently in evolutionary processes. They are often linked to plants that display specific morphological features or are descendants of a more recent origin. In the Mediterranean flora, variations in chromosome size, base number, and symmetry between closely related species are not new. Many processes, such as polyploidy, aneuploidy, or dysploidy, can explain these changes (Stebbins 1971; Levin 2002; Guerra 2008; Choi *et al.* 2008) and morphological differences could result from the expression of these genetic variations (Thompson 2005; Thompson 2020). Species belonging to genera such as *Reichardia*, *Brachyscome*, *Crepis* and *Geranium* provide clear examples of this karyotypic variety (Siljak-Yakovlev 1996; Watanabe *et al.* 1999; Dimitrova and Greilhuber 2000; Martin *et al.* 2022). Interestingly, these variations are not limited to interspecific differences but extend to intraspecific levels, giving rise to the emergence of new chromosomal races (Levin 2002). *Prospero autumnale* (Parker *et al.* 1991, Ebert *et al.* 1996, Vaughan *et al.* 1997, Hamouche *et al* .2010), *Ornithogalum tenuifolium* (Stedje 1989), *O. nutans* (Cullen and Rattert, 1967), *Albuca abyssinica* (Stedje 1996), *Bellevalia mauritanica*, and *Muscari neglectum* (Azizi *et al.* 2016b) are notable examples in the Hyacinthaceae family.

CONCLUSION

In terms of karyotypic constitution and asymmetry indices, the cytogenetic data related to the examined species belonging to four genera of the subfamily Scilloideae have revealed, on the one hand, that the populations of the Skikda region are different from other populations previously studied by other researchers, indicating the important genetic diversity that exists in Algeria and on the other hand, significant differences between the species. This suggests that *P. autumnale* is the most stable species and *H. lingulata* is the most evolved species. However, molecular phylogenetic investigations are required to fully comprehend the relationship between the species under issue.

ACKNOWLEDGMENT

The authors would like to thank Dr Errol Véla from the University of Montpellier for the confirmation of the identification of *Oncostema elongata.*

REFERENCES

Almeida da Silva R, Rocha J, Silva A, García-Cabral I, Amich F, Crespí AL. 2014. The Iberian species of *Scilla* (Subfamily Scilloideae, Family Asparagaceae) under climatic change scenarios in southwestern Europe. Syst Bot. 39: 1083-1098.

Almeida da Silva TM, Crespí AL. 2013. *Scilla* L. In: Castroviejo S, Rico E, Crespo MB, Quintanar A, Herrero A, Aedo C. (eds) Flora Iberica, 20. Madrid: Real Jardin Botanico, CSIC. Pp. 145-156.

APD [African Plant Database] 2023.*Oncostema* Raf In African Plant Database. – Published at: https://africanplantdatabase.ch/en/search/*Oncostema*/[last accessed 20 June 2023]

APG IV. 2016. An update of the Angiosperm Phylogeny Group classification for the orders and families of flowering plants: APG IV. Bot. J. Linn. Soc. 181: 1-20.

Arano H, Saito H. 1980. Cytological studies in family Umbelliferae. Karyotypes of seven species in the subtribe Seselinae. La Kromosomo. 2: 471-480.

Azizi N, Amirouche R, Amirouche N. 2016a. Cytotaxonomic diversity of some medicinal species of Hya-

cinthaceae from Algeria. Pharmacogn Commun. 6: 34-38.

Azizi N, Amirouche R, Amirouche N. 2016b. Karyological investigations and new chromosome number reports in *Bellevalia* Lapeyrouse, 1808 and *Muscari* Miller, 1758 (Asparagaceae) from Algeria. Comp Cytogenet. 10: 171-187.

Barone G, Di Gristina E, El Mokni R, Domina G. 2021. Karyological data of four geophytes native to Tunisia. Fl Medit. 31: 341-345.

Battaglia E. 1950. Chromosome mutations in *Scilla peruviana* L. Caryologia. 3: 126-147.

Choi HW, Kim JS, Lee SH, Bang JW. 2008. Physical mapping by FISH and GISH of rDNA loci and discrimination of genomes A and B in *Scilla scilloides* complex distributed in Korea. J PlantBiol. 51:408-412.

Cullen J, Rattert JA. 1967. Taxonomic and cytological notes on Turkish *Ornithogalum*. Notes from the Royal Botanic Gardens. Edinburgh 27: 293-339.

De la Herrán R, Robles F, Cuñado N, Santos JL, Ruiz Rejón M. 2001. A heterochromatic satellite DNA is highly amplified in a single chromosome of *Muscari* (Hyacinthaceae). Chromosoma. 110: 197-202.

Dimitrova D, Greilhuber J. 2000. Karyotype and DNA content in ten species of *Crepis* (Asteraceae) distributed in Bulgaria. Bot J Linn Soc. 132: 281-297.

Dobignard A, Chatelain C. 2010. Index synonymique de la flore de l'Afrique du Nord. Vol 1. Genève: Conservatoire et jardin botaniques de la ville de Genève.

Ebert I, Greilhuber J, Speta F. 1996. Chromosome banding and genome size differentiation in *Prospero* (Hyacinthaceae): dipioids. J Syst Evol. 203:143-177.

Forrest LL, Jong K. 2004. Karyotype asymmetry in *Galtonia* and *pseudo-Galtonia* (Hyacinthaceae). Edinb J Bot. 60: 569-579.

Greilhuber J, Speta F. 1976. C-banded karyotypes in the *Scilla hohenaclceri* group, *S. persica*, and *Puschlcinia* (Liliaceae). Plant Syst Evol. 126: 149-188.

Guerra M. 2008. Chromosome numbers in plant cytotaxonomy: concepts and implications. Cytogenet. Genome Res. 120: 339-50.

Hamouche Y, Amirouche N, Misset MT, Amirouche R. 2010. Cytotaxonomy of autumnal flowering species of Hyacinthaceae from Algeria. Plant Syst Evol. 285: 177-187.

Hamouche Y, Amirouche R, Amirouche N. 2006. Notes taxonomiques et caryologiques de deux espèces du genre, *Scilla* (Hyacinthaceae) de l'ouest Algerois. Annals de l'Institut national Agronomique El-Harrach. 27: 95-105.

Huziwara Y. 1962. Karyotype analysis in some genera of Compositae. VIII. Further studies on the chromosomes of *Aster*. Am J Bot. 49: 116-119.

Jang TS, Emadzade K, Parker J, Temsch EM, R Leitch AR, Speta F, Weiss-Schneeweiss H. 2013. Chromosomal diversification and karyotype evolution of diploids in the cytologically diverse genus *Prospero* (Hyacinthaceae). BMC Evol Biol. 13: 136.

Jang TS, Parker JS, Weiss-Schneeweiss H. 2018. Euchromatic Supernumerary Chromosomal Segments Remnants of Ongoing Karyotype Restructuring in the *Prospero autumnale* Complex?. Genes. 9: 1-10.

Levan A, Fredga K, Sandberg AA. 1964. Nomenclature for centromeric position on chromosomes. Hereditas. 52: 201-220.

Levin DA. 2002. The role of chromosomal change in plant evolution. Oxford University Press, New York.

Maire R. 1958. Flore de l'Afrique du Nord, Dicotyledonae. Vol. 5, Monocotyledonae, Liliales, Liliaceae. Paris: Le chevalier.

Martin E, Kahraman A Dirmenci T, Bozkurt H, Eroğlu HE. 2022. New chromosomal data and karyological relationships in *Geranium*: basic number alterations, dysploidy, polyploidy, and karyotype asymmetry. Braz Arch Biol Technol. 65: 1-16.

Parker JS, Lozano R, Rejon MR (1991). Chromosomal structure of populations of *Scilla autumnalis* in the Iberian peninsula. Heredity. 67: 287-297.

Paszko B. 2006. A critical review and a new proposal of karyotype asymmetry indices. Plant Syst. Evol. 258: 39-48.

Peruzzi L, Eroğlu HE. 2013. Karyotype asymmetry: again, how to measure and what to measure? Comp Cytogenet. 7: 1-9.

Pfosser M, Speta F. 1999. Phylogenetics of Hyacinthaceae Based on plastid DNA Sequences. Ann M Bot Gard. 86: 852-875.

Quézel P, Santa S. 1962. Nouvelle flore de l'Algérie et des régions désertiques méridionales. Vol. 1. Paris: Centre nationale de la recherche scientifique.

Rejoin RM, posse F, Oliver JL. 1980. The B chromosome système of *Scilla autumnalis* (Liliaceae) : Effects atlysozyme level. Chromosoma. 79: 341-348.

Romero zarco C. 1986. A new method for estimating karyotype asymmetry. Taxon. 35: 526-530.

Sato D. 1936. Analysis of Karyotypes of *Scilla permixta* and the allied species with special reference to the dislocation of the chromosome. Bot Mag. 596: 447-456.

Siljak-Yakovlev S. 1996. La dysploidie et l'evolution du caryotype. Bocconea. 5: 211-220.

Speta F. 1979. Karyological investigations in *Scilla* in regard to their importance for taxonomy. Webbia. 34:

419-431.
Stebbins GL. 1971. Chromosomal evaluation in higher plants. London: Edward Arnold.
Stedje B. 1989. Chromosome evolution within the *Ornithogalum tenuifolium* complex (Hyacinthaceae), with special emphasis on the evolution of bimodal karyotypes. Plant Syst Evol. 166: 79-89.
Stedje B. 1996. Karyotypes of some species of Hyacinthaceae from Ethiopia and Kenya. Nord J Bot. 16: 121-126.
Thompson JD. 2005. Plant evolution in the Mediterranean. First Edition. Oxford University Press, Oxford, OX2 6DP, United Kingdom.
Thompson JD. 2020. Plant volution in the Mediterranean insights for conservation. Second Edition. Oxford University Press, Oxford, OX2 6DP, United Kingdom.
Vaughan HE, Taylor S, Parker JS. 1997. The ten cytological races of the *Scilla autumnalis* species complex. Heredity. 79: 371-379.
Véla E, de Bélair G, Rosato M, Rosselló J. 2016. Taxonomic remarks on *Scilla anthericoides* Poir. (Asparagaceae. Scilloideae). a neglected species from Algeria. Phytotaxa. 288: 154-160.
Watanabe K, Yahara T, Denda T, Kosuge K. 1999. Chromosomal evolution in the genus *Brachyscome* (Asteraceae, Astereae): statistical tests regarding correlation between changes in karyotype and habit using phylogenetic information. J Plant Res. 112: 145-161.
Weiss-Schneeweiss H, Schneeweiss GM. 2013. Karyotype diversity and evolutionary trends in angiosperms in plant genome diversity. Springer-Verlag Wien. 209-223.

SUPPLEMENTARY TABLES

Table 4. Karyomorphological analysis of *Hyacinthoides lingulata.*

N	L (μm)	S (μm)	LT (μm)	AR	R value	RL%	F%	CI	CT
1	5.28±0.26	1.20±0.07	6.49±0.33	4.37±0.49	0.22±0.02	21.7±0.63	4.05±0.25	0.18±0.01	st
2	4.30±0.37	1.11±0.20	5.42±0.55	3.93±0.40	0.25±0.03	18.1±1.20	3.73±0.06	0.20±0.01	st
3	4.49±0.20	0.49±0.13	4.98±0.33	9.15±0.69	0.10±0.01	16.7±1.14	1.64±0.06	0.09±0.01	t
4	3.85±0.15	0.22±0.06	4.08±0.20	17.0±0.66	0.05±0.01	13.6±0.50	0.76±0.01	0.05±0.01	t
5	1.54±0.15	1.24±0.15	2.79±0.30	1.24±0.03	0.80±0.02	9.37±1.01	4.18±0.50	0.44±0.01	m
6	1.73±0.01	0.98±0.04	2.71±0.05	1.76±0.07	0.56±0.02	9.12±0.12	3.29±0.12	0.36±0.01	sm
7	1.49±0.16	0.26±0.11	1.75±0.26	5.57±0.30	3.74±0.17	5.89±0.19	0.88±0.38	0.15±0.07	st
8	1.03±0.09	0.50±0.01	1.54±0.11	2.07±0.10	0.48±0.02	5.19±0.38	1.71±0.06	0.33±0.01	sm

Length of chromosome (L: long arm. S: short arm. LT: total length). F%: Form percentage of chromosome. CI: Centromeric index. AR: Arm ratio. R-value: S/L. RL: Relative length. CT: Chromosome type.

Table 5. Karyomorphological analysis of *Prospero autumnale.*

N	L (μm)	S (μm)	LT (μm)	AR	R value	RL%	F%	CI	CT
1	2.03±0.19	0.63±0.04	2.66±0.22	3.18±0.23	0.31±0.02	17.95±0.13	4.25±0.26	0.23±0.01	st
2	1.97±0.03	0.38 ±0.08	2.35±0.12	5.55±0.27	0.18±0.01	15.82±0.13	2.52±0.13	0.16±0.01	st
3	1.36±0.05	0.94±0.08	2.31±0.13	1.41±0.06	0.70±0.03	15.55±0.40	6.38±0.01	0.41±0.01	m-sc
4	1.61±0.10	0.67±0.08	2.29±0.18	2.41±0.12	0.41±0.02	15.42±0.53	4.52±0.01	0.29±0.01	Sm
5	1.42±0.07	0.51±0.01	1.93±0.08	2.76±0.15	0.36±0.02	13.03±0.53	3.45±0.39	0.26±0.02	sm
6	1.20±0.05	0.57±0.05	1.77±0.11	2.14±0.12	0.46±0.02	11.96±0.79	3.85±0.39	0.32±0.01	sm
7	0.92±0. 15	0.59±0.03	1.52±0.1 8	1.53±0.20	0.65±0.08	10.23±0.13	3.98±0.26	0.39±0.03	m

Length of chromosome (L: long arm. S: short arm. LT: total length). F%: Form percentage of chromosome. CI: Centromeric index. AR: Arm ratio. R-value: S/L. RL: Relative length. CT: Chromosome type.

Table 6. Karyomorphological analysis of *Prospero obtusifolium.*

N	L (μm)	S (μm)	LT (μm)	AR	R value	RL%	F%	CI	CT
1	3.49±0.11	1.32±0.28	4.82± 0.17	2.67±0.69	0.37±0.10	29.0± 1.04	7.98±1.73	0.27±0.04	Sm-Sat
2	2.99±0.11	1.48±0.32	4.47± 0.44	2.05±0.38	0.48±0.09	26.9± 2.66	8.91±1.96	0.32±0.04	sm
3	3.22±0.04	0.90±0.17	4.13± 0.13	3.65±0.75	0.27±0.05	24.8± 0.81	5.43±1.04	0.21±0.03	st
4	2.47±0.13	0.69±0.03	3.17± 0.17	3.55±0.01	0.28±0.01	19.0± 1.04	4.16±0.23	0.21±0.01	st

Length of chromosome (L: long arm. S: short arm. LT: total length). F%: Form percentage of chromosome. CI: Centromeric index. AR: Arm ratio. R-value: S/L. RL: Relative length. CT: Chromosome type.

Table 7. Karyomorphological analysis of *Barnardia numidica.*

N	L (μm)	S (μm)	LT (μm)	AR	R value	RL%	F%	CI	CT
1	3.20±0.10	0.77±0.04	3.97±0.02	4.27±0.11	0.23±0.01	18.3±0.09	3.56±0.17	0.19±0.01	st
2	3.20±0.37	0.18±0.10	3.39±0.27	19.2±2.00	0.05±0.01	15.6±1.25	0.86±0.48	0.05±0.01	t
3	2.79±0.12	0.41±0.11	3.20±0.31	6.70±0.62	0.14±0.02	14.8±0.76	1.92±0.19	0.12±0.01	st
4	2.33±0.23	0.79±0.12	3.12±0.19	2.94±0.69	0.33±0.07	14.4±0.19	3.65±0.57	0.25±0.04	sm
5	0.97±0.10	0.83±0.04	1.81±0.11	1.15±0.13	0.86±0.10	8.37±0.10	3.84±0.19	0.46±0.02	m
6	1.14±0.06	0.58±0.16	1.72±0.10	1.92±0.72	0.51±0.17	7.98±0.48	2.69±0.76	0.33±0.07	sm
7	0.99±0.04	0.68±0.06	1.68±0.10	1.50±0.07	0.66±0.08	7.79±0.48	3.17±0.28	0.40±0.01	m
8	0.81±0.06	0.62±0.04	1.43±0.02	1.26±0.18	0.78±0.11	6.64±0.10	2.88±0.19	0.43±0.03	m
9	1.02±0.04	0.24±0.04	1.27±0.07	0.95±0.25	0.25±0.05	5.87±0.09	1.15±0.19	0.19±0.03	st

Length of chromosome (L: long arm. S: short arm. LT: total length). F%: Form percentage of chromosome. CI: Centromeric index. AR: Arm ratio. R-value: S/L. RL: Relative length. CT: Chromosome type.

Table 8. Karyomorphological analysis of *Oncostema elongata.*

N	L (μm)	S (μm)	LT (μm)	AR	R value	RL%	F%	CI	CT
1	4.11±0.12	1.20±0.10	5.38±0.20	3.29±0.38	0.30±0.03	19.0±0.21	4.49±0.35	0.23±0.02	st
2	3.91±0.60	0.88±0.02	4,79±0.62	4,40±0,68	0.22±0,03	16,9±2,13	3,13±0.60	0,18±0.02	st
3	3,64±0.06	1,02±0,02	4,67±0,08	3,60±0,01	0.27±0.02	16.5±0.28	3.63±0.07	0.21±0.02	st
4	3,97±0.06	0,62±0.02	4.59±0.04	6.50±0.30	0.15±0.07	16.2±0.14	2.20±0.07	0.13±0.02	st
5	1,95±0.02	1.14±0.10	3.10±0.08	1.71±0.16	0.58±0.05	10.9±0.28	4.06±0.35	0.36±0.02	sm
6	1.18±0.06	0.80±0.02	1.99±0.06	1.45±0.07	0.68±0.03	7.05±0.21	2.85±0.02	0.40±0.02	m
7	1.47±0.10	0.46±0.02	1.93±0.12	3.27±0.08	0.30±0.11	6.84±0.42	1.63±0.07	0.32±0.04	st
8	1.10±0.10	0.68±0.08	1.79±0.18	1.58±0.04	0.62±0.01	6.34±0.64	2.42±0.28	0.38±0.02	m

Length of chromosome (L: long arm. S: short arm. LT: total length). F%: Form percentage of chromosome. CI: Centromeric index. AR: Arm ratio. R-value: S/L. RL: Relative length. CT: Chromosome type.

Caryologia
International Journal of Cytology, Cytosystematics and Cytogenetics

Firenze University Press
www.fupress.com/caryologia

OPEN ACCESS

Citation: Hosseini, S., & Yaghoobi, H. (2023). Chromosome counts and karyotype features of different ecotypes of *Allium* L. species (Amaryllidaceae – Subg. *Melanocrommyum*) in Iran. *Caryologia* 76(3): 19-27. doi: 10.36253/caryologia-2203

Received: June 27, 2023

Accepted: October 29, 2023

Published: February 29, 2024

Data Availability Statement: All relevant data are within the paper and its Supporting Information files.

Competing Interests: The Author(s) declare(s) no conflict of interest.

Chromosome counts and karyotype features of different ecotypes of *Allium* L. species (Amaryllidaceae – Subg. *Melanocrommyum*) in Iran

Shahla Hosseini*, Hiva Yaghoobi

Department of Biological Science, University of Kurdistan, Sanandaj, Iran
*Corresponding author. E-mail: sh.hosseini@uok.ac.ir

Abstract. This study aimed to investigate the karyotypes of five *Allium* species, which belong to three sections of the subgenus *Melanocrommyum*. Bulbs from these species were collected from natural habitats in Iran, and their somatic chromosomes were analysed. The results revealed that all examined members of subg. *Melanocrommyum* had a basic chromosome number of x=8 and were diploid ($2n$=$2x$=16). Chromosomal data for *A. saralicum* and *A. shatakiense* are reported here for the first time. The karyotypes exhibited a variety of chromosome types and sizes, including variations observed among different accessions of the same species. In particular, *A. saralicum* showed satellite chromosomes ranging in size from 2.2 to 3.71 µm, located on the short arm. Seven accessions of *A. saralicum*, *A. stipitatum*, and *A. haemanthoides* demonstrated the presence of 1-3 B chromosomes with centromeres located in the median or subterminal position. Notably, the number of B chromosomes varied even among different accessions of the same species. Based on various indices, the karyotypes of the species were classified into symmetric and asymmetric groups. All karyotype asymmetry methods consistently identified *A. stipitatum* as the species with the most asymmetric chromosomes, while *A. ubipetrense* was recognized as the most symmetric species. This study contributes to the karyological knowledge of the genus *Allium* and provides valuable data for future taxonomic research. It emphasizes the significance of chromosomal characteristics in understanding plant evolution and species diversity within the *Allium* genus.

Keywords: *Allium*, B chromosome, ideogram, karyology, *Melanocrommyum*.

INTRODUCTION

Allium is a notable monocot genus comprising over 900 species, primarily concentrated in the eastern Mediterranean region, Southwest, and Central Asia. Within different plant communities, *Allium* species play a significant role (Fritsch and Abbasi, 2013). Iran exhibits diverse geographic and climatic conditions, allowing *Allium* species to thrive in a range of habitats. These plants typically inhabit open, sunny, and relatively dry

sites, adapting to both arid and moderately humid climates (Fritsch and Friesen, 2002). Subgenus *Melanocrommyum* of *Allium* encompasses Iranian species that occupy various ecological habitats, spanning from lowlands to highlands. Although they can be found in dry steppes, semi-deserts, and arid mountains, the majority of these species thrive in such environments (Fritsch and Abbasi, 2013). Currently, Iran is home to 148 recognized *Allium* species and subspecies, representing eight subgenera and 32 sections (Fritsch and Amini Rad, 2013). Subgenus *Melanocrommyum* is the second-largest subgenus within *Allium*, encompassing approximately 170 species worldwide, classified into 20 sections (Fritsch, 2012).

Chromosomes serve as the carriers of genetic information, and alterations in their number and structure play a crucial role in plant evolution (Escudero et al., 2014). Chromosomal characteristics, including number, size, and shape (karyotype), serve as defining features for numerous plant taxa across different taxonomic levels (Baltisberger and Hörandl, 2016). In the genus *Allium*, a basic chromosome number of x=8 is predominant, although a few sections exhibit x=7, 9, and 11 (Friesen et al., 2006). Subgenus *Melanocrommyum* typically possesses a basic chromosome number of x=8. However, a small number of species, such as *A. karataviense* Regel and *A. rnonophyllum* Vved. have been identified with basic chromosome numbers of x = 9 and x=10, respectively (Fritsch and Astanova, 1998). Satellite chromosomes have proven to be a valuable cytological marker in *Allium*, and different types of satellites have been studied based on the centromere position and secondary constrictions on chromosome arms (Dolatyari et al., 2018).

Several karyological investigations have been conducted on Iranian Allium species, revealing symmetrical karyotypes composed of metacentric and submetacentric chromosomes in the Melanocrommyum subgenus (Pedersen and Wendelbo, 1966; Pogosian, 1983; Fritsch and Astanova, 1998; Gurushidze et al., 2010, 2012; Hosseini and Go, 2010; Akhavan et al., 2015; Dolatyari et al., 2018; Hosseini, 2018). Approximately 55% of Iranian Allium species have been karyologically characterized, providing a valuable foundation for future taxonomic research (Dolatyari et al., 2018). Nonetheless, the karyological data for many species, including endemic ones in Iran, remains completely unknown. This study aims to contribute to the karyological investigation of selected Iranian Allium accessions, expanding our knowledge of the chromosomes within the genus Allium.

MATERIALS AND METHODS

In this study, bulbs of five species (seven ecotypes) were collected from their natural habitats in 2018 (Figure 1). The species include *A. ubipetrense* R.M. Fritsch, *A. haemanthoides* Boiss. & Reut. *A. stipitatum* Regel, *A. saralicum* R.M. Fritsch, and *A. shatakiense* Rech. f. Details about the collected materials can be found in Table 1. Among the species studied, *A. ubipetrense* was determined to be endemic to Iran, while the other species were indigenous and had distributions in various regions, including Iran, Iraq, Turkey, Tajikistan, Afghanistan, Kazakhstan, Kyrgyzstan, Pakistan, Turkmenistan, and Uzbekistan.

To break the dormancy of the bulbs, they were stored at 4 °C. Subsequently, the bulbs were rooted in wet, sterile cotton gauze in a refrigerator. For somatic chromosome analysis, fresh root tips measuring 1–1.2 cm were collected from the cultivated bulbs in the early morning. The roots underwent a pre-treatment with a-bromo naphthalene for 3 hours at 4 °C, followed by three washes with distilled water (each lasting 5 minutes) at room temperature. The roots were then fixed overnight at 4 °C in Carnoy's fixative, which consists of glacial acetic acid and ethanol in a 3:1 ratio. After thor-

Table 1. Characterization and sampling location of the studied taxa.

Section	Species	Species code	Locality	Voucher specimen	Origin
sect. *Acanthoprason*	*A. ubipetrense*	S1	Kurdistan, Marivan road, kalatarzan, jannat boo village	UOK-130	Native- endemic
	A. haemanthoides	S5	Kurdistan, Saral Area, Zardavan	UOK-131	Native-non endemic
sect. *Melanocrommyum*	*A. saralicum*	S2-E1	Kurdistan, Saral Area, hezarkanian Village	UOK-113	Native-non endemic
	A. saralicum	S2-E2	Kurdistan, Saral Area, Chatan Village	UOK-114	Native-non endemic
	A. shatakiense	S3	Kurdistan, Saral Area, zardavan	UOK-126	Native-non endemic
sect. *Procerallium*	*A. stipitatum*	S4-E1	Kurdistan, Saral Area, Kapak Village	UOK-101	Native-non endemic
	A. stipitatum	S4-E2	Kurdistan, Saral Area, zardavan	UOK- 102	Native-non endemic

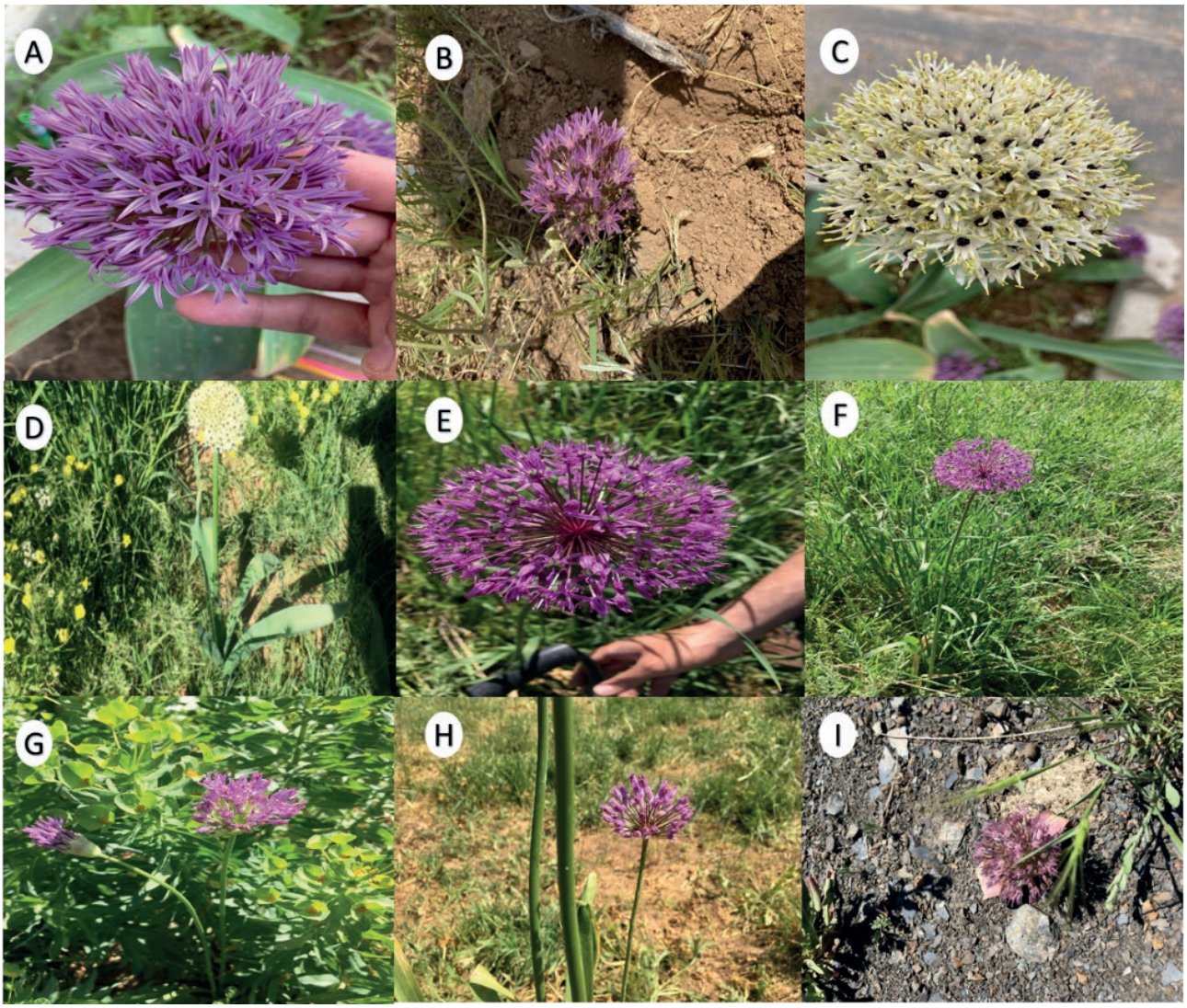

Figure 1. Studied species in their habitat in saral region in Kurdistan. A, B: *A. ubipetrense*; C, D: *A. saralicum*; E, F: *A. stipitatum*; G, H: *A. shatakiense*; I; *A. haemanthoides*.

ough washing with distilled water, the excised roots were transferred to 70% (v/v) aqueous ethanol and stored in a refrigerator until further use.

Hydrolysis was carried out by treating the root tips with 1 M HCl for 15 minutes at 60 °C. Subsequently, the root tips were stained with feulgen solution for 1 hour and then squashed in a drop of 45% (v/v) acetic acid. The best metaphase plates were photographed using a DP72 digital camera attached to the BX51 Olympus microscope. At least five metaphase plates were analyzed for each accession, and the short (S) and long arms (L) of the chromosomes were measured using IdeoKar software (http://agri.uok.ac.ir/ideokar/index.html) (Mirzaghaderi and Marzangi 2015). The morphology of the chromosomes was determined based on the nomenclature proposed by Levan et al. (1964). Karyotype formulas were established using centromere indices (CI) and arm ratio (AR).

In addition to the basic karyological data such as $2n$ (chromosome number), x (basic chromosome number), and the total chromosome length of the haploid (HCL), several chromosomal parameters were analyzed. These parameters include the long arm (L), short arm (S), chromosome length (CL), arm ratio (AR), r value, relative length of chromosome (RL), chromosome form percentage (F %), and centromeric index (CI %). Furthermore, 12 karyotype parameters were calculated to quantify the asymmetry of the karyotypes. These parameters

include the mean centromeric asymmetry (MCA), coefficient of variation of chromosome length (CVCL), coefficient of variation of centromeric index (CVCI), total form percentage (TF %), mean centromeric index (XCI), asymmetry index (AI), degree of karyotype asymmetry (A), percentage of karyotype symmetry (S%), intra chromosomal asymmetry index (A1 and A2), and percentage karyotype asymmetry index (AsK %). It's worth noting that B chromosomes were not considered in the computation of these parameters due to their effects on calculating asymmetry factors.

RESULTS

The analysis focused on metaphase plates of five species belonging to the *Melanocrommyum* subgenus of the genus *Allium*. These species are diploid, and their basic chromosome number is x=8. The chromosomal data for *A. saralicum* and A. *shatakiense* are presented for the first time in this study. Among the three species analyzed (*A. saralicum*, *A. stipitatum*, *A. haemanthoides*), seven accessions showed the presence of 1–3 B chromosomes with centromeres located in the median or subterminal position (Figure 2). Notably, the number of B chromosomes varied even among different accessions of the same species. Karyotypes of somatic complement and the ideograms of the haploid complement of studied Alliums are demonstrated in Figures 3.

There were significant differences in size between the longest and shortest chromosomes in each complement. *Allium haemanthoides* had the longest chromosome (14.2 µm), while *A. stipitatum* had the shortest chromosome (5.42 µm). The mean total chromosome length (TL) ranged from 9.27 µm (*A. stipitatum*) to 11.37 µm (*A. haemanthoides*), with an overall mean value of 10.15 µm. The centromeric index (CI) of the complements varied from 37% (*A. stipitatum*) to 41% (*A. ubipetrense*). Based on the nomenclature proposed by Levan et al. (1964), two chromosome types, 'm' (centromere at the median region) and 'sm' (centromere at the submedian region), formed six different karyotype formulas (Table 2). Additionally, there were pairs of satellites with sizes ranging from 2.2 to 3.71 µm in *A. saralicum* (S2-E1 and S2-E2) located on the short arm.

The karyotypes of all five species were classified into the 1A, 1B, and 2B classes of Stebbins classification (Stebbins 1971). Various methods were used to assess karyotype asymmetry, and most methods identified different species as symmetric or asymmetric. For example, *A. ubipetrense* had the highest value of total form percentage (TF %) at 41.56 (indicating the most symmetric species), while *A. stipitatum* had the lowest value at 37.52 (the most asymmetric species). The coefficient of variation (CV %) showed the highest value in *A. stipitatum* (26.88%, the most asymmetric) and the lowest value in *A. ubipetrense* (11.77%, the most symmetric). The highest XCA value (mean centromeric asymmetry) was observed in *A. stipitatum* (24.11%), while the lowest value was found in *A. shatakiense* (17.95%). The mean coefficient of variation of centromeric index (CVCI) was determined as 13.56 µm, ranging from 7.7 µm (*A. ubipetrense*) to 14.32 µm (*A. stipitatum*). *Allium stipitatum* had the highest value of asymmetry index (A) at 0.24, while *A. ubipetrense* and *A. shatakiense* showed the lowest value at 0.17. The highest and lowest values of percentage of karyotype symmetry (S %) were observed in *A. ubipetrense* (68.83) and *A. stipitatum* (43.20), respectively. *Allium stipitatum* had the highest value of percentage karyotype asymmetry index (AsK %) at 62.24 but *A. ubipetrense* showed the lowest value (54.90) (Table 2). According to the data presented in Table 2, all the karyotype asymmetry methods consistently identified *A. stipitatum* as the species with the most asymmetric chromosomes, while *A. ubipetrense* was recognized as the most symmetric species. These findings highlight the distinct karyotype characteristics and asymmetry levels among the studied Allium species.

DISCUSSION

The karyotypic characteristics of several *Allium* species, including *A. saralicum*, *A. shatakiense*, *A. stipitatum*, *A. ubipetrense* and *A. haemanthoides* are discussed in this study. All studied taxa were found to be diploid with a chromosome number of $2n$=$2x$=16. *Allium stipitatum*, on the other hand, exhibited the same diploid chromosome number of $2n$=$2x$=16, which is consistent with previous studies (Fritsch and Astanova, 1998; Ohri and Pistrick, 2001; Oroji Salmasi et al., 2019). However, reports also exist of *A. stipitatum* having a basic chromosome number of $2n$=16 and $2n$=48 (Pogosian 1983).

In *A. saralicum*, a pair of satellite chromosomes was observed, located on the short arm of the chromosomes. The present study identified two chromosome types, 'm', 'sm', and 'st', in five different *Allium* species. The karyotypic analysis, combined with previously published data on the *Melanocrommyum* subgenus, indicated a common symmetric karyotype with 2-8 metacentric and 0-4 submetacentric chromosomes, as well as 0-4 subtelocentric chromosome pairs.

Chromosomes in the *Acanthoprason* section (*A. ubipetrense* and *A. haemanthoides*) displayed a median or

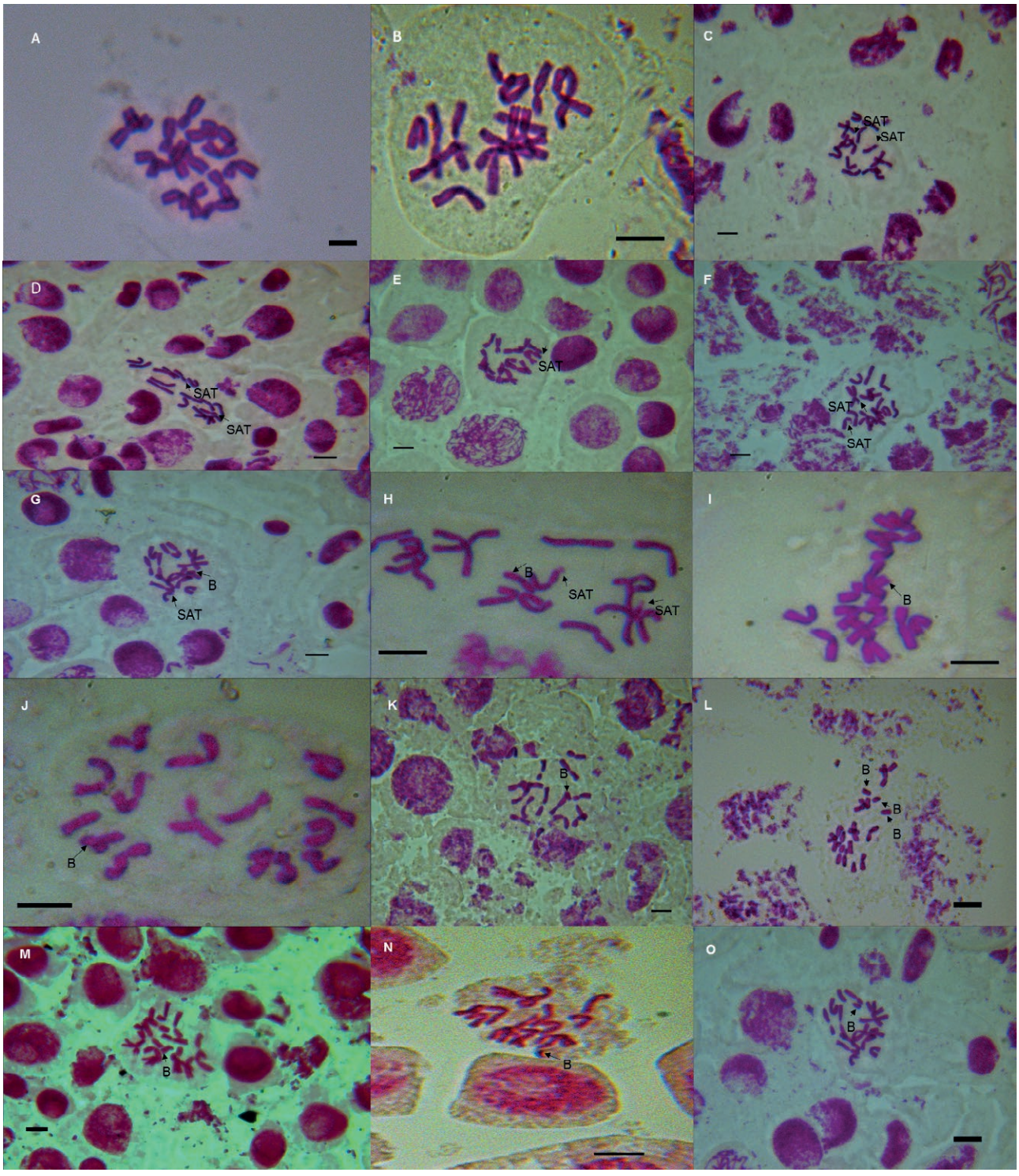

Figure 2. Mitotic metaphase plates of the investigated accessions of selected *Allium*, subg. *Melanocrommyum*: A, B: *A. ubipetrense*; C-F: *A. saralicum* (E1); G, H; *A. saralicum* (E2); I-K; *A. stipitatum* (E1); L; *A. stipitatum* (E2); M; *A. haemanthoides*; N,O; *A. shatakiense*. Scale bars = 10µm.

submedian centromere position and a gradual decline in arm lengths. *Allium ubipetrense* had chromosomes with centromeres only in the median position, while *A. haemanthoides* exhibited submedian centromeres and one B

Figure 3. Idiograms and karyotypes of the investigated accessions of selected *Allium* subg. *Melanocrommyum*. A: *A. ubipetrense*; B; *A. saralicum*; C: *A. shatakiense*; D: *A. stipitatum*; E: *A. haemanthoides*. Scale bars = 10µm.

chromosome in addition to metacentric ones. The coefficient of variation for centromere index (CVCI) in *A. stipitatum* was more than twice (14.32) that of *A. ubipetrense* (6.35). The coefficient of variation for centromere length (CVCL) index confirmed *A. ubipetrense* as having the most symmetric chromosomes. A study by Dolatyari et al. (2018) on *A. haemanthoides* did not detect any B chromosomes but identified two satellite (SAT) chromosomes with centromeres positioned between the median and sub median positions.

Allium ubipetrense is primarily found in the northwestern parts of the Zagros mountain range in Iran. This species exhibits different morphotypes, which sometimes leads to misidentifications. *Allium haeman-*

Table 2. Mean chromosomal and karyotypic parameters of *Allium* spp. S1: *A. ubipetrense* S2: *A. saralicum*, S3: *A. shatakiense*, S4: *A. stipitatum*, S5: *A. haemanthoides.*

	Species						Range	
Parameters	S1	S2	S3	S4	S5	Mean	Min	Max
S (µm)	4.09	4.30	3.89	3.47	4.52	4.05	3.47-4.52	S4	S5
L (µm)	5.79	6.55	5.50	5.79	6.84	6.09	5.50-6.84	S3	S5
TL (µm)	9.89	10.86	9.40	9.27	11.37	10.15	9.27-11.37	S4	S5
AR	1.44	1.63	1.45	1.69	1.54	1.55	1.44-1.69	S1	S4
r value	0.69	0.64	0.70	0.60	0.66	0.65	0.60-0.70	S4	S3
HCL	79.21	89.03	75.27	75.74	93.61	82.57	75.27-93.61	S3	S5
RL%	12.49	12.24	12.49	12.25	12.14	12.32	12.14-12.49	S5	S1,S3
F %	5.15	4.86	5.13	4.60	4.83	4.91	4.60-5.15	S4	S1
CI	0.41	0.38	0.40	0.37	0.39	0.39	0.37-0.41	S4	S1
TF %	41.56	39.65	41.20	37.52	40.00	39.98	37.52-41.56	S4	S1
CVCL	11.77	19.89	20.72	26.88	18.90	19.63	11.77-26.88	S1	S4
A1	0.30	0.33	0.28	0.37	0.32	0.32	0.28-0.37	S3	S4
A2	0.11	0.19	0.20	0.26	0.18	0.18	0.11-0.26	S1	S4
AI	185.24	155.31	170.48	214.10	174.87	180	155.31-214.10	S2	S4
AsK %	54.90	60.34	58.43	62.24	58.79	58.94	54.90-62.24	S1	S4
S%	68.83	52.49	51.91	43.20	54.90	54.26	43.20-68.83	S4	S1
A	0.17	0.21	0.17	0.24	0.19	0.19	0.17-0.24	S1,S3	S4
XcA	17.95	21.72	17.53	24.11	19.74	20.21	17.53-24.11	S3	S4
XcI	0.17	0.39	0.41	0.37	0.40	0.34	0.17-0.41	S1	S3
CVCI	6.35	12.47	12.09	14.32	11.45	13.56	6.35-14.32	S1	S4

	Species						
	S1	S2-E1	S2-E2	S3	S4-E1	S4-E2	S5
ST[a]	1A	1A	1A	1A	2B	2B	1B
KF[b]	16m	10m+6sm	10m+6sm+ 1smB	12m+4sm+1smB	8m+8sm+1stB	12m+4sm+3stB	10m+6sm+1smB

[a] ST Stebbin's (1971) classification; [b] KF Karyotype formula.

thoides, classified under sect. *Acanthoprason*, shares one subgroup with *A. ubipetrense* and *A. kurdistanicum* from the Kurdistan province, based on molecular markers (ITS sequences of nuclear rDNA) (Fritsch and Abbasi 2013). Chromosomal parameters suggest a high probability of differentiation between the two species, *A. haemanthoides* and *A. ubipetrense*, into different subgroups.

Regarding the *Melanocrommyum* section, *A. saralicum* and *A. shatakiense* demonstrated closely similar values for all parameters and indices. The karyotypes of both species consisted of metacentric and sub metacentric chromosomes, with one B chromosome and centromeres in the median position. This study reports the symmetric karyotype of section *Melanocrommyum* for the first time in *A. saralicum* and *A. shatakiense*. Previous studies have also shown this symmetric karyotype in the *Melanocrommyum* section (Fritsch & Astanova 1998; Hosseini and Go, 2010; Akhavan & al. 2015; Dolatyari et al., 2018; Hosseini, 2018).

Allium stipitatum, the only species analyzed karyologically in section *Procerallium*, was also diploid with $2n$=16. However, its karyotype differed from the other species in subg. *Melanocrommyum*, as it included 1-3 subtelocentric B chromosomes. Among the studied taxa, *Allium stipitatum* exhibited the highest values for all asymmetric indices, such as CVCL (26.88), CVCI (14.32), ASK% (62.24), and the lowest values for TF% (37.52), rvalue (0.6), F% (4.6), and CI (0.37).

Nevertheless, when it comes to distinguishing closely related taxa at the section level, the uniformity of karyotypes and comparable chromosome counts do not hold significant value. This research focused on a five species across three different sections, and it would be inaccurate to apply these findings universally to the entire *Allium* genus. To achieve a clearer understanding

of sectional boundaries, it would be beneficial to conduct future studies that involve a larger variety of species from diverse sections, while also examining chromosomal karyotypes in greater detail.

CONCLUSION

In conclusion, the karyological investigation of five *Allium* species belonging to the *Melanocrommyum* subgenus provides valuable insights into the chromosomal characteristics and karyotype diversity within this genus. The species studied, *A. ubipetrense*, *A. haemanthoides*, *A. stipitatum*, *A. saralicum*, and *A. shatakiense*, exhibited diploid chromosome numbers and a basic chromosome number of x=8. However, some variations were observed, such as the presence of 1-3 B chromosomes in certain accessions. The karyotypes of these species displayed a combination of metacentric, submetacentric, and subtelocentric chromosomes, with centromeres positioned at the median or submedian regions. Additionally, satellite chromosomes were observed in *A. saralicum*. The karyotype asymmetry analysis revealed variations among the species, with *A. stipitatum* exhibiting the most asymmetric chromosomes and *A. ubipetrense* displaying the most symmetric chromosomes.

These findings contribute to the understanding of the genetic diversity and evolutionary patterns within the *Allium* genus, particularly the *Melanocrommyum* subgenus. The data obtained from this study adds to the existing knowledge of *Allium* species in Iran and serves as a foundation for future taxonomic and evolutionary research. Further investigations of karyological characteristics and chromosomal variations in other Iranian *Allium* species would provide a more comprehensive understanding of their genetic makeup and phylogenetic relationships.

ACKNOWLEDGMENTS

This research was funded by the University of Kurdistan (UOK), Iran, as a research grant (11.99.5722).

REFERENCES

Akhavan, A., Saeidi, H., Zarre, S., & Rahiminejad, M. (2015). Chromosome Numbers and Karyotype Features of Selected Species of *Allium* L. (Amaryllidaceae) Sect. Acanthoprason in Iran. *Iranian Jornal of Botany, 21*(2), 158-164.

Baltisberger, M., & Hörandl, E. (2016). Karyotype evolution supports the molecular phylogeny in the genus Ranunculus (Ranunculaceae). *Perspectives in Plant Ecology, Evolution and Systematics, 18*, 1-14.

Dolatyari, A., Saeidi Mehrvarz, S., Shahzadeh Fazeli, S. A., Naghavi, M. R., & Fritsch, R. M. (2018). Karyological studies of Iranian Allium L. (Amaryllidaceae) species with focus on sect. Acanthoprason. 1. Mitotic chromosomes. *Plant Systematics and Evolution, 304*, 583-606.

Escudero, M., Martín-Bravo, S., Mayrose, I., Fernández-Mazuecos, M., Fiz-Palacios, O., Hipp, A. L., et al. (2014). Karyotypic changes through dysploidy persist longer over evolutionary time than polyploid changes. *PLoS One, 9*(1), e85266.

Friesen, N., Fritsch, R. M., & Blattner, F. R. (2006). Phylogeny and new intrageneric classification of Allium (Alliaceae) based on nuclear ribosomal DNA ITS sequences. *Aliso: A Journal of Systematic and Evolutionary Botany, 22*(1), 372-395.

Fritsch, R., & Abbasi, M. (2013). A taxonomic review of Allium subg. *Melanocrommyum in Iran. Gatersleben: IPK*.

Fritsch, R., & Amini Rad, M. (2013). Allium pseudostrictum (Amaryllidaceae), a new record from Iran. *Rostaniha, 14*(1), 81-84.

Fritsch, R., & Astanova, S. (1998). Uniform karyotypes in different sections of Allium L. subgen. Melanocrommyum (WEBB & BERTH.) ROUY from Central Asia. *Feddes repertorium, 109*, 539-549.

Fritsch, R., & Friesen, N. (2002). Evolution, domestication and taxonomy *Allium crop science: recent advances* (pp. 5-30): CABI publishing Wallingford UK.

Fritsch, R. M. (2012). Illustrated key to the sections and subsections and brief general circumscription of Allium subg. Melanocrommyum. *Phyton (Horn), 52*(1), 1-37.

Gurushidze, M., Fritsch, R. M., & Blattner, F. R. (2010). Species-level phylogeny of Allium subgenus Melanocrommyum: Incomplete lineage sorting, hybridization and trnF gene duplication. *Taxon, 59*(3), 829-840 https://doi.org/810.1002/tax.593012.

Gurushidze, M., Fuchs, J., & Blattner, F. R. (2012). The evolution of genome size variation in drumstick onions (Allium subgenus Melanocrommyum). *Systematic Botany, 37*(1), 96-104.

Hosseini, S. (2018). Karyological studies of some Allium L. (Amaryllidaceae) species in Iran. *The Iranian Journal of Botany, 24*(1), 65-71.

Hosseini, S., & Go, R. (2010). Cytogenetic study of some Allium species (Subgenus allium and Melanocrommyum) in Iran. *Cytologia, 75*(1), 99-108.

Levan, A., Fredga, K., & Sandberg, A. A. (1964). Nomenclature for centromeric position on chromosomes. *Hereditas (Lund), 52*(201-220).

Mirzaghaderi G, Marzangi K. 2015. IdeoKar: an ideogram constructing and karyotype analyzing software. Caryologia. 68(1):31-35.

Ohri, D., & Pistrick, K. (2001). Phenology and Genome Size Variation in Allium L. - a Tight Correlation? *Plant Biology, 3*(6), 654-660.

Oroji Salmasi, K., Javadi, H., & Miri, S. M. (2019). Karyotype analysis of some Allium species in Iran. *Journal of Plant Physiology and Breeding, 9*(2), 115-127.

Pedersen, K., & Wendelbo, P. (1966). *Chromosome numbers of some SW Asian Allium species*.

Pogosian, A. (1983). Chromosome numbers of some species of the genus Allium (Alliaceae) distributed in Armenia and Iran. *Bot. Z., 68*, 652-660.

Stebbins, G. L. (1971). *Chromosomal evolution in higher plants*: Edward Arnold Publisher, London.

Caryologia
International Journal of Cytology, Cytosystematics and Cytogenetics

Firenze University Press
www.fupress.com/caryologia

OPEN ACCESS

Citation: Sofi, I.I., Verma, S., Ganie, A.H., Sharma, N., & Shah, M.A. (2023). Meiotic behavior and its implications on the reproductive success of *Arnebia euchroma* (Royle ex Benth.) I.M.Johnst. (Boraginaceae), an important medicinal plant of Trans-Himalaya. *Caryologia* 76(3): 29-37. doi: 10.36253/caryologia-2154

Received: July 4, 2023

Accepted: November 13, 2023

Published: February 29, 2024

Data Availability Statement: All relevant data are within the paper and its Supporting Information files.

Competing Interests: The Author(s) declare(s) no conflict of interest.

Meiotic behavior and its implications on the reproductive success of *Arnebia euchroma* (Royle ex Benth.) I.M.Johnst. (Boraginaceae), an important medicinal plant of Trans-Himalaya

Irfan Iqbal Sofi[1,*], Shivali Verma[2], Aijaz H. Ganie[1], Namrata Sharma[2], Manzoor A. Shah[1]

[1] *University of Kashmir, Srinagar-19006, Jammu and Kashmir, India*
[2] *University of Jammu, Jammu Tawi-18006, Jammu and Kashmir, India*
*Corresponding author. E-mail: sofi.irfan98@gmail.com

Abstract. The present study reports the chromosome number, meiotic behavior and its relation with pollen fertility and seed set of *Arnebia euchroma* (Royle ex Benth.) I.M.Johnst. The species shows a chromosome count of $2n = 2x = 14$. The meiotic abnormalities such as chromatin stickiness, cytomixis, laggard formation, chromosomal bridges, were also observed in the Pollen Mother Cells (PMCs) of the target plant species. The linear model of regression showed a significant reduction of seed set with increasing meiotic abnormality and correlation analysis highlighted positive relationship between pollen viability and seed set. Meiotic abnormalities within the species hinder its reproductive process, causing a decline in reproductive efficiency. This study highlights the importance of addressing these intrinsic factors in future conservation programs to prevent a decline in the species population in nature.

Keywords: chromosome number, meiotic abnormalities, pollen viability, seed set.

INTRODUCTION

Reproduction is an essential and vital stage in the life history of plants and a necessary natural process for survival, multiplication and evolution (Wani et al. 2022). The meiotic abnormalities are one of the factors that affect the reproductive success of plant species (Wani et al. 2022). The decline in seed set and loss of genetic variability, are some of the repercussions of the meiotic depression (Cohen et al. 2021). The studies on reproduction, meiotic behaviour and seed biology may aid in identifying the key factors that affect the reproductive success of species as well as sustenance or survival of its population (Gan et al. 2013). The study is also critical for developing strategies for sustainable utilisation and effective conservation measures of threatened species (Rashid et al. 2022a).

The restricted distribution pattern of *Arnebia euchroma* (Royle ex Benth.) I.M.Johnst., in Himalaya is further declining and this species is at risk of disappearing because of habitat deterioration, fragmentation and climate change (Lal et al. 2020; Sofi et al. 2022a). Therefore, understanding of the meiotic behavior may improve the knowledge about reproduction and inherent bottlenecks of the species. The foundation of conservation biology, reintroduction, and mass production and multiplication rely on quality of germplasm. Understanding the biological characteristics of the species will unveil the attributes of the germplasm (Ma et al. 2022).

Therefore, the present study was conducted to study the meiotic behaviour and its impact on pollen fertility and seed set. Understanding the aspects of meiotic behaviour, pollen fertility and seed production may provide vital clues for sustainable development of this important medicinal plant species of the Trans-Himalaya.

MATERIAL AND METHODS

Study area

The study was conducted in the four studied sites (Table 1) of the trans-Himalayan range of Ladakh, India. The area is dominated by mountains and harsh climatic conditions, however, regarded as cold biodiversity hotspot because of presence of rich species diversity (Sofi et al. 2022b).

Analysis of pollen mother cell (PMC) meiosis

During the present investigation, floral buds of *A. euchroma* from four different natural populations were fixed for meiotic studies. Young, unopened flower buds of suitable sizes were randomly collected from various plants within each studied population. The collected buds were preserved for 24 hours in Carnoy's fixative, which is a mixture of ethanol, chloroform, and glacial acetic acid (6: 3: 1 v/v). The materials were then transferred to 70% ethanol and kept at 4°C under refrigeration until use. Anthers were squashed in 1% propiocarmine and slides were observed under microscope. Pollen mother Cells (PMCs) were observed to count the chromosome number and meiotic abnormalities if any. Photomicrographs of chromosomes were taken from freshly prepared slides using an EVOS XL microscope. Chiasmata number was counted for cells at diplotene.

Pollen fertility estimation

Pollen fertility was estimated by collecting 10-15 fresh floral buds with dehiscing anthers followed by squashing in 2% acetocarmine and glycerol (Marks 1954). Well-filled pollen grains with uniformly stained

Table 1. Proportion of Meiotic abnormalities in PMCs of *Arnebia euchroma*.

Population /Site	Meiotic stage	No. of PMCs	Normal PMCs	PMCs with stickiness/ clumping	PMCs with laggards	PMCs with chromatin bridges	PMCs with cytoplasmic channels	PMCs with satellite chromosomes
Matayen	Diplotene	52	52	-	-	-	-	-
	Diakinesis	47	47	-	-	-	-	-
	Metaphase-I	93	56	7	9	7	14	-
	Anaphase-I	20	-	11	6	3	-	-
Karpokhar	Diplotene	24	24	-	-	-	-	-
	Diakinesis	17	13	-	-	-	-	-
	Metaphase-I	54	20	6	-	-	11	4
	Anaphase-I	13	-	3	-	10	-	-
	Telophase-I	6	-	-	-	-	-	-
Changoyal	Diplotene	34	34	-	-	-	-	-
	Metaphase-I	42	16	9	6	-	-	-
	Anaphase-I	16	-	16	-	-	-	-
Rungdum	Diplotene	19	19	-	-	-	-	-
	Metaphase-I	29	21	8	-	-	-	-
	Anaphase-I	21	-	20	-	1(6:3)	-	-
	Telophase-I	7	7	-	-	-	-	-
	Telophase-II	5	5	-	-	-	-	-

cytoplasm were considered fertile while shrivelled and unstained pollen grains were counted as sterile. Percentage pollen fertility/viability was calculated as follows:

$$\text{Pollen viability} = \frac{\text{Number of fertile pollen grains}}{\text{Total number of pollen grains observed}} \times 100$$

Seed set calculation

Individual plants were randomly chosen, labelled, and tallied according to the Lubbers and Christensen (1986) technique for the quantity of seeds produced per plant in order to estimate the seed set.

$$\text{Seed set} = \frac{\text{Total number of seeds produced per flower}}{\text{Total number of ovules borne per flower}} \times 100$$

Statistical analysis

Statistical analysis including linear model regression and correlation analysis was used to depict relationship between different parameters; the analysis was carried using the software r.

RESULTS

All the four populations of *A. euchroma* matched in having 14 chromosomes in their PMCs revealing $2n = 14$ (diploid chromosome count) and $x=7$ (haploid chromosome count), i.e., $2n = 2x = 14$. The PMCs were analysed at diplotene, diakinesis, metaphase-I, anaphase-I and telophase I.

In Matayen population, a total of 212 cells were scanned with 52 cells (24.52%) at diplotene (Fig. 1 A), 47 cells (22.16%) at diakinesis (Fig. 1 B), 93 cells (43.86%) at metaphase and 20 cells (9.43%) at anaphase I (Table 1). At diakinesis, we found perfect 7IIs and 6 cells had 2IVs+4IIs (Fig. 1 B). At metaphase-I, studied PMCs with6 IIs (Figs. 1 C, D) perfect 7IIs (Figs. 1 E, F), clumping (Fig. 1 G), laggards, chromatin bridges and cytoplas-

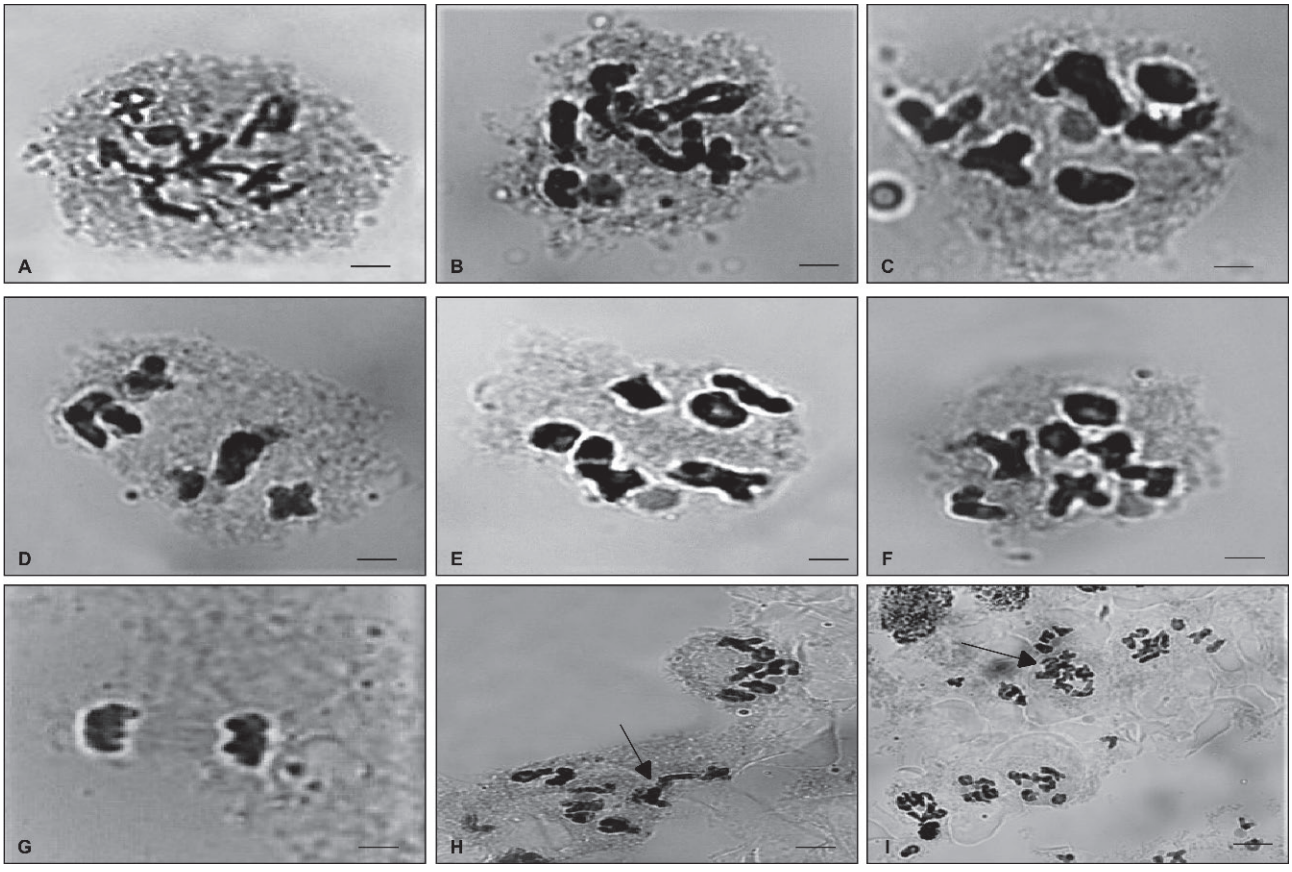

Figure 1. (A) A PMC at diplotene, (B) A PMC at diakinesis, (C & D) A PMC at metaphase with 6 IIs, (E & F) A PMC at metaphase with 7 IIs, (G) A PMC at anaphase showing clumping of chromosomes, (H, & I) PMCs at metaphase showing migration of chromatin material. Scale bars =10 μm.

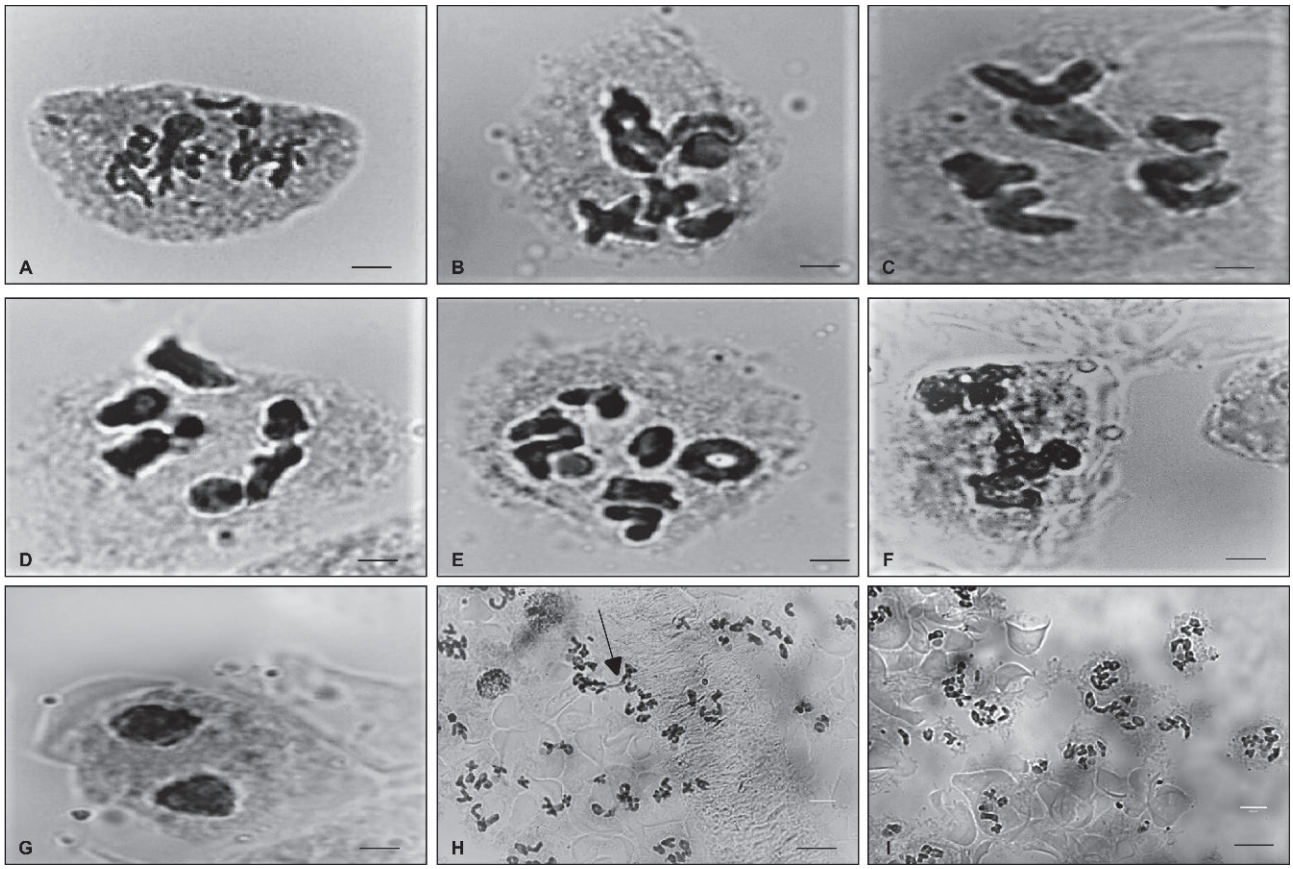

Figure 2. (A) A PMC at diplotene, (B) A PMC at diakinesis, (C) A PMC at metaphase with 5 IIs, (D) A PMC at metaphase with 6 IIs and 1 satellite, (E) A PMC at metaphase with 7 IIs, (F) A PMC at anaphase with chromatin bridge formation, (G) A PMC at telophase, (H & I) PMCs showing migration of chromosomes through cytoplasmic channels. Scale bars =10 μm.

mic channels (Figs. 1 H, I) were observed. At anaphase-I no PMC with normal segregation was observed out of 20 cells scanned (Table 1). Chiasmata frequency per PMC calculated at diplotene in this population is 10.9 while RI calculated is 17.9.

In Karpokhar population, a total of 114 cells were scanned at different stages of meiosis with 24 cells (21.05%) at diplotene (Fig. 2 A), 17 cells (14.91%) at diakinesis, 54 cells (47.36%) at metaphase, 13 cells (11.40%) at anaphase I and 6 cells at telophase-I (5.26%) (Table 1). At diakinesis stage perfect 7IIs and 4 cells with 1IV+5IIs (Fig. 2 B) were found. At metaphase-I, 5IIs (Fig. 2 C), 6IIs (Fig. 2 D), cells with perfect 7IIs (Fig. 2 E), clumping, satellite chromosomes (Fig. 2 D) and cytoplasmic channels (Figs. 2 H, I) were observed. At anaphase-I no PMC with normal segregation was observed, PMC's with chromatin bridges (Fig. 2 F) and clumping (Fig. 2 F) were recorded (Table 1). Chiasmata frequency per PMC calculated at diplotene in this population is 11.3 while RI calculated is 18.3.

In Changoyal, a total of 92 cells were scanned at different stages of meiosis with 34 cells (36.95%) at diplotene (Fig. 3 A), 42 cells (45.65%) at metaphase and 16 cells (17.39%) at anaphase I (Table 1). At metaphase-I, perfect 7IIs (Fig. 3 B), 5IIs (Fig. 3 C), 14 cells with Is (Fig. 3 D), clumping (Fig. 3 E) and laggards (Fig. 3 F) were observed. At anaphase-I no PMC with normal segregation was observed out of 16 cells scanned, all the cells with huge clumping (Fig. 3 G) were recorded. Chiasmata frequency per PMC calculated at diplotene in this population is 12.4 while RI calculated is 19.4.

Similarly, in Rungdum population, a total of 81 cells were scanned at different stages of meiosis with 19 cells (23.45%) at diplotene (Fig. 4 A), 29 cells (35.80%) at metaphase, 21 cells (25.92%) at anaphase I, 7 cells (8.64%) at telophase-I and 5 cells (6.17%) at telophase-II (Table 1). At metaphase-I, perfect 7IIs (Figs. 5 B-E) and clumping (Figs. 4 F, G) containing 7IIs were observed. At anaphase-I a PMC with abnormal segregation of 6:3 (Fig. 4 G) with a chromatin bridge was observed. However,

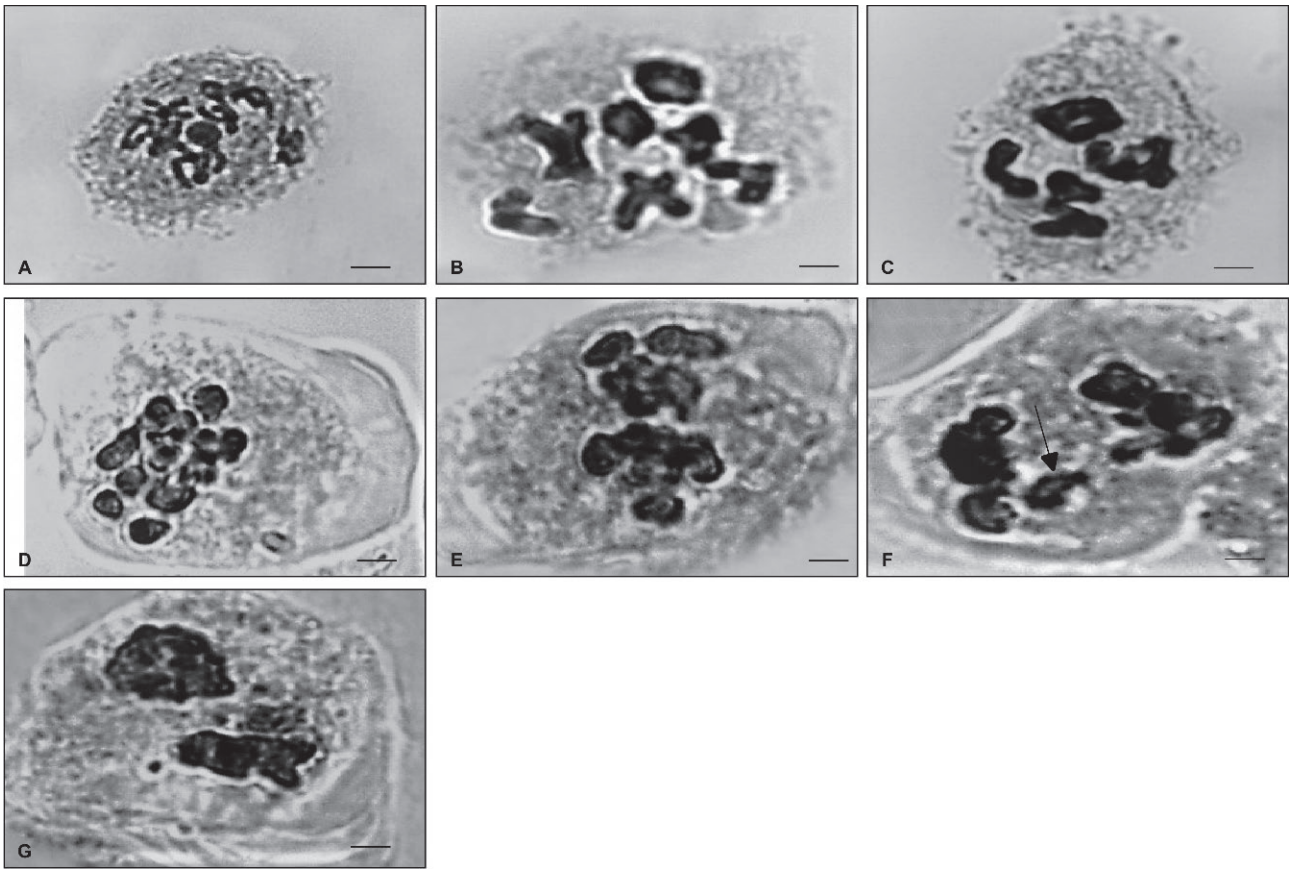

Figure 3. (A) A PMC at diplotene, (B) A PMC at metaphase with 7 IIs, (C) A PMC at metaphase with 5 II s, (D) A PMC at metaphase with 14 Is, (E) A PMC at metaphase showing clumping of chromosomes, (F) A PMC at metaphase showing laggards, (G) A PMC at anaphase. Scale bars =10 µm.

in rest of cells clumping were observed. Chiasmata frequency per PMC calculated at diplotene in this population is 12 while RI calculated is 19.

The average proportion of meiotic irregularity, pollen fertility, and seed set observed in the four studied populations of the *Arnebia euchroma* is shown in Table 2. It was evident from results that the percentage of pollen fertility and seed set declined with increase in percentage of meiotic anomalies in the four populations under study.

The linear regression between seed set (%) and meiotic abnormality (%) revealed a significant ($p<0.001$) decline of seed set with the increase in meiotic abnormality in the studied sites of target plant species (Fig. 5). The correlation analysis also depicted negative relationship between meiotic abnormality and pollen viability ($r = -0.96$), meiotic abnormality and seed set ($r = -0.99$) and positive correlation between pollen viability and seed set ($r = 0.98$), (Fig. 6).

DISCUSSION

The present study has documented chromosome number and meiotic behaviour of *Arnebia euchroma* from the four natural populations. The study confirms chromosome number $2n = 2x = 14$ in accordance with previous studies (Sharma et al. 2013). The presence of chromosomal stickiness, cytomixis, laggard formation and other chromosomal abnormalities have been observed in all the studied populations. The most prevalent chromosome abnormality observed was chromosomal stickiness and chromosomal clumping in all studied sites. During the current study, cytomixis which involves the transfer of chromatin material primarily between proximal PMCs (Guan et al. 2012) was also observed. As a result of the chromatin material being transferred between PMCs, the irregularities associated with this transfer including chromosomes stickiness, sterility of pollen grains (Páez et al. 2021) was observed. This phenomenon functions as an additional potential

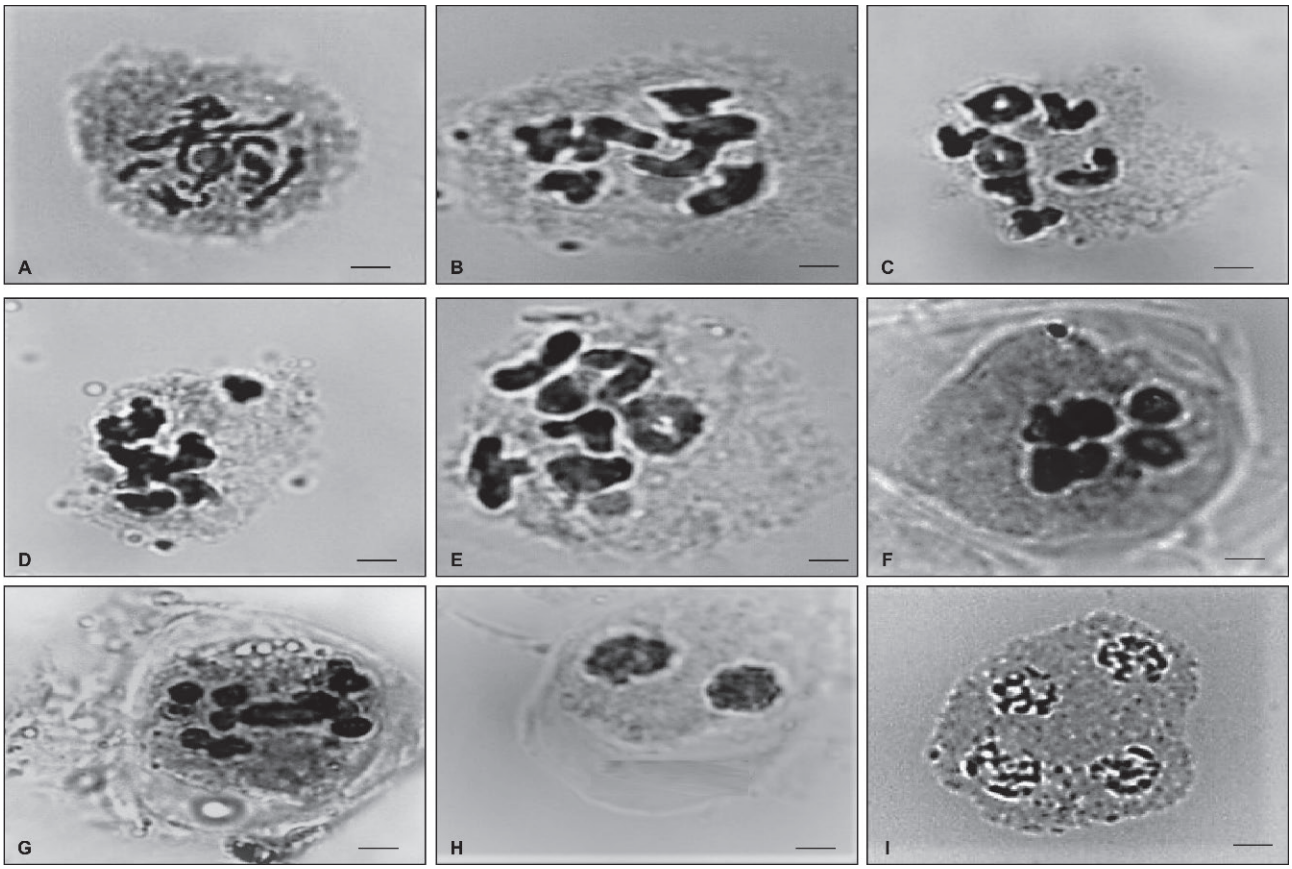

Figure 4. (A) A PMC at diplotene, (B-E) PMCs at metaphase with 7 IIs, (F) A PMC at metaphase showing clumping, (G) A PMC at anaphase showing chromatin bridge, (H) A PMC at telophase I, (I) A PMC at telophase II. Scale bars =10 μm.

genetic recombination mechanism (Mursalimov and Deineko 2017; Rashid et al. 2022b) and is a natural meiotic aberration that may have evolutionary importance (Singhal et al. 2018). The cytoplasmic channels and chromatin migration has also been reported in meiocytes of *Arnebia hispidissima* (Baquar and Husain., 1969). The phenomenon of cytomixis and its effects on meiotic developments and pollen fertility has been reported in various taxa of Himalayan region (Tantary et al. 2021). Cytomixis causes various meiotic abnormalities which include interbivalent connections, chromosome stickiness, laggards, bridges, late disjunction, pyknotic chromatin and unorganized chromatin threads (Singhal and Kumar 2008) as observed in present study also. Unreduced gametes or aneuploids and polyploids plants with certain morphological traits can both result from cytomixis (Falistocco et al. 1995; Arabi et al. 2022) leading to increase or decrease of basic chromosome count of the species (Tantary et al. 2021).

Chromosome clustering in *A. euchroma* was associated with both the intense (entire genome affected) and mild (few chromosomes affected) chromosomal stickiness that was observed in some PMCs. The presence of clumping distorts the chromosome shape making it difficult to determine the chromosome count. In the majority of cases stickiness was observed at Metaphase-I, and Anaphase-I in the present study. The cause of chromosome stickiness in many plant species has been attributed to environmental and genetic causes, as well as the interplay between the two (Pessim et al. 2015; Arabi et al. 2022). The sticky chromatin in various flowering plants have been attributed to gene mutation that disrupts proteins which in normal circumstances helps the chromosomes stay apart and prevents adherence (Tantary et al. 2021). However, the low temperature and high UV exposure in the alpine habitats (Rashid et al. 2022b) may be responsible for the observed chromosomal stickiness in the *Arnebia euchroma*. Chromosomal stickiness and the ensuing lack of chromosomal segregation at anaphase I can be suspected as the cause of meiotic abnormalities in the current investigation as seen in case of other studies (Masoud et al. 2010; Sin-

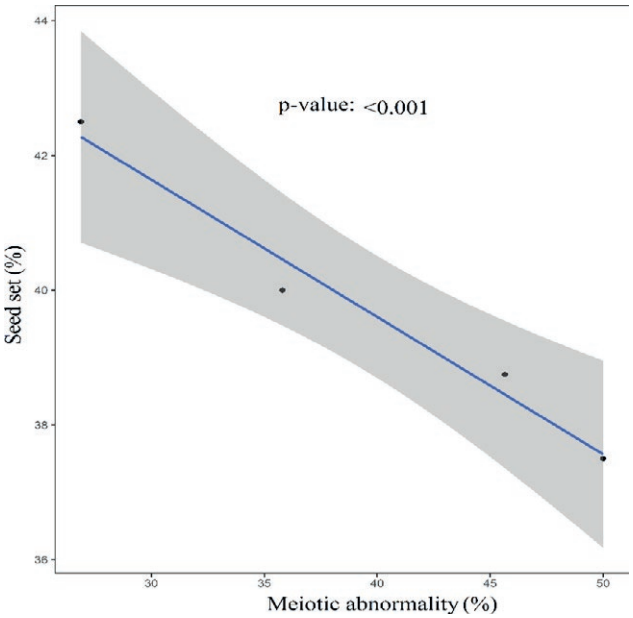

Figure 5. Relationship between seed set and meiotic abnormality as shown by linear model of regression with 95% confidence interval highlighted in grey shade.

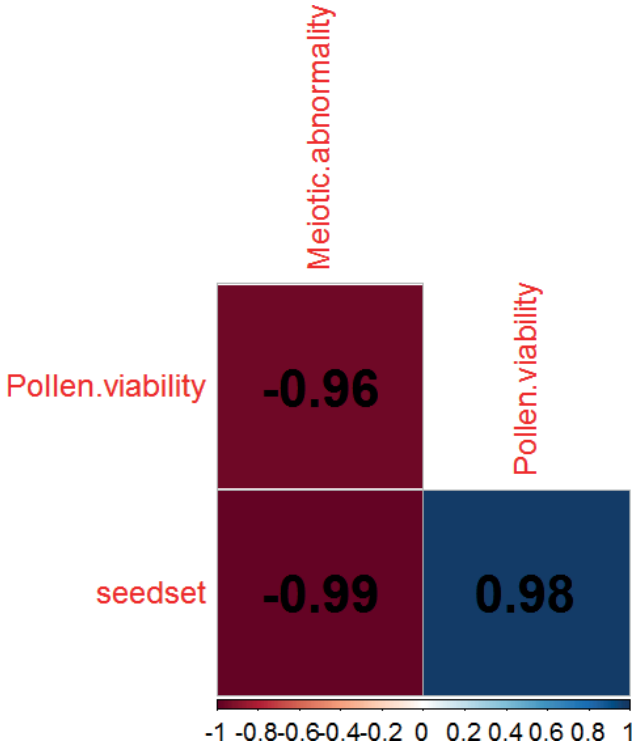

Figure 6. Relationship between meiotic abnormalities, seed set, and pollen viability as depicted by correlation plot.

Table 2. Coordinates of sites and mean meiotic irregularity, pollen fertility, and seed set observed in the 4 studied populations of the *Arnebia euchroma*

Population	Latitude	Longitude	Mean		
			Meiotic abnormality	Pollen viability	Seed set
Matayen	34.37	75.59	26.88	85	42.5
Karpokhar	34.24	75.97	50.00	67	37.5
Changoyal	34.35	76.13	45.65	75	38.75
Rungdum	34.05	76.20	35.80	78	40

gh et al. 2022). The chromosome bridges may occur as a result of chiasma interlocking in bivalents, and laggards may develop as a result of delayed terminalisation of stickiness at the ends of chromosomes (Chaudhari and Chaudhary 2012). Pollen fertility may be totally or partially impacted by chromatin stickiness, depending on degree of presence (Rana et al. 2013). The presence of five and six bivalents and few quadrivalents in some cells of the studied populations as against the normal seven bivalent formation can lead to development of aneuploids in the target plant species. The rarity of quadrivalents points to translocation instead of segmental allopolyploidy as the cause (Dawson et al. 1993; Lattoo et al. 2006). Normal segregation of chromosomes occurs as a result of optimal spindle orientation and chiasma development, while any deviation can lead to laggard formation (Arabi et al. 2022). The frequency of abnormal PMCs decreased as the cells progressed during meiosis, as seen by a comparison of the stages during the course of meiosis. A recovery mechanism that may successfully combat the anomalous behaviour of PMCs and restores fidelity during division with cell cycle advancement (Grewal and Rani 2022). The meiotic aberrations present in the target species can lead to abnormal microsporogenesis without micronuclei. This type of atypical meiotic behaviour results in sterile pollen grains, which lowers pollen viability, seed and fruit set as seen during the present study.

The intrinsic factors (meiotic abnormalities) associated with the species is a constrain in its reproductive process. Therefore, these factors can lead to loss of reproductive efficiency with low seed and fruit formation and reduction in the pollen fertility of the species (Rashid et al. 2022a; Rashid et al. 2022a). It is evident from the current study that designing of effective future conservation programs of the target species should also consider the intrinsic factors that hold capacity to reduce the population of the species in nature.

AUTHOR CONTRIBUTIONS

MAS envisioned the idea of the present work. IIS and SV collected the data and carried the cytological work. SV and IIS wrote the manuscript, the other authors helped to revise and finalise the manuscript.

ACKNOWLEDGEMENTS

The financial support of MoEF&CC under the National Mission on Himalayan Studies (NMHS) through its project ID NMHS/2017-18/ MG43/27 is highly acknowledged.

REFERENCES

Arabi M, Norouzi M, Noori SAS, Mortazavian SMM. 2022. Chromosome Count, Male Meiotic Behavior and Pollen Analysis of Eight Populations of *Trachyspermum ammi* (L.) Sprague (Apiaceae) from Iran. Cytologia 87: 29-34.

Baquar, SR, Husain, SA. 1969. Cytoplasmic channels and chromatin migration in the meiocytes of *Arnebia hispidissima* (Sieb.) DC. Annals of Botany 33: 821-831.

Chaudhari AK, BR C. 2012. Meiotic chromosome behaviour and karyomorphology of Aloe vera (L.) Burm. f. Chromosome Botany. 7:23-9.

Cohen H, Philpott SM, Liere H, Lin BB, Jha S. 2021. The relationship between pollinator community and pollination services is mediated by floral abundance in urban landscapes. Urban Ecosystems 24: 275-290.

Dafni A. 1992. Pollination ecology. New York: Oxford University Press.

Dawson J, Wilson ZA, Aarts MGM, Braithwaite AF, Briarty, LG, Mulligan BJ. 1993. Microspore and pollen development in six male-sterile mutants of *Arabidopsis thaliana.* Canadian Journal of Botany **7**1: 629-638.

Falistocco E, Tosti N, Falcinelli M. 1995. Cytomixis in pollen mother cells of diploid Dactylis, one of the origins of 2n gametes. J. Hered 86: 448–453.

Gan X, Cao L, Zhang X, Li H. 2013. Floral biology, breeding system and pollination ecology of an endangered tree *Tetracentron sinense* Oliv.(Trochodendraceae). Botanical Studies, 54: 1-9.

Grewal A, Rani P. 2022. New record of chromosome count and B-chromosome in *Tinantia erecta* (Jacq.) Fenzl collected from different localities of Mussoorie, Uttarakhand (India). The Nucleus 65: 73-79.

Guan, JZ, Wang JJ, Cheng ZH, Liu Y Li ZY. 2012. Cytomixis and meiotic abnormalities during microsporogenesis are responsible for male sterility and chromosome variations in Houttuynia cordata. Genet Mol Res **11**: 121-30.

Lal M, Samant SS, Kumar R, Sharma L, Paul S, Dutt S, Negi D, Devi K. 2020. Population ecology and niche modelling of endangered *Arnebia euchroma* in Himachal Pradesh, India-An approach for conservation. Med. Plants Int. J. Phytomed. Relat. Ind. 12: 90–104.

Lattoo SK, Khan S, Bamotra S, Dhar AK. 2006. Cytomixis impairs meiosis and influences reproductive success in Chlorophytum comosum (Thunb) Jacq.--an additional strategy and possible implications. Journal of Biosciences, 31: 5.

Lubbers AE, Christensen NL. 1986. Intraseasonal variation in seed production among flowers and plants of *Thalictrum thalictroides* (Ranunculaceae). Am. J. Bot. 73: 190–203.

Ma Y, Cui Z, Cheng CY, Li R, Wu H, Jin L, Wang Z. 2022. Flowering characteristics and mating system of *Fritillaria cirrhosa* (Liliaceae), an endangered plant in China. Brazilian Journal of Botany 45: 1307-1318.

Marks GE. 1954. An acetocarmine glycerol jelly for use in pollen fertility counts. Stain Technol. 29: 277.

Mursalimov S, Deineko E. 2017. Cytomixis in tobacco microsporogenesis: Are there any genome parts predisposed to migration? Protoplasma 254: 1379–1384.

Masoud S, Alijanpoo B, Khayyami M. 2010. Contribution to cytology of genus Salvia L.(Lamiaceae) in Iran. Caryologia 63:405-10.

Páez VDLA, Andrada AR, Kumar P Caro MS. 2021. Cytomixis in angiosperms from Northwestern Argentina. Botany Letters 168: 536-545.

Pessim C, Pagliarini MS, Silva N, Jank L. 2015. Chromosome stickiness impairs meiosis and influences reproductive success in *Panicum maximum* (Poaceae) hybrid plants. Genet. Mol. Res. 14: 4195-4202.

Rana PK, Kumar P, Singhal VK. 2013. Spindle irregularities, chromatin transfer, and chromatin stickiness during male meiosis in Anemone tetrasepala (Ranunculaceae). Turkish Journal of Botany. 37:167-76.

Rashid K, Rashid S, Ganie AH, Nawchoo, IA, Khuroo AA. 2021a. Meiotic studies, pollen fertility and seed set of *Trillium govanianum*, an endangered endemic plant species of the Himalaya. Cytologia 86: 245-249.

Rashid S, Rashid K, Ganie AH, Nawchoo IA, Khuroo AA. 2022b. Meiotic studies, pollen fertility and seed set of *Actaea kashmiriana*, an endemic medicinal plant species of Kashmir Himalaya. Cytologia 87: 239-244.

Schurr L, Affre L, Flacher F, Tatoni T, Le Mire Pecheux L, Geslin B. 2019. Pollination insights for the conserva-

tion of a rare threatened plant species, *Astragalus tragacantha* (Fabaceae). Biodiversity and Conservation 28: 1389-1409.

Sharma V, Gupta RC, Bala S. Singh B. 2013. New chromosome number reports in some medicinally important angiosperms of North India. Cytologia 78: 285-296.

Singh P, Tiwari S, Agrawal SB. 2022. Chromosomal and molecular indicators: a new insight in biomonitoring programs. InNew Paradigms in Environmental Biomonitoring Using Plants 317-340.

Singhal VK, Kumar P. 2008. Impact of cytomixis on meiosis, pollen viability and pollen size in wild populations of Himalayan poppy (*Meconopsis aculeata* Royle). Journal of Biosciences, 33: 371-380

Sofi II, Verma S, Ganie AH, Sharma N, Shah, MA. 2022a. Threat status of three important medicinal Himalayan plant species and conservation implications. Nature Conservation Research. 7: 1.

Sofi II, Zargar SA, Ganie AH, Shah MA. 2022b. Distribution dynamics of *Arnebia euchroma* (Royle) IM Johnst. and associated plant communities in Trans-Himalayan Ladakh region in relation to local livelihoods under climate change. Trees, Forests and People 7: 100213.

Tantray YR, Jan I, Wani MS, Singhal VK, Gupta RC. 2021. Chromosome numbers and meiotic behavior in some species of Asteraceae from high altitudinal regions of Kashmir Himalayas. Journal of Asia-Pacific Biodiversity, 14(4), 590-606.

Wani IA, Verma S, Ahmad P, El-Serehy HA, Hashim MJ. 2022. Reproductive Biology of *Rheum webbianum* Royle, a Vulnerable Medicinal Herb From Alpines of North-Western Himalaya. Frontiers in Plant Science, 13: 10.

Caryologia
International Journal of Cytology, Cytosystematics and Cytogenetics

Firenze University Press
www.fupress.com/caryologia

OPEN ACCESS

Citation: Giovino, A., Marchese, A., Bonanno, F., Sala, G., Marra, F.P., & Domina, G. (2023). Morphological and molecular characterization of Sicilian carob (*Ceratonia siliqua* L.) accessions. *Caryologia* 76(3): 39-49. doi: 10.36253/caryologia-2279

Received: August 7, 2023

Accepted: December 14, 2023

Published: February 29, 2024

Data Availability Statement: All relevant data are within the paper and its Supporting Information files.

Competing Interests: The Author(s) declare(s) no conflict of interest.

Morphological and molecular characterization of Sicilian carob (*Ceratonia siliqua* L.) accessions

Antonio Giovino[1], Annalisa Marchese[2,*], Floriana Bonanno[1], Giovanna Sala[2], Francesco Paolo Marra[3], Gianniantonio Domina[2]

[1] *Council for Agricultural Research and Economics (CREA), Research Centre for Plant Protection and Certification (CREA-DC), 90128 Palermo, Italy*
[2] *Department of Agricultural, Food and Forest Sciences, University of Palermo, Viale delle Scienze– Ed. 4, 90128 Palermo, Italy*
[3] *Department of Architecture (DARCH), University of Palermo, Viale delle Scienze—Ed. 8, 90128 Palermo, Italy*
*Corresponding author. E-mail: annalisa.marchese@unipa.it

Abstract. The evergreen carob tree (*Ceratonia siliqua*) is considered one of the oldest trees in the world, cultivated since ancient times in the Mediterranean Basin, for its edible and high nutritional fruits, adapted to human and animal consumption. Spain is the main producer, followed by Italy, Portugal, Greece, Morocco, and Turkey. In Italy, the cultivation of carob is concentrated in a few provinces and insists on an area of more than 5,500 hectares. In this work 19 accessions, showing interesting fruit traits were analysed morphologically and genetically. Overall, 13 quantitative characters were considered regarding leaf (5 characters), pod (5) and seed (3). To investigate the genetic diversity 8 fluorescently labelled SSR primers were used, indicated as polymorphic in the literature. A UPGMA dendrogram was constructed to depict identity cases and relationships among the accessions. Clustering showed discrimination among accessions from Eastern and Western Sicily. The morphological characterisation does not clearly discriminate any of the cultivars recognized by the growers, similarly, the molecular analysis showed a reduced level of diversity. Since most of these local accessions are of unknown origin and that they are representative of the local germplasm they still warrant protection for their economic and environmental value.

Keywords: carob tree, morphological analysis, microsatellites or SSR markers, genetic diversity, conservation.

INTRODUCTION

The evergreen and rustic carob tree, *Ceratonia siliqua* L., a diploid species ($2n = 48$) belonging to the Fabaceae family, is grown since ancient times in most countries of the Mediterranean basin for economic and environmental value.

This tree characterizes the Mediterranean vegetation and landscape. In the Mediterranean area, pastures with carob trees were traditional agro-sil-

vo-pastoral systems, representing multifunctional systems that can contribute to the preservation of agrobiodiversity and traditional knowledge (Venturi et al. 2022). Carob trees planted with other trees such as olive, fig, grapevines, or almonds and with annual perennial crops between the rows represents an agroforestry practice aiming at integrating woody perennials and an agricultural crop growing as part of the understory.

The carob tree can thrive in calcareous and dry soils (Batlle 1997; Tous et al. 2013), making the species suitable for the valorization of marginal areas for agriculture. Its fruits (pods) are legumes and can have elongated, compressed, or curved shapes (Batlle 1997), they are rich in nutritional values and bioactive molecules properties, showing a wide range of biological properties with important health-promoting effects (prevention of cancers, lowering of LDL cholesterol, antidiabetic effects) (Avallone et al. 1997; Zunft et al. 2003; Goulas et al. 2016; Theophilou et al. 2017). Carob seeds can be used to produce carob bean gum, a food-thickening agent (Bouzouita et al. 2007; Kyratzis et al. 2019).

The carob is considered native to the Eastern Mediterranean and it was mainly spread in cultivation in the Western Mediterranean countries by Greeks, and Romans who selected and propagated genotypes by scion grafting (Baumel et al. 2022). Anyway, multiple origins of domestication were identified both in the Eastern and Western Mediterranean Basin (Baumel et al. 2022). The differences between cultivated varieties and wild progenitors are relative to the size and position of fruits (La Malfa et al. 2007). The cultivation in specialized orchards has taken place only recently, because in the past carob cultivation essentially comprised wild rootstocks distributed naturally and randomly grafted with phenotypes of selected scions (La Malfa et al. 2014).

Spain is the main producer of Carob followed by Italy, Portugal, Greece, Morocco, and Turkey (Batlle 1997; Bulca 2016).

Nowadays in Italy, carob cultivation is prevalent in South-eastern Sicily, in the provinces of Syracuse and Ragusa, where it has represented an important economic resource for centuries. In the Monti Iblei (South-eastern Sicily) the enclosed fields with carob trees are included in the "National Catalogue of Historical Rural Landscapes" where a dense network of low walls marks out plots where carob trees provide food and shade to livestock left grazing there after the wheat harvest (Agnoletti, 2011; 2013).

Carob pods in Sicily are directly marketed or transformed into derivatives for animal or human feed (Caruso et al. 2008; La Malfa et al. 2012). In the last twenty years, on the island, the demand for carob has undergone a transformation moving from products exclusively for animal feed and widespread culinary traditions towards a sought-after product (chocolate, liqueurs, and cough sweets) thanks to local companies that improved the processing of carob. According to the latest published statistical data, carob cultivation in Sicily concerns about 5,415 ha (ISTAT 2022).

In Sicily, the carob genotypes were introduced at different times by Phoenicians, before the Greek and Roman dominations and later during the Arab domination (Ramón-Laca and Mabberley 2004; Baumel et al. 2022). The Sicilian carob germplasm includes peculiar cultivars multiplicated by seeds or grafted. In the field farmers in general grow few phenotypes.

Different studies have been performed on carob genetic diversity by using different molecular markers (Barracosa et al. 2008; Caruso et al. 2008; La Malfa et al. 2014; Viruel et al. 2018; Di Guardo et al. 2019; Kyratzis et al. 2019; Baumel et al. 2022). Similarly, many studies have been conducted to check the nutritional composition of carob products (Avallone et al. 1997; Zunft et al. 2003; Bouzouita et al. 2007; Bulca, 2016; Goulas et al. 2016; Theophilou et al. 2017).

Although among the molecular markers, microsatellite or SSR (Simple Sequence Repeats) represent the marker of choice for fingerprinting study and a powerful instrument for germplasm management, allowing diversity assessment among standardized databases (e.g. peach – Marchese et al. 2005; palm – Giovino et al. 2021, 2023; fig – Costa et al. 2017; apple – Venison et al. 2022; sweet cherry – Ordidge et al. 2021; Trifonova et al. 2021; almond – Dangl et al. 2009; Cimò et al. 2017; hazelnut – Fiore et al. 2022; olive – Atrouz et al. 2021; Marchese et al. 2023), in the carob species La Malfa et al. (2014) found low genetic diversity by using a set of EST-SSR. Viruel et al. (2018) tried to improve the detection of diversity by using next-generation sequencing of SSR loci, screening populations throughout the Mediterranean Basin – from Spain, Greece, Lebanon, and Morocco. They found hidden SNP mutations in the SSR amplicons which can be considered an additional source of genetic variation, however, the differences among populations were not so large.

The purpose of the current study was to characterize carob accessions from Sicilian farms using morphological and SSR markers to detect the level of diversity and for conservation purposes.

MATERIALS AND METHODS

Plant material

The specimens used for morphological statistical analysis and molecular analysis were collected in the private farms and the regional collection field and voucher specimens were deposited in herbarium SAAF-University of Palermo. A total of 19 accessions were georeferenced and collected from local farms (Table 1, Figure 1).

Morphological characterization

Overall, 14 accessions were used for morphological analysis (Table 1). For each accession, 10 measurements were taken for each quantitative character on 3 different samples. Overall, 15 descriptors were considered regarding leaf (6 characters), pod (5), and seed (4) based on carob descriptors developed by Batlle and Tous (1997) (Table 2).

A principal component analysis (PCA) and a discriminant analysis (DA) were performed, following Boyd (2002), Giovino et al. (2015), and Domina et al. (2017; 2022). The PCA was based on logarithmic values of continuous quantitative characters, using PAST version 4.11 (Hammer et al. 2001; Hammer et al. 2022). The DA, with the individuals a priori assigned to the postulated cultivars, was performed on continuous and discrete numerical characters. Each of the 13 continuous characters was also subjected to univariate analysis.

Table 1. Carob trees accessions analyzed in this study.

Code	Accession	Country	Geographic coordinates	Morphological analysis	Molecular analysis	Voucher
1	Cicero	Italy	36° 51' 09" N 14° 55' 05" E	X	X	SAF100086
2	Fratantonio_E	Italy	36° 53' 10" N 14° 54' 25" E	X	X	SAF100087
3	Fratantonio_G	Italy	36° 48' 24" N 14° 54' 20" E	X	X	SAF100088
4	Fratantonio_S	Italy	36° 53' 33" N 14° 54' 14" E	X	X	SAF100089
5	Iacono	Italy	36° 50' 42" N 14° 34' 07" E	X	X	SAF100090
6	Licitra	Italy	36° 52' 49" N 14° 54' 17" E (collection field)	X	X	SAF100091
7	Maltese	Italy	36° 46' 49" N 14° 42' 54" E	X	X	SAF100092
8	Racemosa	Italy	36° 52' 49" N 14° 54' 17" E (collection field)	X	X	SAF100093
9	Scrofani	Italy	36° 51' 10" N 14° 41' 40" E	X	X	SAF100094
10	Tantillo	Italy	36° 52' 49" N 14° 54' 17" E (collection field)	X	X	SAF100095
11	Tenuta Chiaramonte	Italy	36° 50' 00" N 14° 38' 27" E	X	X	SAF100096
12	Latinissima	Italy	36° 52' 49" N 14° 54' 17" E (collection field)	X	X	SAF100097
13	Pasta	Italy	36° 52' 49" N 14° 54' 17" E (collection field)	X	X	SAF100098
14	Saccarata	Italy	36° 52' 49" N 14° 54' 17" E (collection field)	X	X	SAF100099
15	Torretta	Italy	36°86'56.17"N 14°83'70.71"E		X	SAF100100
16	Terrasini	Italy	36°86'55.48"N 14°83'75.43"E		X	SAF100101
17	Cinisi	Italy	36°86'55.48"N 14°83'75.43"E		X	SAF100102
18	NA CAR	Israel			X	SAF100103
19	Israel CAR	Israel			X	SAF100104

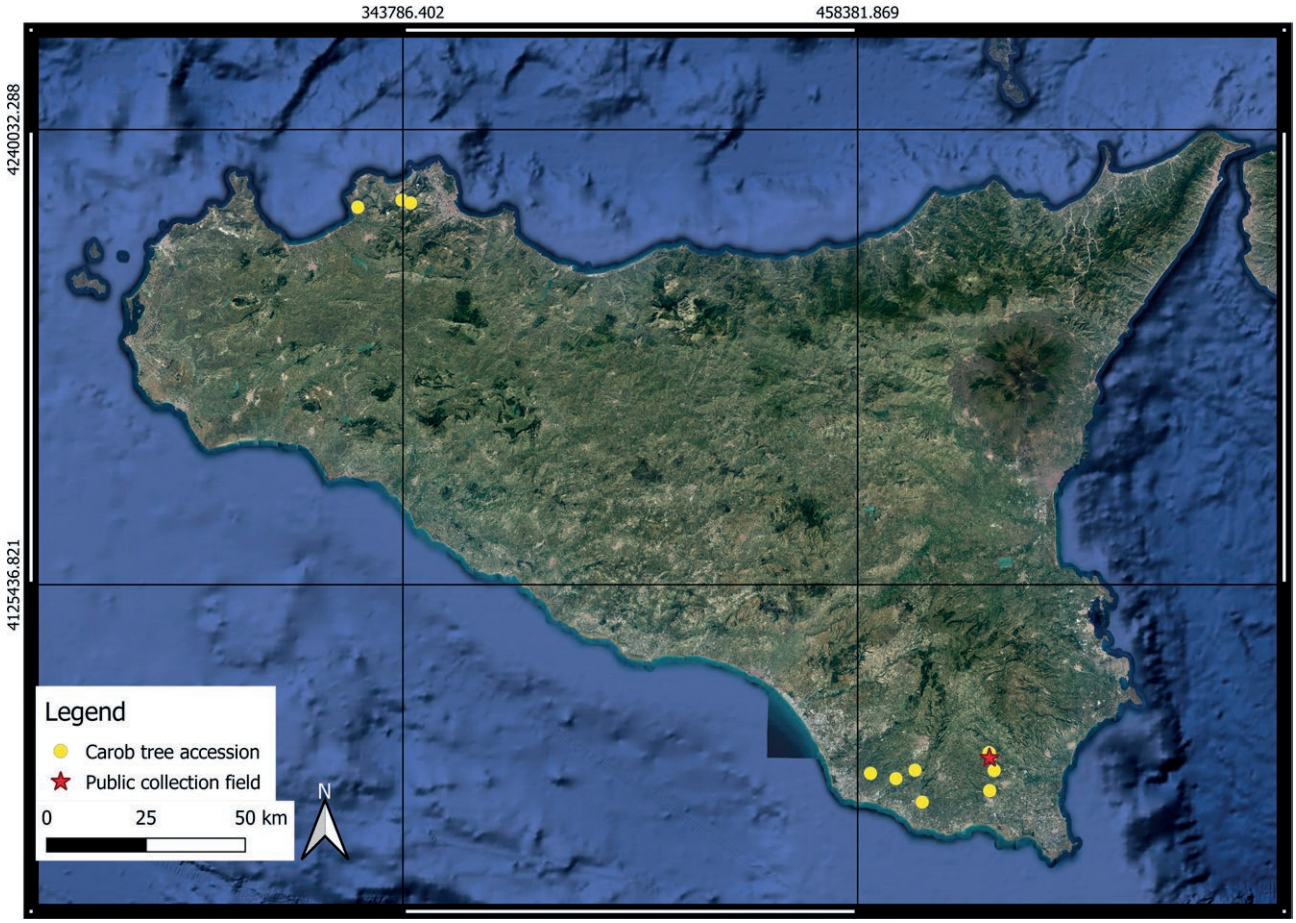

Figure 1. Location sites of carob trees where accessions were sampled (yellow pointer) and of regional collection field (red star).

Genomic DNA Extraction and SSR genotyping

Overall, 19 accessions were used for molecular analysis (Table 1). Genomic DNA extraction was performed from young leaves by using the Doyle and Doyle protocol (1987). DNA quantifications were carried out with NanoDrop 1000 Spectrophotometer and dilution were made to the final concentration of 150 ng/µl. Eight Single Sequence Repeats (SSRs) loci were chosen: Cesi_98_gct6; Cesi_187_at15; Cesi_673_ct9; Cesi_722_ag9; Cesi_976_ta5tg6 and Cesi_1187_at9 reported by La Malfa et al. (2014), and two C09 and C24 developed by Viruel et al. (2018) following number and range of expected alleles, reported heterozygosity in the literature, to set multiplexes PCR reactions. For multiplexing, the SSR loci were used for the amplification of eight genotypes and once detected their expected allele size range in comparison with the literature. Fluorescent dyes (FAM, HEX, NED, and PET; Life Technologies, Thermo Fisher, Foster City, CA, USA) were used for each locus, and multiplexes PCR were developed, and the markers used are shown in Table 3.

Table 2. Morphological traits among studied *Ceratonia siliqua* accessions.

	Descriptor	Type
Leaf	No. leaflets	discrete
	leaflet length	mm, continuous
	leaflet width	mm, continuous
	leaf axis length	mm, continuous
	Distance of the first pair of leaflets from the base	mm, continuous
	leaflets petiole length	mm, continuous
Pod	length	mm, continuous
	width	mm, continuous
	edge thickness	mm, continuous
	groove thickness	mm, continuous
	pod weight	gr, continuous
Seed	length	mm, continuous
	width	mm, continuous
	thickness	mm, continuous
	No. seeds per Pod	discrete

Table 3. Specific biomarkers for the determination of intraspecific variability

Marker	Sequence 5'-3'
Cesi_976F	TCCTGAAGGCTGAAGATGATG
Cesi_976R	CAAACCAATGAAGGGCTCTA
Cesi_98F	GCCACCACTTTGAAGGAAGA
Cesi_98R	GCTAGAAGCAGGAGCAGGAG
Cesi_1187F	TTCTCGTCGCCCAAACTG
Cesi_1187R	CTCCCTCATCTCCTTCGTTG
Cesi_187F	ATAACTGGGCGTTCTTTGCTT
Cesi_187R	ATTATCTCTTGCTTTGTGGTCCT
Cesi_509_F	GCCACCTCTCCCTCTTCTC
Cesi_509_R	TTTTGTTCTAATTTTGCTTGCA
Cesi_673F	GAATAGGGCAGAGAGAACAGG
Cesi_673R	TCAAAGGAAGATGAGAAAGAAATCC
Cesi_722F	AGGCTCACACGAAACCCTAA
Cesi_722R	CTGCCACAAGATGATAGATTTG
VirC-09_F	AAGACTCGGCAGCATCTCCAGGCTTTGTAGCTGCCCATTG
VirC-09_R	GCGATCGTCACTGTTCTCCAGAAGGTTGGATAGCGTCCTG
VirC-24_F	AAGACTCGGCAGCATCTCCAAGCTGCAATTTGAGGAATAAAGC
VirC-24_R	GCGATCGTCACTGTTCTCCAACATCCAAAACCCTAGAGCAAG

The PCR reactions were performed in 8 µl reactions containing 1.5 ng template genomic DNA, 1 x Multiplex PCR master mix (Qiagen) and 0.2 µM of each primer on a Geneamp Pcr System 9700 Thermocycler (Thermo Fisher) using the following touch-down protocol: initial denaturation at 95°C for 5 minutes followed by 10 cycles of 95°C for 45 s, 65°C for 30 s with a reduction in temperatures of 1°C per cycle and 72°C for 45 s, then 25 cycles of 95°C for 45 s, 55°C for 30 s, 72°C for 45 s. The final extension was performed at 72°C for 30 minutes.

The SSR analysis was performed with an ABI 3135xl Genetic Analyzer (Applied Biosystems, Thermo Fisher, Foster City, CA, USA), using ABI GeneScan and Genotyper software for allele sizing and scoring.

SSR diversity analysis

By analyzing SSR in a plant's genome, researchers can create a unique fingerprint for that species and use it to identify and differentiate it from other closely related species. SSRs have been successfully used for the identification of genetic diversity between cultivars of the same species (Glynn et al. 2009; Marra et al. 2013; Fiore et al. 2022). The SSR data were analyzed using the software package Cervus 3.0 (Kalinowski et al. 2007). The total number of alleles (Na), the number of effective alleles (Ne), Polymorphic Information Content (PIC), He and Ho, and null alleles were computed.

A UPGMA dendrogram was constructed by using the software Darwin6 (Perrier and Jacquemoud-Collet 2006).

RESULTS

Morphological analysis

Leaf width and length ranged from 27.4 mm (Scrofani) to 46.3 mm (Latinissima) and from 41.5 mm (Scrofani) to 67.6 mm (Tantillo), respectively. The number of leaflets/leaves was found between 7.6 and 9.9. The average pod dimensions (width, length, and thickness) were found between 20 and 26.1 mm, 130.3 and 232 mm and 6-11 mm for the accessions. The pod weight was variable and ranged from 14.7 g (Tantillo) to 50.1 g (Saccarata) among genotypes (Table 4).

Figure 2 shows the quality of representation of the variables by cos2. The results of PCA indicated that the first two principal components explained 68% of the data variability, the plot shows the loading of each studied variable (arrows), and the arrow lengths approximate their variance, whereas the angles between them represent their correlations. The seed characters are positively correlated, they are grouped together, and on the opposite side there are the leaves descriptors. The seed length was positively correlated with pod thickness and negatively correlated with the number of leaflets. Furthermore, pod weight is negatively correlated with the leaflet

Table 4. Leaf, pod and seed descriptors of carob accessions.

	Leaflets					Pod				Seed			
	N. Leaflets	length (mm)	width (mm)	leaf axis length (mm)	distance first pair leaflets from the base	petiole length (mm)	pod weight (mm)	length (mm)	width (mm)	groove thickness 1 (mm)	groove thickness 2 (mm)	N. seeds per pod (mm)	length (mm)	width (mm)	thickness (mm)
Cicero	8.4	49.4	36.3	95.8	23.4	2.6	25.8	139.0	24.4	9.4	4.7	13.3	8.8	6.2	2.3
Fratantonio_E	8.3	52.5	39.8	112.4	26.3	2.7	32.2	141.5	26.1	11.4	5.0	12.0	9.3	6.8	2.5
Fratantonio_G	8.0	55.2	38.2	98.5	24.7	2.5	19.2	132.2	23.3	9.9	5.5	12.0	8.3	6.0	2.5
Fratantonio_S	8.9	43.0	29.4	88.6	19.5	2.5	38.0	156.7	24.7	8.3	5.7	13.0	9.7	7.0	3.0
Iacono	7.6	42.7	34.1	68.3	23.5	2.5	36.1	142.2	23.7	10.2	6.0	13.0	10.0	7.3	2.8
Licitra	7.6	42.7	34.1	68.3	23.5	2.5	36.1	142.2	23.7	10.2	6.0	13.0	10.0	7.3	2.8
Maltese	8.8	46.1	35.7	103.0	21.8	2.3	24.9	131.1	25.2	10.1	5.3	12.0	9.8	6.7	2.7
Racemosa	8.8	54.9	42.6	112.8	23.4	2.5	29.1	150.0	20.0	6.0	4.5	13.0	7.0	4.5	2.0
Scrofani	8.7	41.5	27.4	90.8	19.3	2.3	17.2	133.5	21.8	7.6	5.5	13.5	8.3	5.8	3.3
Tantillo	8.6	67.6	45.7	135.1	30.9	2.5	14.7	145.0	20.0	8.5	5.0	15.0	9.5	7.0	3.0
Tenuta Chiaramonte	7.8	48.1	33.6	97.6	24.0	2.5	27.2	130.3	23.9	9.9	6.2	12.7	9.3	7.0	2.8
Latinissima	9.4	58.9	46.3	140.5	26.5	3.1	36.6	152.5	23.0	8.3	4.8	12.0	10.5	8.0	3.3
Pasta	9.9	47.7	30.5	131.6	26.7	2.7	38.1	232.0	25.7	9.4	5.0	15.0	8.8	7.8	3.3
Saccarata	9.2	53.4	42.5	138.7	30.0	3.2	50.1	155.0	25.0	10.0	6.0	11.0	10.0	7.5	3.0

Figure 2. Biplot illustration of PCA analysis, squared cosine (cos2) shows how accurate the representation of our variables or individuals on the PC plane.

Figure 3. Correlation matrix of different descriptor in different accession of carob tree.

length and width. The trait correlations are also indicated using absolute Pearson correlation coefficients, with red shades indicating high absolute correlation and blue shades indicating low absolute correlation (Figure 3). We found a negative correlation between seed length and the number of seeds in the pod and a positive correlation between leaflets length and leaf axis length.

No continuous numerical morphological character discriminates the single cultivars since all the values overlap. Both the PCA and the DA are of little significance because they represent a small portion of the vari-

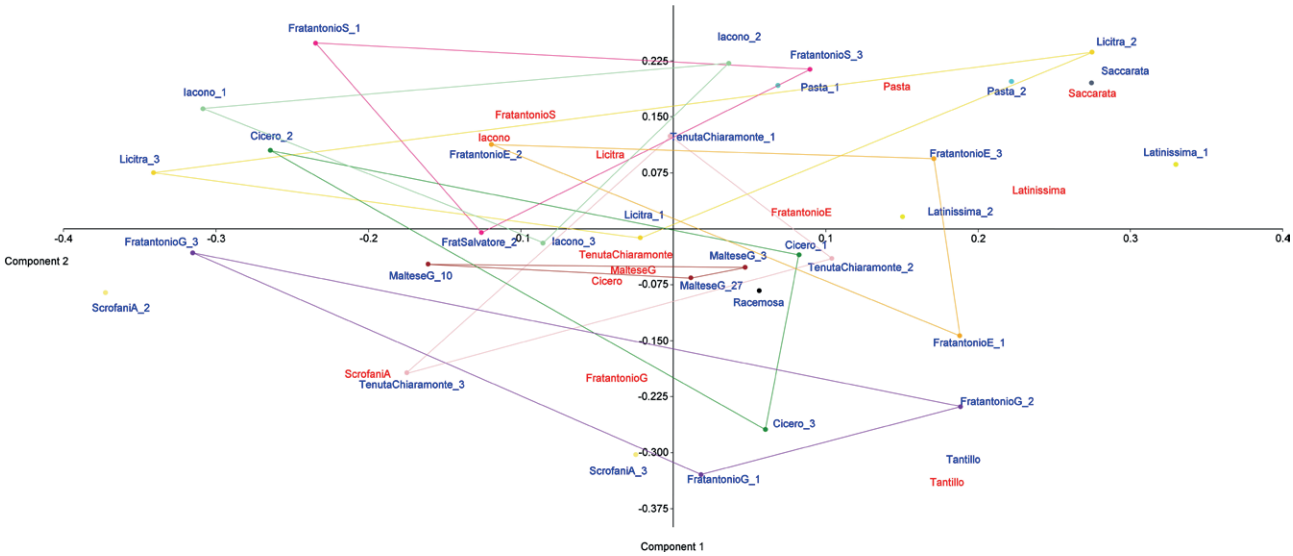

Figure 4. Principal Component Analysis based on the 13 continuous morphological characters, with groups corresponding to the 18 studied accessions. PC1: Eigenvalue 0.0367, % variance 32.969; PC2: Eigenvalue 0.0293, % variance 26.284.

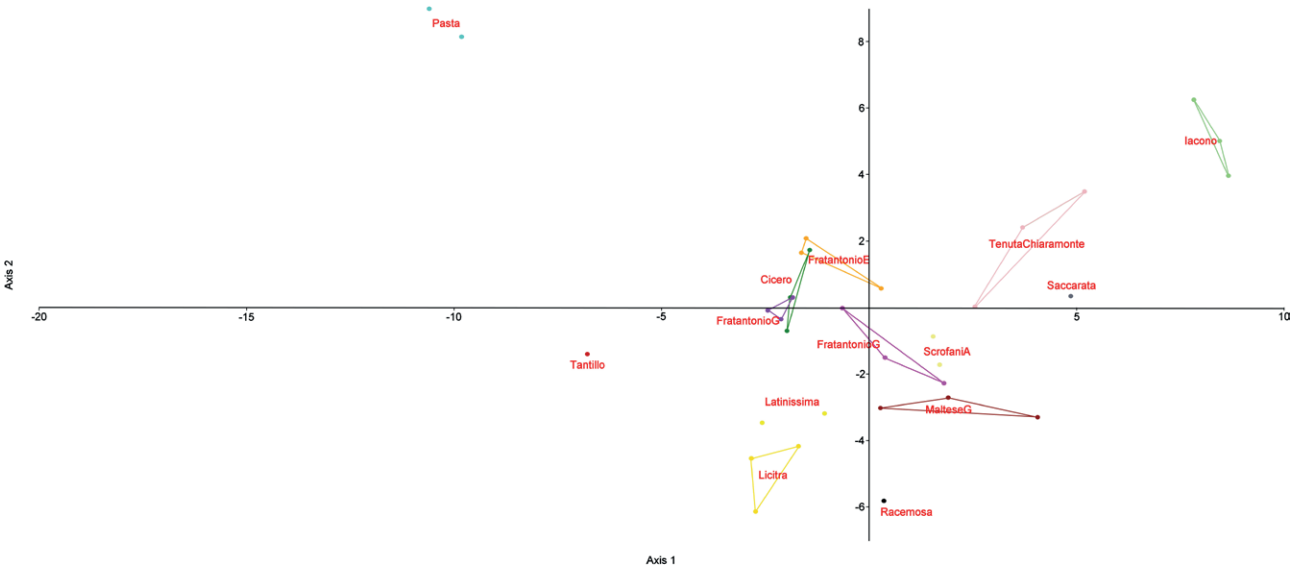

Figure 5. Discriminant analysis (DA), based on the 15 considered morphological characters with groups corresponding to the nine studied taxa. Axis 1: Eigenvalue 31.498, % variance 22.37; Axis 2 Eigenvalue 21.532, % variance 28.97.

ability. The PCA done on the complete dataset (Figure 4) shows an almost complete overlapping of all examined accessions. The DA on the complete dataset discriminates only the accessions "Iacono" and "Pasta" (Figure 5).

SSR marker diversity

The 8 SSR markers used in this analysis showed a low level of polymorphism; the mean number of alleles per locus resulted 3.875; the mean proportion of loci typed was 0.8750; the mean expected heterozygosity was 0.5029 and the mean polymorphic information content (PIC) was 0.4129. The most polymorphic primer pair was Cesi_187 which amplified 6 alleles, while Cesi_722 and Cesi_1187 only three alleles. The Primer Cesi_673 resulted monomorphic thus it was eliminated from the cluster analysis.

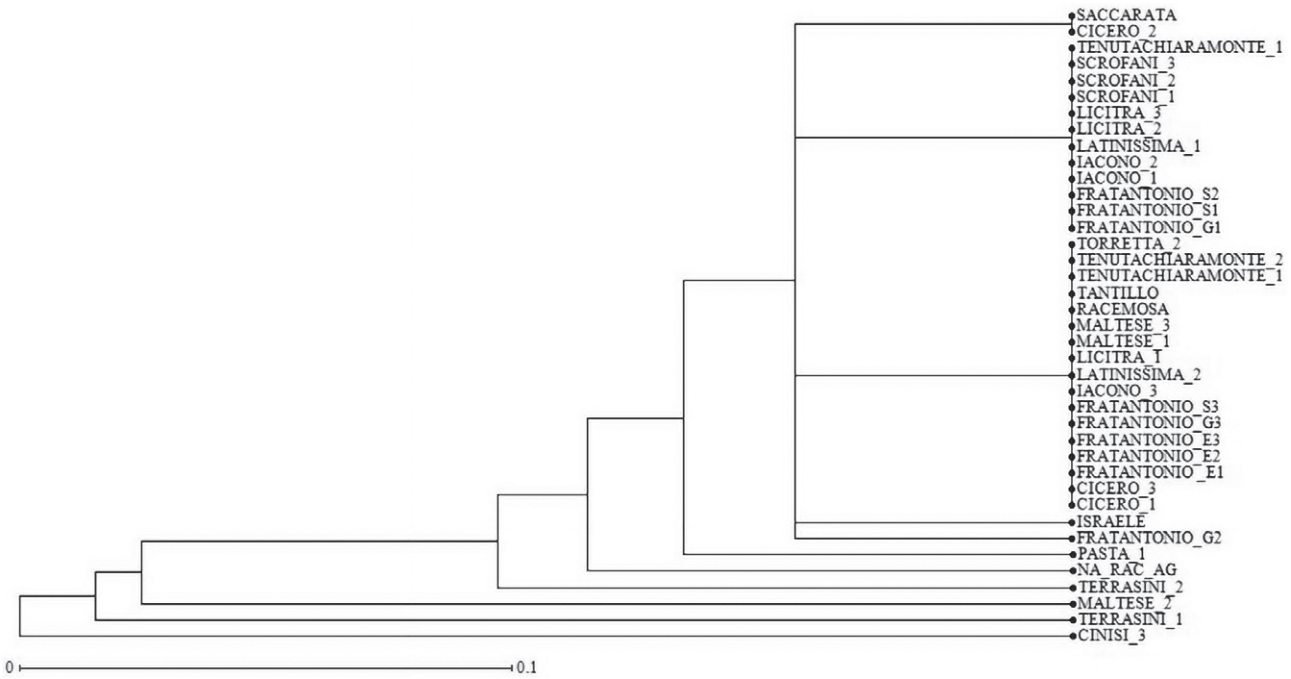

Figure 6. Dendrogram of 19 carob accessions based on simple matching coefficients.

Cluster analysis

As depicted in the UPGMA dendrogram, based on 7 SSRs, as Cesi_673 was monomorphic, constructed with the Dice dissimilarity index by using DARwin 6 software (CIRAD), only 9 accessions studied were discriminated, while most were undiscriminated (Figure 6).

DISCUSSION

The carob species represents a genetic resource of adaptation to the environmental and dry climatic conditions of Sicily, which is the leading Italian region for carob production, producing 98% of the Italian carobs, accounting for 35,0838 tons (ISTAT 2022). Carob pods are mainly produced in Ragusa areas in the south-eastern part of Sicily, where the most common varieties are "Latinissima" (or known synonyms "Giubiliana", "Cipriana", "Cipriota", "Masculina"), Racemosa (or "Moresca", "Spada", "Sciabulara"), Saccarata (or "Latina", "Fimminedda", "Milara") (Caruso et al. 2006, Blangiforti et al., 2022).

Most carob present in specialized orchards are nowadays grafted trees; the grafted carob trees improve phenotypic traits: fleshiness, size and sweetness of the pod and productivity (Batlle and Tous 1997; Tous et al. 2013). Female cultivars are the most important trees in commercial orchards in Mediterranean countries (Albanell et al. 1996) appreciated for their pods and seeds employed as raw materials in the food, pharmaceutical and cosmetic industries (Vourdoubas et al. 2002). Carob pods have been investigated as a material for bioethanol production (Biner et al. 2007).

The carob characterization can be performed at both the morphological and genetic levels. In our study, all the accessions were female, and it was evident the low phenotypical diversity among them that was almost overlapping. The DA analysis enabled the discrimination of only the accessions Iacono and Pasta. Barbagallo et al. (1997) recorded that pod size and numbers of normal and aborted seeds were the characters with a certain degree of polymorphism in analyzing a survey of sixteen Sicilian carob cultivars. They recognized cultivar groups according to a geographic criterion.

Our accessions, in general, showed many leaflets between 7.6 and 9.9 with higher values than the number reported by Korkmaz et al., (2020) analyzing Turkish genotypes where it ranged from 5.9 to 7.1. Regarding the morphological character of pod carob cultivars in Sicily, La Malfa et al. (2012) reported average pod weight, pod width, pod length, and pod thickness as 13.7–33.4 g, 19.3–26.8 mm, 14.9–22.9 cm and 6.8–14.0 mm, respectively, which is in accordance with our study.

Similarly, our dendrogram (Figure 6) showed a limited SSR variability. The most diverse accessions were Terrasini_1, Maltese_2, Cinisi_3, NA_RAC_AG, and

Pasta_1, mostly from Western Sicily. Three groups of identity were found: Saccarata/ Cicero_2; a group of Latinissima_1 accessions and a group of Latinissima_2/ Racemosa/Maltese accessions closely related to a plant derived from a seed originated in Israel and Frantantonio_G2. Clustering showed discrimination among accessions from Eastern Sicily and Western Sicily.

As observed for the whole Mediterranean area (Baumel et al. 2022), the morphological and genetic diversity recorded in the Sicilian carob accessions turned out to be very low.

Sicilian farmers can distinguish vegetatively or sexually propagated accessions to which local names are given but the analysis of this germplasm has shown that the morphological and genetic variations are minimal. The low level of diversity within a given geographic area can be explained by the asexual propagation of selected clones (La Malfa et al. 2014). However, considering that most of the local accessions are of unknown origin and that they are representative of a typical germplasm they still deserve attention and protection.

Baumel et al. (2022) also observed higher genetic variability in the eastern and western Mediterranean basin and lower in the central Mediterranean. Further molecular analysis including SNP sequencing may better shed light on the carob genetic diversity and origin.

Nonetheless, given the multiple origins of domestication and the presence of haplotypes peculiar to the central Mediterranean (Baumel et al. 2022), the knowledge and conservation of the Sicilian germplasm is found to be extremely important for the conservation of carob biodiversity to protect both the agro-forest ecosystem and landscape of Mediterranean region. The cultivation of this multi-functional tree is ideal for agricultural diversification in semi-arid areas therefore in the next coming year it is expected to increase due to climate change, considering its resistance to drought, high rusticity, low requirements for orchard management, and low environmental footprint (Zemouri et al. 2020; Tzatzani et al. 2023).

ACKNOWLEDGMENTS

This work was supported by 'PSR SICILIA 2014-2020 – Programma di Sviluppo Rurale – Misura 16 – Cooperazione – Sottomisura 16.1 – "Sostegno per la costituzione e la gestione dei gruppi operativi del PEI in materia di produttività e sostenibilità dell'agricoltura" – Gruppo Operativo: ATS GO CARRUBO – Project Title: "SISTEMI INNOVATIVI PER LO SVILUPPO DELLA FILIERA DEL "CARRUBO" for the technical support.

We gratefully thank Daniela Trippa for her help in the laboratory activity.

REFERENCES

Atrouz K, Bousba R, Marra FP, Marchese A, Conforti FL, Perrone B, Harkat H, Salimonti A, Zelasco S. 2021. Algerian olive germplasm and its relationships with the Central-Western Mediterranean varieties contributes to clarify cultivated olive diversification. Plants 10(4):678. https://doi.org/10.3390/plants10040678

Avallone R, Plessi M, Baraldi M, Monzani A. 1997. Determination of chemical composition of carob (*Ceratonia siliqua*): protein, fat, carbohydrates, and tannins. J food Compos Anal. 10(2):166–172. https://doi.org/10.1006/jfca.1997.0528

Agnoletti M. (Editor) 2011. Paesaggi rurali storici: per un catalogo nazionale. Roma; Laterza.

Agnoletti M. (Editor) 2013. Italian historical rural landscape. Cultural Values for the Environment and Rural Development; Springer Dordrecht, The Netherlands. https://doi.org/10.1007/978-94-007-5354-9

Albanell E, Caja G, Plaixats J. 1996. Characterization of carob fruits (*Ceratonia siliqua* L.), cultivated in Spain for Agroindustrial use. Int. Tree Crops J. 9:1-9. https://doi.org/10.1080/01435698.1996.9752955

Barbagallo MG, Di Lorenzo R, Meli R, Crescimanno FG. 1997. Characterization of carob germplasm (*Ceratonia siliqua* L.) in Sicily. J Hortic Sci. 72(4):537–543. https://doi.org/10.1080/14620316.1997.11515541

Barracosa P, Lima MB, Cravador A. 2008. Analysis of genetic diversity in Portuguese *Ceratonia siliqua* L. cultivars using RAPD and AFLP markers. Sci Hortic (Amsterdam). 118(3):189–199. https://doi.org/10.1016/j.scienta.2008.06.020

Batlle I and Tous J. 1997. Carob tree: Ceratonia siliqua L.-Promoting the conservation and use of underutilized and neglected crops. 17. Institute of Plant Genetics and Crop Plant Research, Gatersleben/ International Plant Genetic Resources Institute, Rome, Italy.

Baumel A, Nieto Feliner G, Médail F, La Malfa S, Di Guardo M, Bou Dagher Kharrat M, Lakhal-Mirleau F, Frelon V, Ouahmane L, Diadema K. 2022. Genome-wide footprints in the carob tree (*Ceratonia siliqua*) unveil a new domestication pattern of a fruit tree in the Mediterranean. Mol Ecol. 31(15):4095–4111. https://doi.org/10.1111/mec.16563

Biner B, Gubbuk H, Karhan M, Aksu M, Pekmezci M. 2007. Sugar profiles of the pods of cultivated and wild types of carob bean (*Ceratonia siliqua* L.) in

Turkey. Food Chemistry. 100(4):453-1455. https://doi.org/10.1016/j.foodchem.2005.11.037.

Blangiforti C, D'Amato A, La Malfa S. 2022. Il carrubo è l'uomo. Memoria, storia e storie attorno a un albero emblematico. Abulafia ISBN: 8894623750

Bouzouita N, Khaldi A, Zgoulli S, Chebil L, Chekki R, Chaabouni MM, Thonart P. 2007. The analysis of crude and purified locust bean gum: A comparison of samples from different carob tree populations in Tunisia. Food Chem. 101(4):1508–1515. https://doi.org/10.1016/j.foodchem.2006.03.056

Boyd A. 2002. Morphological analysis of Sky Island populations of *Macromeria viridiflora* (*Boraginaceae*). Syst Bot. 27(1):116–126. https://doi.org/10.1043/0363-6445-27.1.116

Bulca S. 2016. Some properties of carob pod and its use in different areas including food technology. Sci Bull Ser F Biotechnol. 20:142–147.

Caruso M, La Malfa S, La Rosa G, Gentile A, Tribulato E, Frutos Tomás D. 2006. Molecular characterization and evaluation of carob germplasm. In I International Symposium on Pomegranate and Minor Mediterranean Fruits 818: 95–102. https://doi.org/10.17660/ActaHortic.2009.818.12

Caruso M, La Malfa S, Pavlíček T, Frutos Tomñs D, Gentile A, Tribulato E. 2008. Characterisation and assessment of genetic diversity in cultivated and wild carob (*Ceratonia siliqua* L.) genotypes using AFLP markers. J Hortic Sci Biotechnol. 83(2):177–182. https://doi.org/10.1080/14620316.2008.11512367

Cimò G, Marchese A, Germanà M.A. 2017. Microspore embryogenesis induced through in vitro anther culture of almond (*Prunus dulcis* Mill.). Plant Cell, Tissue and Organ Culture (PCTOC). 128:85–95. https://doi.org/10.1007/s11240-016-1086-2

Costa F, Marchese A, Mafrica R, Di Vaio C, Ferrara G, Fretto S, Quartararo A, Marra FP, Mennone C, Vitale F, Reale S, Caruso T. 2017. Genetic diversity of fig (*Ficus carica* L.) genotypes grown in Southern Italy revealed by the use of SSR markers. Acta Hortic. 1173:75-80. https://doi.org/10.17660/ActaHortic.2017.1173.13

Di Guardo M, Scollo F, Ninot A, Rovira M, Hermoso JF, Distefano G, La Malfa S, Batlle I. 2019. Genetic structure analysis and selection of a core collection for carob tree germplasm conservation and management. Tree Genet Genomes. 15:1–14. https://doi.org/10.1007/s11295-019-1345-6

Domina G, Di Gristina E, Barone G. 2022. A new species within the *Centaurea busambarensis* complex (Asteraceae, Cardueae) from Sicily. Biodivers Data J. 10:e91505. https://doi.org/10.3897/BDJ.10.e91505

Domina G, Greuter W, Raimondo FM. 2017. A taxonomic reassessment of the *Centaurea busambarensis* complex (Compositae, Cardueae), with description of a new species from the Egadi Islands (W Sicily). Isr J Plant Sci. 64(1–2):48–56. https://doi.org/10.1080/07929978.2016.1257146

Doyle JJ, Doyle JL. 1987. A rapid DNA isolation procedure for small quantities of fresh leaf tissue. Phytochemical Bulletin. 19(1):11-15.

Fiore MC, Marchese A, Mauceri A, Digangi I, Scialabba A. 2022. Diversity assessment and DNA-based fingerprinting of Sicilian hazelnut (*Corylus avellana* L.) germplasm. Plants. 11(5):631. https://doi.org/10.3390/plants11050631

Giovino A, Domina G, Bazan G, Campisi P, Scibetta S. 2015. Taxonomy and conservation of *Pancratium maritimum* (Amaryllidaceae) and relatives in the Central Mediterranean. Acta Bot Gall. 162(4):289–299. https://doi.org/10.1080/12538078.2015.1089416

Giovino A, Guarino C, Marchese A, Sciarillo R, Domina G, Tolone M, Mateu-Andrés I, Khadari B, Schillaci C, Guara-Requena M, Saia S. 2023. Genetic variability of *Chamaerops humilis* (Arecaceae) throughout its native range highlights 2 species movement pathways from its area of origin. Botanical Journal of the Linnean Society. 201:3: 361–376. https://doi.org/10.1093/botlinnean/boac053

Giovino A, Marchese A, Domina G. 2021. Morphological and genetic variation of *Chamaerops humilis* (Arecaceae) in relation to the altitude. Caryologia. International Journal of Cytology, Cytosystematics and Cytogenetics. 73(4):85–98. https://doi.org/10.13128/caryologia-1011

Goulas V, Stylos E, Chatziathanasiadou M V, Mavromoustakos T, Tzakos AG. 2016. Functional components of carob fruit: Linking the chemical and biological space. Int J Mol Sci. 17(11):1875. https://doi.org/10.3390/ijms17111875

Hammer Ø, Harper DA, Ryan PD. 2022. Past Software. Nat Hist Museum.

Hammer Ø, Harper DAT, Ryan PD. 2001. PAST: Paleontological statistics software package for education and data analysis. Palaeontol Electron. 4(1):9.

ISTAT Italian National Institute of Statistics Cultivations 2022. Available at: http://dati.istat.it/Index.aspx?DataSetCode=DCSP_COLTIVAZIONI# (accessed June, 2023).

Kalinowski ST, Taper ML, Marshall TC. 2007. Revising how the computer program CERVUS accommodates genotyping error increases success in paternity assignment. Mol Ecol. 16(5):1099–1106. 10.1111/j.1365-294X.2007.03089.x

Korkmaz N, Akin M, Koc A, Eyduran S, İlhan G, Sağbaş H, Ercişli S. 2020. Morphological and biochemical diversity among wild-grown carob trees (*Ceratonia siliqua* L.). Folia Horticulturae. 32(1). https://doi.org/0.2478/fhort-2020-0007

Kyratzis AC, Nikoloudakis N, Katsiotis A. 2019. Genetic variability in landraces populations and the risk to lose genetic variation. The example of landrace 'Kyperounda'and its implications for ex situ conservation. PLoS One. 14(10):e0224255. https://doi.org/10.1371/journal.pone.0224255

La Malfa S, Avola C, Brugaletta M, La Rosa G, Muratore G. 2012. Morphological and technological characterization of different carob cultivars in Sicily. Acta Horticulturae, In: XXVIII Int Hortic Congr Sci Hortic People Int Symp. 940: 207–212. https://doi.org/10.17660/ActaHortic.2012.940.27

La Malfa S, Brugaletta M, Caruso M, Gentile A. 2007. La biodiversità del carrubo: aspetti bioagronomici e molecolari. Riv di Fruttic e di Ortofloric. 69(6):44–48.

La Malfa S, Currò S, Douglas AB, Brugaletta M, Caruso M, Gentile A. 2014. Genetic diversity revealed by EST-SSR markers in carob tree (*Ceratonia siliqua* L.). Biochem Syst Ecol. 55:205–211. https://doi.org/10.1016/j.bse.2014.03.022

Marchese A, Tobutt KR, Caruso T. 2005. Molecular characterisation of Sicilian *Prunus persica* cultivars using microsatellites. J. Hortic. Sci. Biotechnol. 80(1):121–129. https://doi.org/10.1080/14620316.2005.11511902

Marchese A, Bonanno F, Marra FP, Trippa DA, Zelasco S, Rizzo S, Giovino A, Imperiale V, Ioppolo A, Sala G, Granata I, Caruso, T. 2023. Recovery and genotyping ancient Sicilian monumental olive trees. Frontiers in Conservation Science. 4: p.1206832. https://doi.org/10.3389/fcosc.2023.1206832

Marra FP, Caruso T, Costa F, Di Vaio C, Mafrica R, Marchese A. 2013. Genetic relationships, structure and parentage simulation among the olive tree (*Olea europaea* L. subsp. *europaea*) cultivated in Southern Italy revealed by SSR markers. Tree Genet genomes. 9:961–973. https://doi.org/10.1007/s11295-013-0609-9

Ordidge M, Litthauer S, Venison E, Blouin-Delmas M, Fernandez-Fernandez F, Höfer M, Kägi C, Kellerhals, M, Marchese A, Mariette S, Nybom H. 2021. Towards a Joint International Database: Alignment of SSR marker data for European collections of cherry germplasm. Plants, 10(6): 1243. https://doi.org/10.3390/plants10061243

Perrier X, Jacquemoud-Collet JP. 2006. DARwin software, https://darwin.cirad.fr/

Ramón-Laca L, Mabberley DJ. 2004. The ecological status of the carob-tree (*Ceratonia siliqua*, Leguminosae) in the Mediterranean. Bot J Linn Soc. 144(4):431–436. https://doi.org/10.1111/j.1095-8339.2003.00254.x

Theophilou IC, Neophytou CM, Constantinou AI. 2017. Carob and its Components in the Management of Gastrointestinal Disorders. J Hepatol Gastroenterol. 1(5).

Tous J, Romero A, Batlle I. 2013. The Carob tree: Botany, horticulture, and genetic resources. Hortic Rev 41:385–456. https://doi.org/10.1002/9781118707418.ch08

Tzatzani TT, Ouzounidou G. 2023. Carob as an Agrifood Chain Product of Cultural, Agricultural and Economic Importance in the Mediterranean Region. Journal of Innovation Economics Management, I140-21.

Venison EP, Litthauer S, Laws P, Denancé C, Fernández-Fernández F, Durel CE, Ordidge M. 2022. Microsatellite markers as a tool for active germplasm management and bridging the gap between national and local collections of apple. Genet. Resour. Crop Evol. 69(5):1817–1832. https://doi.org/10.1007/s10722-022-01342-5

Venturi M, Piras F, Corrieri F. et al. 2022. The multifunctional role of linear features in traditional silvopastoral systems: the sabana de morro in Dolores (El Salvador) and the pastures with carob trees in Ragusa (Italy). Biodivers Conserv 31, 2315–2327. https://doi.org/10.1007/s10531-021-02220-9

Viruel J, Haguenauer A, Juin M, Mirleau F, Bouteiller D, Boudagher-Kharrat M, Ouahmane L, La Malfa S, Médail F, Sanguin H. 2018. Advances in genotyping microsatellite markers through sequencing and consequences of scoring methods for *Ceratonia siliqua* (Leguminosae). Appl Plant Sci. 6(12):e01201. https://doi.org/10.1002/aps3.1201

Vourdoubas J, Makris P, Kefalas J, Kaliakatsos G 2002. In Proceedings of the 12th National Conference and Technology Exhibition on Biomass for Energy, Industry and Climate Protection, Amsterdam:489-493

Zemouri Z, Djabeur A, Frimehdi N, Khelil O, Kaid-Harche M, 2020. The seed diversity of Carob (*Ceratonia siliqua* L.) and the relationship between seeds color and coat dormancy. Scientia Horticulturae. 274:p.109679. https://doi.org/10.1016/j.scienta.2020.10967

Zunft HJF, Lüder W, Harde A, Haber B, Graubaum HJ, Koebnick C, Grünwald J. 2003. Carob pulp preparation rich in insoluble fibre lowers total and LDL cholesterol in hypercholesterolemic patients. Eur J Nutr. 42:235–242. https://doi.org/10.1007/s00394-003-0438-y

Caryologia
International Journal of Cytology, Cytosystematics and Cytogenetics

Firenze University Press
www.fupress.com/caryologia

OPEN ACCESS

Citation: Köseoğlu, E., & Aytürk, Ö. (2023). Microtubule response to salt stress. *Caryologia* 76(3): 51-62. doi: 10.36253/caryologia-2229

Received: July 5, 2023

Accepted: January 19, 2024

Published: February 29, 2024

Data Availability Statement: All relevant data are within the paper and its Supporting Information files.

Competing Interests: The Author(s) declare(s) no conflict of interest.

ORCID

ÖA: 0000-0002-8652-7545

Microtubule response to salt stress

Emre Köseoğlu, Özlem Aytürk*

Department of Gastronomy and Culinary, University of Maltepe, Istanbul, Turkey
*Corresponding author. E-mail: ozlemayturk@maltepe.edu.tr

Abstract. This study has aimed to investigate the relationship between salt stress, programmed cell death (PCD) and microtubule distribution in terms of duration and stress dose. PCD is an important mechanism that benefits living organisms throughout their lives. On the other hand, PCD is an indirect effect that reduces efficiency when it occurs under stress. In this research The maize (*Zea mays*) roots were exposed to salt stress with 0, 50, 100, 300 and 500 mM NaCl. The prepared paraffin sections of these five groups were subjected to DAPI (4-6-diamidino-2-phenylindole) and TUNEL analysis to study the morphological changes caused by stress-induced nuclear degeneration. PCD was determined. Microtubule labeling analysis was performed on the tissues to determine whether there were stress-induced microtubule changes in these cells and disturbances were found; they exhibited aggregation, regional thickening, and random distribution around the nucleus and vacuole and under the cell wall. When all groups were evaluated, cells exposed to a salt concentration of 50 mM (even after 24 hours) were significantly less damaged than cells at other concentrations (100, 300, and 500 mM) at each time point. The rate of progression and spread to the whole tissue was significantly higher at 300 and 500 mM salt concentrations compared to the other groups. To reduce economic losses in salty soils, it is of great importance to fully investigate stress. The data that will emerge from our research, which is the subject of a small number of studies, will help to understand the mechanism of stress, microtubule and PCD.

Keywords: maize, microtubules, programmed cell death, salt stress, TUNEL.

INTRODUCTION

Due to their stability in the soil, plants come in for abiotic stress factors along their lifetime that affect their physiological and biochemical mechanisms (Salika and Riffat 2021; Koyro et al. 2012). This effect leads to a decrease in plant yield (Yadav et al 2020) or has more serious consequences. Since stress conditions reduce the productivity of plants and the number of people in the world are growing day by day, it is necessary to reverse the negative situations in plants that people consume as food, increase the quality of plants and minimize their losses. With this planned study, one of the impacts of salt stress on maize was investigated and support was provided to solve the stress-related problems for which people are sought as food.

Maize belongs to the Poaceae family. It is generally grown in hot and humid areas. (Rouf et al 2016) The maize plant is used worldwide for both

consumption and industrial purposes. Its seed is one of the cold-tolerant seeds that can be kept a few years under optimal conditions and has low moisture content (Macar 2017). Its kernel contains 70% starch, 10% protein, 5% fat, 2% sugar, and a lot of vitamin A. Environmental factors (drought, salinity, high temperatures, etc.) are important factors affecting the maize yield worldwide and Turkey. (Tollenaar and Lee 2002) Our literature research of maize plants revealed that research on stress-programmed cell death and microtubules in maize is insufficient.

We chose salt, an element that stresses plants, as a research topic. In an earlier study, the salt tolerance of Maize *(Zea mays* L.) plants was determined to be 50-75 mM in sensitive genotypes and 125-150 mM in resistant genotypes. It was found that 17 different maize varieties were seriously affected at all levels after 150 mM. (Aydınoğlu and Akgül 2021). The time at which the maize is exposed to salt stress is also important. In short-term exposure, growth is affected by osmotic stress. There is an accumulation of sodium in the roots of the plant, the seed cannot absorb enough water, and germination does not occur in time (Farooq et al. 2016). Akay et al. (2019) showed that by increasing salinity, root length is negatively affected, and its elongation decreases by 82%, as well as, germination rate, seedling vigor and root to stem ratio decreases. These studies show that plants undergo some morphological changes under stress conditions. Salt stress, which is our research topic, causes many negative conditions for the maize plant. For example, the stress factors salinity, UV radiation, temperature, water, light, etc. can trigger the Programmed cell death (PCD) process (Sychta et al. 2021; Petrov et al. 2015).

PCD is a controllable mechanism. PCD is observed as long as the plant life cycle continues (Rocha and Hernandez, 2017). Characteristic features indicating the presence of PCD have been identified in plant tissue studies. DNA fragmentation, increased vacuolization, chromatin condensation are some of the most obvious (Sychta et al 2021). Internucleosomal fragmentation, which is a common consequence of PCD, is detected by the TUNEL assay (Petrov et al. 2015). The PCD process occupies an important place in the developmental stages of the plant. All these stages take place regularly. For example, the formation of unisexual flowers, the degradation of root tissue, the opening of anthers (Gunawardena 2008). Although PCD is important for the continuation of the life cycle of the plant, it is a process that seriously damages the maize plant under stress (Choudhury et al. 2017; Rocha and Hernandez 2017), there is almost no information on how this process affects microtubules. Here, the relation between PCD and microtubule distribution is investigated in detail.

Microtubules, which are dynamic structures, are perfect transformation devices (Mollinedo and Gajate 2003). Microtubules play a role in various cellular tasks such as intracellular movement, intracellular transport, and proliferation. (Borowiak et al. 2015). A microtubule has an average diameter of 21 nm and can be up to 10 µm long. Microtubules appear as bundles around chromatin concentrated in the nuclei of newly formed plant cells. (Lü et al. 2007). Plant cortical microtubules create a non-centrosomal arrangement that anchors laterally to the plasma membrane (Gutierrez et al., 2009; Crowell et al., 2011; Sampathkumar et al., 2013). This arrangement's course is directed by cellulose synthase-interacting proteins (Bringmann et al., 2012; Li et al., 2012), which act on the complex (Paredez et al., 2006).

Many different factors, including stress, can affect microtubule organization. For example, in the studies of Blancaflor et al. (1998), it was observed that when roots are exposed to aluminum stress, microtubule sensitivity decreases, their arrangement is disrupted, they are randomly organized, and their reorganization is prevented in the inner cortex, outer cortex, and epidermis. In addition, symbiotic and non-pathogenic fungi are known to alter the sequence of microtubules in plant cells (Uetake and Peterson 1998).

These findings contribute to the latest research in the field. Based on the lack of parts of literature, our study aimed to investigate the effect of salt concentrations (50 mM, 100 mM, 300 mM, and 500 mM) on maize roots. The study utilized TUNEL analysis to examine whether programmed cell death (PCD) was induced, and also analyzed the microtubule organization under PCD stress.

MATERIAL AND METHOD

In this project, monoecious maize, which belongs to the Poaccea family, was selected as the study material. The research was conducted on five groups under laboratory conditions using maize plant seeds, with three replicates for each group (Table 1).

Fluorescence microscopic studies

Fluorescent staining applications, DAPI (4-6-diamidino-2-phenylindole) and TUNEL (terminal deoxynucleotidyl transferase dUTP nick end labeling: in situ end labeling) used to detect PCD and microtubule proteins used for imaging. 1.5-2.0 cm long roots under salt stress

Table 1. Salinity of the solutions used to generate salt stress.

	groups				
	1. group	2. group	3. group	4. group	5. group
salt concentration	control-0 mM	50 mM	100 mM	300 mM	500 mM
salt treatment time	0	15min 30min 1h 2h 6h 12h 24h			

were fixed with FAA (formalin-acetic-alcohol). Then, 3 µm sections were taken using the paraffin embedding method. Fluorescence microscopic observations using Olympus BX -51 fluorescence microscopy were made by staining the obtained sections with dyes suitable for the method to be used. To detect changes in nuclear morphology caused by salt concentration, we performed staining with 4',6-diamidine-2'phenylindole dihydrochloride (DAPI), taking into account the studies conducted by Schweizer (1976). We stained our samples with 1 µg ml-1 DAPI for 1 hour in the dark. After staining, we washed the samples 4-6 times with PBS so that no residual dye was present. We performed our TUNEL (terminal deoxynucleotidyl transferase dUTP nick end labeling: in situ end labeling) analysis using the ApopTag® Plus Fluorescein In situ Apoptosis Detection Kit according to the kit manufacturer's instructions (Chemicon, Temecula, CA, USA).

Microtubule labeling analysis

The characteristics of the intracellular skeletal system of maize cells were examined. Microtubules were labeled with FITC (fluorescein isothiocyanate) and their changes were followed, and data were obtained on the change (relationship, location) of microtubules in the cytoplasm, nucleus, and cell wall. The microtubule labeling study performed on our thin-sectioned samples was carried out using a method obtained by modifying the data from the studies of Kumagai et al. (2001). The sectioned samples were placed on slides coated with poly-L-lysine. First, the samples were washed thoroughly in 50 mM PBS (pH 6.8) for 30 min. To destroy the cell wall, the preparations were treated with enzymes dissolved in 0.4 M mannitol: 0.5% cellulose for 25 minutes, 2% driselase for 15 minutes, and finally 1% cellulysin for 16 minutes. The air-dried slides were permeabilized in methanol cooled at -20°C for 10 minutes. Then they were rehydrated with these chemicals: 1% Triton X-100, 0.1 M PIPES, 2 mM EGTA, 1 mM MgSO4, and 0.4 M mannitol (pH 6.9) buffer for 30 minutes. Then the labeling step with antibodies was started. Samples were incubated with anti-a-tubulin antibody (IgG, Sigma-Aldrich)/buffer (ratio 1/50) for 1 hour at 37°C in a humidified oven in the dark. After incubation, samples were washed 1-2 times with a buffer. Fluorescent Goat Anti-Rabbit IgG (secondary antibody, Sigma-Aldrich) / buffer (ratio 1/24) was incubated in an oven at 37°C for 30 minutes. After incubation, slides were washed 3 times with a buffer for 2 minutes. To prevent the loss of fluorescence radiation, the samples were bound with 1,4-diazabicyclo-(2,2,2) (DABCO) and observations were started in a short time. A KAMERAM fluorescence camera and an Olympus BX -51 fluorescence microscope (wavelength of 420-490 nm) were used for imaging, analyzes were performed using KAMERAM software, and photographs were taken.

RESULTS

Here, root tissue was first exposed to different salt concentrations considering the results of literature studies. Five groups were formed, namely the control group (group 1) and 50 Mm (group 2), followed by 100 Mm (group 3), 300 Mm (group 4) and 500 Mm (group 5). The preparations of these five groups were subjected to DAPI (4-6-diamidino-2-phenylindole) and TUNEL analysis to study in detail the morphological changes caused by stress-induced nuclear degeneration. It was determined that the tissue cells were subjected to PCD. Microtubule labeling analysis was performed on the tissues to determine whether there were stress-induced microtubule changes in these cells, and all results were discussed below.

Findings of DAPI Staining

Findings of the group 1 (control)

In this group, which we determined to be the control, the plant roots were treated with pure water only. Fluorescence microscopy observations of DAPI staining in the cells showed that the nuclear morphologies were mostly smooth and spherical (Figure 1a-d).

Findings of the group 2

The cells of root tissue stressed with 50 mM salt for 15 minutes, chromatin condensation disorder was rare, seen in a few cells at the edge of the root tissue (figure 1e, arrows). When the time was increased to 30 minutes, chromatin condensation of cells in the edge region was almost twice as high as after 15 minutes. In case of extension to 1 hour, the number of cells with chromatin condensation increased rapidly in the central region, but their numbers were relatively small compared with the peripheral region. In case of extension to 2 hour (figure 1f, arrows), and then up to 6 hours, the cells with chromatin condensation increased in almost the whole tissue, while it has not been observed that the cells in the lower part of the root tissue have not changed up to this stage, additionally the cells whose nuclei were fragmented in 6 hours began to increase. When the duration was extended to 12 h (figure 1g, arrows) and 24 h, there wasn't a crucial difference between them. It was shown that the nuclei in relatively many cells of the 1.5-2.0 cm tissue lost their spherical shape, except for the region of the root tip, and the tissue was extremely damaged.

Findings of the group 3

By examining the DAPI staining and fluorescence microscopy images of the cells of root tissue stressed with 100 mM salt for 15. minute, it was found that these cells that showed chromatin condensation in the root tissue were regional and had a similar degree of deterioration as the 15 min and 30 min of 2. groups. In contrast to the 15. minute of the 2. group, a few cells in the middle region showed deterioration in the form of chromatin condensation (figure 1h, arrows). When the time of salt concentration was increased toward 24 h, 30 min in the form of 1, 2h (figure 1i, arrows), 6, 12 (figure 1j, arrows), and 24 h, a similar tissue change was observed as in the 2. group, but with faster and more intense chromatin condensation and further nuclear fragmentation.

Findings of the group 4

Examination of fluorescence microscopy images of the cells of root tissue stressed with 300 mM salt for 15 minutes shows that they are in a similar state to cells of root tissue exposed to a salt concentration of 100 mM for 2 hours, and that damage has and that damage has progressed to a very early stage observed. It was found that when the time was increased from 15 minutes (figure 1k, arrows) to 30 minutes, 1, 2 (figure 1l, arrows), 6, 12 (figure 1m, arrows), and 24 hours, the damage increased greatly in the marginal and middle regions, while it was less advanced in the cells of the root tip tissue. It was observed that chromatin was not properly distributed in the degraded cells, but partially condensed and the cells lost their spherical shape . In contrast to the 2nd and 3rd groups, it was observed that the staining was intense at all stages. While there was a high level of stress induced degradation of the cells, particularly after the 1st hour, it was observed that the integrity of the tissue was not compromised, and the pseudo-blinding was more intense than in the previous two groups.

Findings of the group 5

Examination of the fluorescence microscopy images of the cells of root tissue stressed with 500 mM salt for 15 minutes showed a similar picture to the cells exposed to a salt concentration of 300 mM for 30 minutes and 1 hour and cellular defects were seen in more than half of the tissue (figure 1n, arrows). In case of extension to 30 minutes, 1, 2 (figure 1o, arrows), 6, 12 (figure 1p, arrows), and 24 hours, it was found that the defects started in the marginal and middle region as in all previous groups, but spread very early and rapidly to more than half of the tissue. It was found that the pseudo glare became more intense from the 1st hour and the integrity of the tissue was severely damaged.

When all groups were evaluated, cells exposed to a salt concentration of 50 mM (even after 24 hours) were significantly less damaged than cells at other concentrations (100, 300, and 500 mM) at each time point. The rate of progression and spread to the whole tissue was higher at 300 and 500 mM salt concentrations compared to the other groups.

Findings of TUNEL analysis

Starting from the control group, fluorescence microscopy images of DAPI staining root tissues

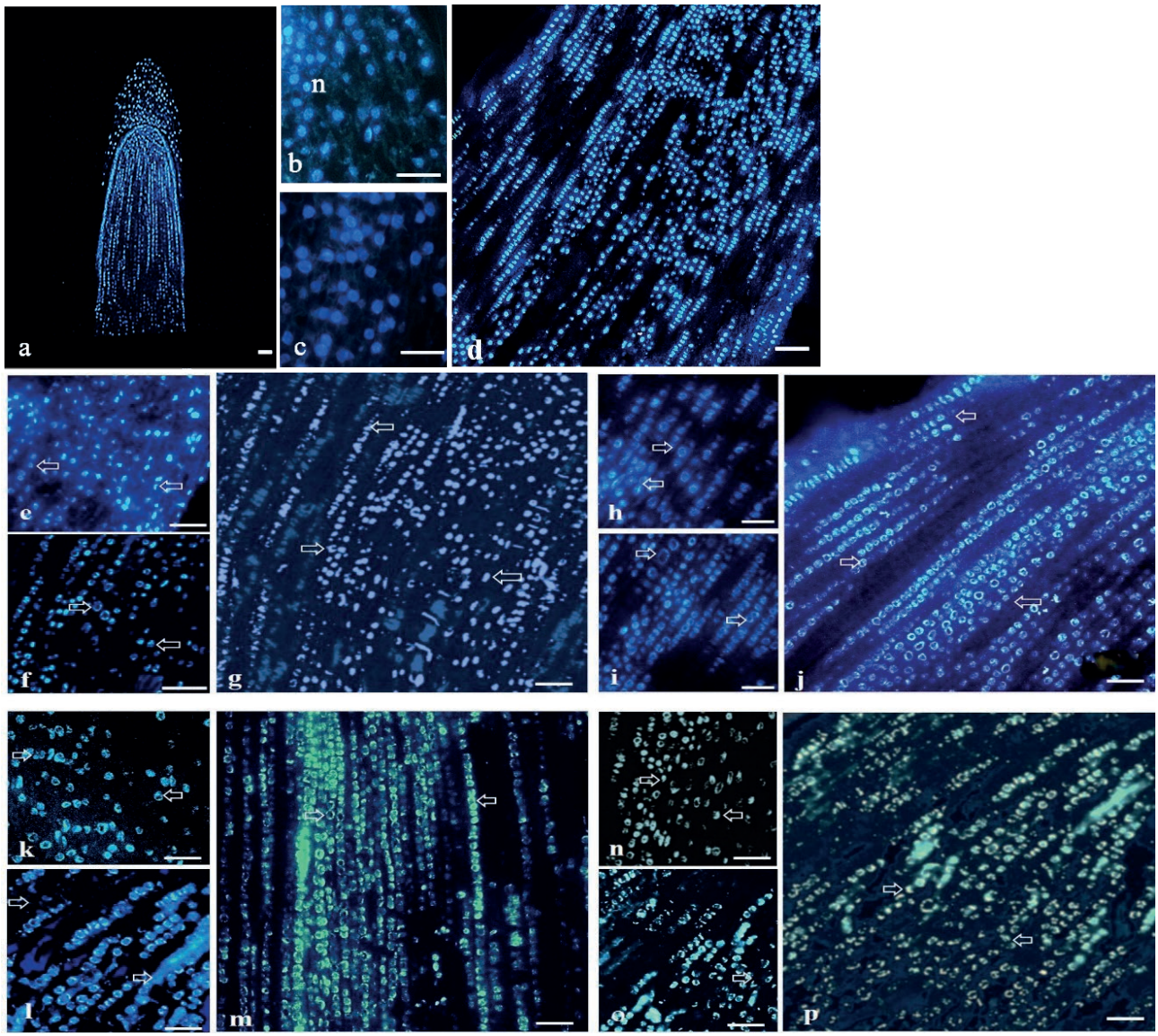

Figure 1a-p. Fluorescence micrographs showing DAPI staining in the cells of maize root tissue (arrow). a-d. group (control): **a.** overall view of root tissue, **b, c.** image of nuclei, d. magnified view of texture. e-p*. Condition of the cells exposed to salt concentration. **e-g.** at 50 mM; e. 15min, f. 2h, g. 12h. **h-j.** at 100 mM, h. 15min, i. 2h, j. 12h. **k-m.** at 300 mM, k. 15min, l. 2h, m. 12h. **n-p.** at 500 mM, n. 15min, o. 2h, p. 12h. Bars, a. 50 µm, b,c.10 µm and d-p.50 µm. * To avoid repetition in similar phases, the situation is presented with the images of only 3 groups.

exposed to salt stress in the 50, 100, 300, and 500 mM groups respectively for 15 and 30 minutes and for 1, 2, 6, 12, and 24 hours were examined (Figure 2a-d7). Unusual differences in the tissue cells, such as rapid vacuolization, enlargement and elongation of the cells, as well as increased staining, irregularities in nuclear shape, and changes in chromatin condensation, indicated that stress-induced apoptosis might occur in these tissues. To confirm this assumption, TUNEL analysis was performed on the tissues and a detailed study of cell death was continued. The TUNEL reaction confirmed the formation of DNA breaks and the appearance of PCD in these cells by fluorescent labeling.

Findings of the group 1 (control)

When the fluorescence microscopy image of the TUNEL staining of the maize plant was examined, the TUNEL staining in the cells of the control group showed negative results.

Findings of the group 2

When the fluorescence microscopy images of TUNEL analysis of the cells of root tissue stressed with 50 mM salt for 15 minutes were examined, it was found that the labeled cells were located at the edges of the tissue, and a slightly positive result was obtained. In the case of extension to 30 minutes, it was found that the labeled cells formed at the edges and at the center of the tissue, and the labeled cells increased relatively compared to 15 minutes at the edge of the tissue. When the salt stress was applied for 1 hour by doubling the time, it was determined that the cells labeled at both the edge and at the center of the tissue increased rapidly. When the time is continuously increased to 2, 6, 12 and 24 hours, it is seen that the signs spread to the entire root tissue from the second hour, that is, the number of positive cells increases up to the 24 hour group. In each group, relatively less radiating cells were observed in the root tip cells than in the middle and marginal cells of the root tissue. At the stage when the time was increased to 24 hours, some of these radiations might be pseudo-radiation, because the number of radiating cells increased greatly, but the nuclei lost their structure due to the damage caused by the stress in the tissue. No completely obvious auto fluorescence was found in the root tissue at any stage (Figure 2a-a7).

Findings of the group 3

Examination of fluorescence microscope images of TUNEL analysis of stem tissue cells stressed with 100 mM salt for 15 minutes, as in group 2, revealed that there was a slight positive labeling in the peripheral parts of this tissue, which was more pronounced than in the central parts.In case of extension to 30 minutes and then to 1 hour, a significantly rapid increase in positive reaction was observed in the edge region. When the time was continuously increased up to 2, 6, 12, and 24 hours : after 1 hour, the positive reaction spread to the entire maize root tissue, unlike the 2. group, i.e., marks formed at the edge and center, at the root tip, and at the upper parts of the root. Both in the 12 and 24-hour

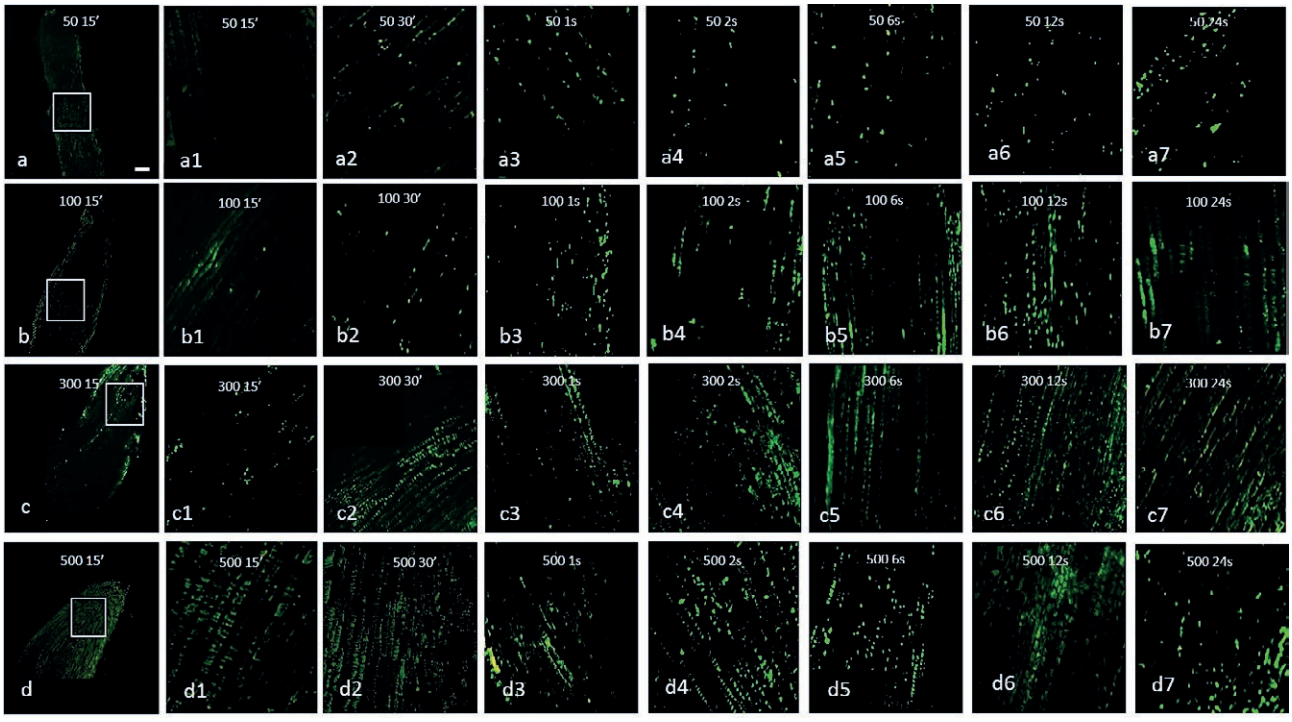

Figure 2a-d7. Fluorescence micrographs with TUNEL staining in cells of root tissue exposed from 50 to 500 mM salt concentration. The a'-g' photos show an enlarged view of the marked area (square) in the a-g photos. Bars 10 µm (a'-g'), 50 µm (a-g). 7a-g'. Fluorescence micrographs with TUNEL staining in cells of root tissue exposed to 100 mM salt concentration. The a'-g' photos show an enlarged view of the marked area (square) in the a-g photos. Bars 10 µm (a'-g'), 50 µm (a-g).8a-g'. Fluorescence micrographs with TUNEL staining in cells of root tissue exposed to 300 mM salt concentration. The a'-g' photos show an enlarged view of the marked area (square) in the a-g photos. Bars 10 µm (a'-g'), 50 µm (a-g).9a-g'. Fluorescence micrographs with TUNEL staining in cells of root tissue exposed to 500 mM salt concentration. The a'-g' photos show an enlarged view of the marked area (square) in the a-g photos. bars 10 µm (a'-g'), 50 µm (a-g).

groups, as well as in the 24-hour group of the 2. group, it was observed that the structures of the cells deteriorated due to the damage caused by the stress, so some of the radiations formed in the tissues were considered as pseudo-radiations. Thus, it was found that the deterioration caused by 100 mM salt concentration occurred in a shorter time than the deterioration caused by 50 mM salt concentration, but the degree of damage was similar in these two groups (Figure 2b-b7)

Findings of the group 4

When we applied the TUNEL assay to cells of root tissue stressed with 300 mM salt for 15 minutes, we saw that the result was different from the results of the 2. and 3. groups for 15 minutes: the marking was more pronounced in the peripheral region. At 30 minutes, the irradiation rapidly increased in both the middle and marginal sections, and the markings in the nuclei exposed to PCD were more frequent than in the 2. and 3. groups. At 1 hour, the irradiation spread to all parts of the root, as in the 3. group, but the markings in the nuclei exposed to PCD increased more. When the time was gradually increased to 2, 6, 12, and 24, it was determined that the density of the positive in the root tissue was similar in all these periods, the nuclei lost their structure, and the markings spread throughout the root. As a result the positive reaction formed by the 300 mM salt concentration was much more intense from the 1st hour, in contrast to the positive reactions formed by the 50 and 100 mM salt concentrations. (Figure 2c-c7)

Findings of the group 5

Examination of fluorescence microscopy images of TUNEL analysis of the cells of root tissue stressed with 500 mM salt for 15 minutes revealed that the tissue showed a positive response of low intensity, with flash spreading to the entire root tissue compared to the previous groups, but the intensity was weaker. The situation seen at 15 min continued at 30 min, with most cells in the edge and middle parts of the root tissue being positive. When the time was doubled, i.e., to 1 hour, it was observed that false glow occurred everywhere in the root and their structures could not be determined, i.e., there were cells with compromised integrity. This situation was observed in the last stages in groups 2 and 3. In the 4. group, it was observed later, almost 12 hours, in contrast to the 5. group. When the time was gradually increased to 2, 6, 12, and 24 hours, the false positive reactions were more evident at the edge and middle of the root, they were intense in the nuclei exposed to PCD, and these positive reactions were strongly positive. The intensity of the positive response persisted after 24 hours, as well as the presence of amorphous cells and nuclei, and that the positive reaction in most roots were false radiations. The structure of the root tissue after 12 and 24 hours was similar to that of the 4. group (Figure 2d-d7)

Findings of microtubule labeling

In our study, the characteristics of microtubule changes associated with stress and PCD of cells of root tissue were determined. For this purpose, root tissue sections were collected. Microtubule proteins belonging to these tissue cells were labeled with FITC (fluorescein isothiocyanate) and visualized by fluorescence staining analysis, and data were obtained on the changes (relationship, location) of microtubules in the cell wall, nucleus and cytoplasm, which we have described below against salt stress.

Findings of the group 1 (control)

In the first group, which we determined to be the control, it was observed that the microtubules in the cells of the root tissue were mostly concentrated around the nucleus and under the cell wall (anchors laterally to the plasma membrane) and rarely formed short extensions from the nucleus to the cell wall. It was observed that the microtubules under the cell wall formed a thin layer in a parallel arrangement, while the microtubules around the nucleus tightly surrounded the nucleus. They were also found to be located around the vacuoles and generally homogeneously distributed in the cytoplasm (Figure 3a-c).

Findings of the group 2

When the cells of root tissue stressed with 50 mM salt for 15 minutes were examined, it was observed that the regular state of microtubules under the cell wall was disturbed at a low level and very weak clusters were formed at this stage, in which PCD was weakly positive. It was observed that the density of microtubules in the cytoplasm and around the nucleus increased slightly. When the duration was extended to 30 minutes, a situation similar to that observed at 15 minutes was observed, except for the increase in microtubule density. However, when the time was advanced to 1 and 2 hours,

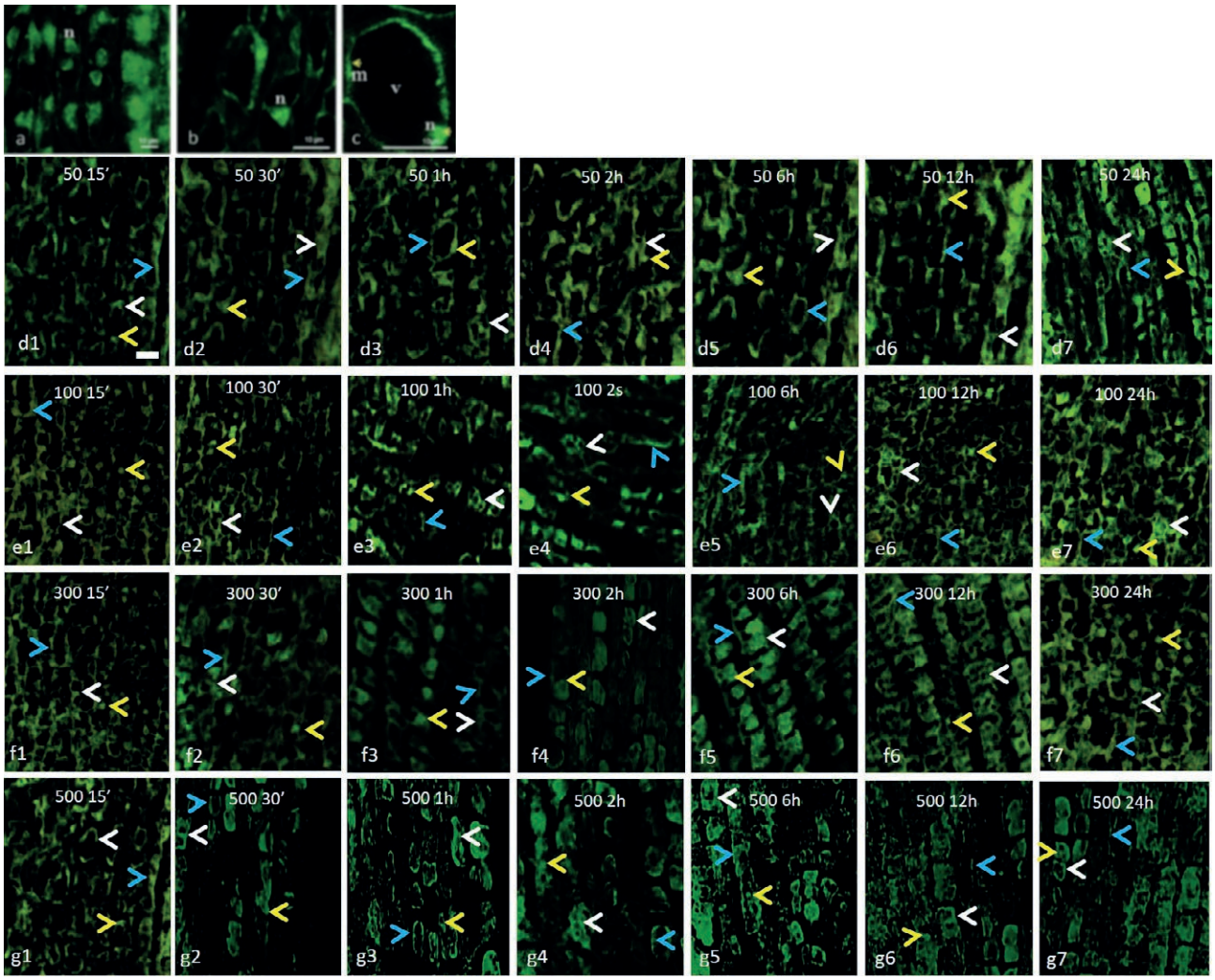

Figure 3a-g7. Analysis of fluorescence staining of microtubule proteins labeled with FITC (flurecein isothiocyanate) in root tissue cells exposed to different salt concentrations. hungry. Control, d1-d7. 50mm, e1-e7. 100mm, f1-f7. 300mM, g1-g7. 500mM. Arrows show where microtubules were examined: under the cell wall (blue arrow), around the nucleus (yellow arrow), around the vacuole (white arrow). Bars, 50 µm (a,b), 10 µm (c-g7).

it was determined that microtubule irregularities, aggregation, and condensation showed a more significant increase. At this stage, it was observed that the regularity of microtubules around the nucleus began to give way to random organization. When the time was extended to 2 hours and then to 6 hours, the microtubule changes observed in the first hour progressed at a moderate rate. It was found that after 6 hours, the change occurred mainly in the form of microtubule condensation, and the increase in irregularities and aggregations was similar to the situation at 2 hours. After 12 and 24 hours, it was observed that the appearance of microtubules changed into a band in which the nucleus and vacuoles were wrapped. At these stages, when PCD was strongly positive, the microtubule bundles were dense and irregularly shaped in many places, and the increase in aggregation was evident (Figure 3d1-d7).

Findings of the group 3

Examination of fluorescence microscopy images of microtubule labeling analyzes of the cells of root tissue stressed with 100 mM salt for 15 minutes revealed that at this stage, when PCD was observed as a weak positive intensity, the regular state of microtubules under the cell wall was disturbed at a relatively low level and aggregates were formed. In the cytoplasm and micro-

tubules around the nucleus, it was observed that the density increased slightly as under the cell wall. It was observed that the situation did not change significantly when the time was extended to 30 minutes, and when it was extended to 1 hour, microtubule density and microtubule disruption increased significantly in all regions. After 2 and 6 hours, microtubule irregularity, aggregation, and condensation had slightly increased. In addition to density, it was observed that random order began to deteriorate, especially for microtubules around the nucleus. When time was extended to 12 hours, microtubule condensation, increased reticular appearance, and irregular shape changed relatively little. After 24 hours, the irregularity was more pronounced than expected. The density around the nuclei and vacuoles covered a quarter of the cell (Figure 3e1-e7).

Findings of the group 4

When the fluorescence microscopy images of microtubule labeling analysis of the cells of root tissue stressed with 300 mM salt for 15 minutes were examined, It was observed that the microtubules under the cell wall, normally in the form of parallel extensions, were rearranged by 50% and these parallel arrays began to aggregate. The aggregation increased at this stage where PCD was observed to be moderately positive. A rapid increase in the density of microtubules in the cytoplasm and around the nucleus was observed. When the time was extended to 30 minutes and then to 1 hour, it was observed that, in contrast to the salt concentrations of 50 and 100 mM, high aggregations occurred in all regions at these stages and the regularity of microtubules was severely disturbed. When the time was gradually prolonged to 2, 6, 12, and 24 hours, it was observed that the appearance of microtubules changed into a dense band, and at these stages, when PCD was strongly positive, the microtubule bundles were irregularly shaped in many places and the increase in aggregation was obvious (Figure 3f1-f7).

Findings of the group 5

Examination of fluorescence microscopy images of microtubule labeling analysis of the cells of root tissue stressed with 500 mM salt for 15 min revealed a rapid increase in microtubule density in the cytoplasm and around the nucleus, where PCD was observed to be moderately positive. When the time was extended to 30 minutes, it was observed that their regular state under the cell wall was relatively disturbed and an intense increase in their aggregation was observed. It was observed that after these stages at 1, 2 and 6 hours, the microtubule bundles formed densely and irregularly in many places, and the clusters increased even more. After 12 and 24 hours, they had a similar appearance. The microtubules were difficult to observe because most of the cells of the root tissue were destroyed. At these stages, almost the entire cell was covered with irregular microtubule clusters and pseudo-staining (Figure 3g1-g7).

In this study, a fluorescence microscope was used to examine microtubule changes in cellular changes that maize plants undergo when exposed to salt stress. In this study, which is one of the few studies, the relationship between PCD and microtubule distribution was investigated in detail. If we evaluate the results of increased salinity (50, 100, 300 and 500 Mm), we can say that: The results of 15-minute, 30-minute, 1-hour and 2-hour applications are similar to each other, and the results of 6-hour, 12-hour and 24-hour applications are similar. In the PCD process seen as a result of the response of root tissue cells to salt stress of 50 mM, microtubule organization showed clustering, regional thickening, and random distribution around the nucleus and vacuole.

DISCUSSION

In our study, it was found that low and high salt stress can cause programmed cell death (PCD). A review of the literature shows that some studies support our findings, for example, in *Halopyrum mucronatum* at salt stress of 0, 90, 180 and 360 mM, it was found that growth was inhibited with increasing salinity, followed by plant death (Khan and Ungar 2001). TUNEL analysis was applied to determine the damage that occurred when 200, 300, 400, and 500 mM salt stress acted on the cells of the root tissue of the rice plant. TUNEL analysis gave positive results and it was found that the plant underwent PCD. As a result of 500 mM salt stress, chromatin condensation and cellular deformation were observed in the cells of the root tissue; DNA agarose gel electrophoresis was performed and breaks were observed (Yazdani and Mahdieh 2012). Another study discovered that the high salt concentrations augmented the quantity of cells exhibiting TUNEL-positive nuclei and DNA ladders in roots of both Barley and Arabidopsis. (Huh et al. 2002; Katsuhara and Shibasaka 2000; Li and Dickman 2004). Thus, when the plant is under salt stress, it can induce PCD (Williams and Dickman 2008) As shown in previous studies, stress causes PCD. Cell death can occur at different salt levels. All of these studies support our findings. In addition to salt stress, there are also studies that have found PCD in other types of stress. For

example, when water stress affected root tissue pea cells for 6, 12, and 24 hours, chromatin condensation and clusters were detected in the cells, TUNEL analyzes and DNA agarose gel electrophoresis experiments were performed, and apoptosis-like findings were noted (Gladish et al. 2006). Wang et al. (1996) demonstrated positivity by performing TUNEL analysis to investigate PCD in a toxin-treated tomato plant and found that 50% of the cells were subjected to PCD by the TUNEL assay. The root tissue of the *Vicia faba* plant was exposed to caffeine stress and the differentiations in the cells indicated the formation of PCD. COMET and TUNEL assays were applied and positive PCD results were obtained (Rybaczek et al. 2015).

In our study, it was observed that TUNEL positivity did not increase proportionally with increasing stress. According to the literature, the plant can achieve a certain level of recovery in the early stages of PCD. Cells that have undergone chromatin condensation can perform healing studies by activating early repair mechanisms (Ciniglia et al. 2010). As can be seen from our results, there are also PCD outcomes that do not parallel the dose or duration of stress.

Plant microtubules have been the subject of numerous studies (Zhao et al. 2021; Rui and Dinneny 2020; Hashimoto 2015). The subject of our study, the relationship between stress, PCD, and microtubules, is one of the few studies (Smertenko and Franklin-Tong 2011; Yanık et al. 2017). Based on the observations of DAPI staining, our studies have shown that prolonged salt can cause stress-induced damage even at low doses. The initial dose of stress-induced cell death was slightly higher and the time of onset was slightly longer. Microtubule change in stressed tissue progressed more slowly than stress-induced damage. Studies have been performed, some of which are consistent with our results. Some of the results are: in the stress study with bisphenol in maize root tissue, it was found that bisphenol disrupted microtubule arrangement and mitosis. It was observed that the microtubule arrangement became disorganized and cell division was disrupted or completely stopped. As the amount of bisphenol increased, the shapes and directions of microtubules changed (Stavropoulou et al. 2018). Cortical microtubules are located under the cell wall (anchors laterally to the plasma membrane). Microtubules were found to affect the shape of the cell as a result of the application of mechanical stress in the maize plant (Landrein and Hamant 2013). It was also observed that microtubules changed when light, auxin, and mechanical stress were applied to the coleoptile tissue of the maize plant. (Fischer and Schopfer, 1997). As additionally to literature in this study, in the PCD process seen as a result of the response of root tissue cells to salt stress of microtubule organization showed clustering, regional thickening, and random distribution around the nucleus and vacuole. It was thought that the rapid vacuolization that occurred during the PCD process triggered the condensation around the nucleus and in the cytoplasm.

ACKNOWLEDGEMENTS

Our investigation was supported by MUKKAM (Maltepe University Cancer and Stem Cell Research Centre). We thank MUKKAM for providing laboratory resources.

FUNDING

This project was supported by Maltepe University Research Foundation (grant number FEN -13571271-604).

REFERENCES

1. Akay HE, Öztürk İ, Sezer M, Bahadır C. 2019. Effects of different salt concentrations on germination and early seedling growth in sugar maize (*Zea mays* L.) cultivars. Turk J Agric For. 7(2):103-108. https://doi.org/10.24925/turjaf.v7isp2.103-108.3160
2. Aydınoğlu F, Akgül B. 2021. Mısır (*Zea mays* L.) bitkisinin üşüme stresine toleransı sırasında yaprak büyüme bölgelerinde mikroRNA aracılıklı redoks regülasyonunun incelenmesi. Anadolu Tarım Dergisi. 2019:1–11. https://doi.org/10.7161/omuanajas.482710
3. Blancaflor EBD, Jones L, Gilroy S. 1998. Alterations in the cytoskeleton accompany aluminum-induced growth inhibition and morphological changes in primary roots of maize. Plant Physiol. 118(1):159–172. https://doi.org/10.1104/pp.118.1.159
4. Borowiak MW, Nahaboo RM, Nekolla K, Jalinot P, Hasserodt J, Rehberg M, Delattre M, Zahler S, Vollmar A, Trauner D, Thorn-Seshold O.. 2015. Photo Switchable Inhibitors of Microtubule Dynamics Optically Control Mitosis and Cell Death. Cell. 162(2):403–411. https://doi.org/10.1016/j.cell.2015.06.049
5. Bringmann, M., Li, E., Sampathkumar, A., Kocabek, T., Hauser, M. T., and Persson, S. 2012. POM-POM2/cellulose synthase interacting1 is essential for the functional association of cellulose synthase and

microtubules in Arabidopsis. Plant Cell 24:163–177. https://doi.org/10.1105/tpc.111.093575
6. Choudhury FKR, Rivero M, Blumwald E, Mittler R. 2017. Reactive oxygen species abiotic stress and stress combination. Plant J. 90(5):856–867. https://doi.org/10.1111/tpj.13299
7. Ciniglia C, Pinto G, Sansone C, Pollio A. 2010. Acridine orange/Ethidium bromide double staining test: A simple In-vitro assay to detect apoptosis induced by phenolic compounds in plant cells. Allelopathy J. 26(2):301–308.
8. Crowell, E. F., Timpano, H., Desprez, T., Franssen-Verheijen, T., Emons, A. M., Hofte, H., et al. 2011. Differential regulation of cellulose orientation at the inner and outer face of epidermal cells in the Arabidopsis hypocotyl. Plant Cell 23:2592–2605. https://doi.org/10.1105/tpc.111.08733
9. Farooq M, Hussain M, Wakeel A, Kadambot HMM, Farooq Hussain M, Wakeel A, Siddique K, HM, Farooq M, Hussain M, Wakeel A. 2016. Salt stress in maize:effects resistance mechanisms and management Agron. Sustain. Dev. 35:461–481. https://doi.org/10.1007/s13593-015-0287-0
10. Fischer K, Schopfer P. 1997. Interaction of auxin light and mechanical stress in orienting microtubules in relation to tropic curvature in the epidermis of maize coleoptiles. Protoplasma. 196(1–2):108–116. https://doi.org/10.1007/BF01281064
11. Gladish D, Xu KJ, Niki T. 2006. Apoptosis-like programmed cell death occurs in procambium and ground meristem of pea (*Pisum sativum*) root tips exposed to sudden flooding. Ann Bot-London. 97(5):895–902. https://doi.org/10.1093/aob/mcl040
12. Gunawardena AH. 2008. Programmed cell death and tissue remodeling in plants. 59(3):445–451. https://doi.org/10.1093/jxb/erm189
13. Gutierrez, R., Lindeboom, J. J., Paredez, A. R., Emons, A. M., and Ehrhardt, D. W. 2009. Arabidopsis cortical microtubules position cellulose synthase delivery to the plasma membrane and interact with cellulose synthase trafficking compartments. Nat. Cell Biol. 11:797–806. doi: https://doi.org/10.1038/ncb1886
14. Hashimoto, T. 2015. Microtubules in plants. The Arabidopsis Book/American Society of Plant Biologists, 13. https://doi.org/10.1023/B:BILE.0000012896.76432.ba
15. Huh G, Damsz HB, Matsumoto TK, Reddy MP, Rus AM, Ibeas JI, Narasimhan ML, Bressan RA, Hasegawa PM. 2002. Salt causes ion disequilibrium-induced Programmed cell death in yeast and plants. Plant J. 29:649–659. https://doi.org/10.1046/j.0960-7412.2001.01247.x
16. Katsuhara M, Shibasaka M. 2000 Cell death and growth recovery of barley after transient salt stress. J. Plant Res. 113:239–243. https://doi.org/10.1007/PL00013934
17. Khan MA, Ungar IA. 2001. Alleviation of salinity stress and the response to temperature in two seed morphs of *Halopyrum mucronatum* (Poaceae). Aust J Bot. 49(6):777-783. https://doi.org/10.1007/PL00013934
18. Koyro HW, Ahmad P, Geissler N. 2012. Abiotic stress responses in plants: an overview. Environmental adaptations and stress tolerance of plants in the era of climate change, 1-28. https://doi.org/10.1071/BT01014
19. Kumagai F, Yoneda NA, Tomida T, Sano T, Nagata T, Hasezawa S. 2001. Fate of nascent microtubules organized at the M/G1 interface, as visualized by synchronized tobacco BY-2 cells stably expressing GFP-tubulin: time-sequence observations of the reorganization of cortical microtubules in living plant cells. Plant and Cell Physiol. 42(7):723-732. https://doi.org/10.1093/pcp/pce091
20. Landrein B, Hamant O. 2013. How mechanical stress controls microtubule behavior and morphogenesis in plants: History experiments and revisited theories. Plant J. 75(2):324–338. https://doi.org/10.1111/tpj.12188
21. Li W, Dickman MB. 2004 Abiotic stress induces apoptotic-like features in tobacco that is inhibited by expression of human Bcl-2. Biotechnol. Lett. 26:87–95. https://doi.org/10.1023/B:BILE.0000012896.76432.ba
22. Li S, Lei L, Somerville CR, and Gu Y. 2012. Cellulose synthase interactive protein 1 (CSI1) links microtubules and cellulose synthase complexes. Proc. Natl. Acad. Sci. U.S.A. 109:185–190. https://doi.org/10.1073/pnas.1118560109
23. Lü B, Gong Z, Wang J, Zhang J, Liang J. 2007. Microtubule dynamics in relation to osmotic stress-induced ABA accumulation in *Zea mays* roots. J.Exp. Bot. 58(10):2565-2572.
24. Macar T. 2017. Genetiği değiştirilmiş (Transgenik) mısır (*Zea mays* L.) tohumlarında bazı biyokimyasal ve fizyolojik parametrelerin araştırılması. Doktora Tezi. Giresun Üniversitesi.
25. Mollinedo F, Gajate C. 2003. Microtubules microtubule-interfering agents and apoptosis. Apoptosis 8(5):413–450. https://doi.org/10.1023/A:1025513106330
26. Paredez AR. Somerville CR. and Ehrhardt DW. 2006. Visualization of cellulose synthase demonstrates functional association with microtubules. Science 312:1491–1495. https://doi.org/10.1126/science.1126551

27. Petrov V, Hille J, Mueller-Roeber B, Gechev TS. 2015. ROS-mediated abiotic stress-induced programmed cell death in plants. Frontiers in Plant Science, 6:69. https://doi.org/10.3389/fpls.2015.00069
28. Rocha GL, Hernandez J. 2017. Programmed Cell Death-Related Proteases in Plants. Enzyme Inhibitors and Activators. book. https://dx.doi.org/10.5772/65938
29. Rouf ST, Prasad K, Kumar P. 2016. Maize—A potential source of human nutrition and health: A review. Cogent Food & Agriculture, 2(1):1166995. https://doi.org/10.1080/23311932.2016.1166995
30. Rui Y and Dinneny JR. 2020. A wall with integrity: surveillance and maintenance of the plant cell wall under stress. New Phytologist, 225(4):1428-1439. https://doi.org/10.1111/nph.16166
31. Rybaczek D, Musialek MW, Balcerczyk A. 2015. Caffeine-induced premature chromosome condensation results in the apoptosis-like programmed cell death in root meristems of *Vicia faba*. PLoS ONE 10(11):1–33. https://doi.org/10.1371/journal.pone.0142307
32. Salika R, Riffat J. 2021. Abiotic stress responses in maize: a review. Acta Physiologica Plantarum, 43(9):130.
33. Sampathkumar A, Gutierrez R, Mcfarlane H, Bringmann M, Lindeboom J, Emons AM. 2013. Patterning and life-time of plasma membrane localized cellulose synthase is dependent on actin organization in Arabidopsis interphase cells. Plant Physiol. 162:675–688. https://doi.org/10.1104/pp.113.215277
34. Schweizer D. 1976. Reverse fluorescent chromosome banding with chromomycin and DAPI. Chromosoma. 58(4):307–324. https://doi.org/10.1007/BF00292840
35. Smertenko A, and Franklin-Tong VE. 2011. Organisation and regulation of the cytoskeleton in plant programmed cell death. Cell Death & Differentiation, 18(8):1263-1270. http://dx.doi.org/10.1038/cdd.2011.39
36. Stavropoulou K, Adamakis IDS, Panteris E, Arseni EM, Eleftheriou EP. 2018. Disruption of actin filaments in *Zea mays* by bisphenol A depends on their crosstalk with microtubules. Chemosphere 195:653–665. https://doi.org/10.1016/j.chemosphere.2017.12.099
37. Sychta K, Słomka A, Kuta E. 2021. Insights into Plant Programmed Cell Death Induced by Heavy Metals-Discovering a Terra Incognita. Cells. 10(1):65. https://doi.org/10.3390/cells10010065
38. Tollenaar M, Lee EA. 2002. Yield potential, yield stability and stress tolerance in maize. Field crops research, 75(2-3):161-169. https://doi.org/10.1016/S0378-4290(02)00024-2
39. Uetake YR, Peterson L. 1998. Association between microtubules and symbiotic fungal hyphae in protocorm cells of the orchid species *Spiranthes sinensis*. New Phyto. 140(4):715–722. https://doi.org/10.1046/j.1469-8137.1998.00310.x
40. Wang H, Li J, Bostock RM, Gilchrist DG. 1996. Apoptosis: a functional paradigm for programmed plant cell death induced by a host-selective phytotoxin and invoked during development. The Plant Cell. 8(3):375-391. https://doi.org/10.1105/tpc.8.3.375
41. Williams B, Dickman M. 2008. Plant programmed cell death: Can't live with it; Can't live without it. Mol. Plant. Path. 9(4):531–544. https://doi.org/10.1111/j.1364-3703.2008.00473.x
42. Yadav S, Modi P, Dave A, Vijapura A, Patel D, Patel M. 2020. Effect of abiotic stress on crops. Sustainable crop production, 3.
43. Yanık F, Aytürk Ö, Vardar F. (2017). Programmed cell death evidence in wheat (*Triticum aestivum* L.) roots induced by aluminum oxide (Al2O3) nanoparticles. Caryologia, 70(2):112-119.https://doi.org/10.1080/00087114.2017.1286126
44. Yazdani M, Mahdieh M. 2012. Salinity Induced Apoptosis in Root Meristematic Cells of Rice. IJBBB. 40–43. https://doi.org/10.7763/IJBBB.2012.V2.66
45. Zhao S, Zhang Q, Liu M, Zhou H, Ma C, Wang P. 2021. Regulation of plant responses to salt stress. International Journal of Molecular Sciences, 22(9):4609. https://doi.org/10.3390/ijms22094609

Caryologia
International Journal of Cytology, Cytosystematics and Cytogenetics

Firenze University Press
www.fupress.com/caryologia

OPEN ACCESS

Citation: Santra, I., Biswas. D., & Ghosh, B. (2023). Chromosomal characterization mediated by karyomorphological analysis and differential banding pattern in fenugreek (*Trigonella foenum-graecum* L.): a neglected legume. *Caryologia* 76(3): 63-70. doi: 10.36253/caryologia-2159

Received: June 2, 2023

Accepted: October 31, 2023

Published: February 29, 2024

Data Availability Statement: All relevant data are within the paper and its Supporting Information files.

Competing Interests: The Author(s) declare(s) no conflict of interest.

ORCID

IS: 0000-0001-7882-0090
DB: 0000-0002-3449-8543
BG: 0000-0002-4396-2088

Chromosomal characterization mediated by karyomorphological analysis and differential banding pattern in fenugreek (*Trigonella foenum-graecum* L.): a neglected legume

Indranil Santra, Diptesh Biswas, Biswajit Ghosh*

Plant Cytogenetics Laboratory, Post Graduate Department of Botany, Ramakrishna Mission Vivekananda Centenary College, Rahara, Kolkata -700118, India
*Corresponding author. E-mail: ghosh_b2000@yahoo.co.in

Abstract. Fenugreek or *Trigonella foenum-graecum* L. is a commercially important yet neglected crop of the family Fabaceae, with potent medicinal applications, and can treat several diseases as well. Conventional breeding studies for higher yields of commercial crops largely depend on chromosomal information of the particular species. Despite a number of cytological research being conducted on *T. foenum-graecum*, a complete characterization of its chromosomes has not been achieved due to the limitations of traditional karyotype analysis methods. A range of chromosomal markers are advantageous to characterize at full extent and identify individual chromosomes rather than relying on only physical metrics. Thus, in this study, in addition to giemsa staining, other approaches like fluorochrome and silver staining were used for the precise karyomorphological analysis of this species. Enzyme maceration and air drying (EMA) based fluorochrome banding with GC-specific stain Chromomycin A3 (CMA), and AT-specific stain 4',6-diamidino-2-phenylindole (DAPI) applied for the first time for chromosome characterization. The results showed $2n = 16$ chromosomes in metaphase cells, with karyotype formula of 2m+6sm. The unique banding pattern observed in the CMA/DAPI and AgNOR staining highlights the AT and GC-rich regions as well as the nucleolar organizer regions (NORs). All this crucial information can further assist in conducting breeding studies of more precision with simultaneously encouraging similar studies that need to be done in other unexploited species of importance.

Keywords: *Trigonella foenum-graecum,* Karyotype, CMA-DAPI, AgNOR, Fenugreek.

INTRODUCTION

Fenugreek (*Trigonella foenum-graecum* L.) belongs to the family Fabaceae and has been consumed by the human race as food, spices and medicine since ancient times; nevertheless, it is still neglected from a global perspective (Mikić 2015). The term "fenugreek" is derived from the Greek language, which translates to "Greek hay," offering a glimpse into the plant's historical usage as a forage crop. The plant is cultivated in various regions, including India, Pakistan, Mediterranean Europe, Australia, and North America

(Acharya et al. 2008). India is a preeminent producer of fenugreek, claiming a staggering 80% of the global production (Rasheed et al. 2015). In addition to its culinary applications, the seeds and leaves of fenugreek have been utilized in traditional medicine to treat a plethora of conditions such as hyperglycemia, cardiovascular disease, neurological disorders, pulmonary fibrosis, obesity, asthma, and inflammation.

Fenugreek also possesses a large variety of nutritional compounds that are important for basic maintenance of biological systems. In general the fenugreek seeds contains 58% carbohydrates, 23-26% proteins, 0.9% fats and 25% fibers (Wani et al. 2018; Syed et al. 2020). Different kinds of minerals for example potassium (603 mg/100 g), magnesium (42 mg/100 g), calcium (75 mg/100 g), zinc (2.4 mg/100 g), manganese (0.9 mg/100 g), copper (0.9 mg/100 g) and iron (25.8 mg/100 g) can be found in *T. foenum-graecum*. Vitamin C (220 mg/100 g) and β carotene (19 mg/100 g) are also present in higher amounts in fenugreek (Al-Jasass and Al-Jasser 2012; Wani et al. 2018). In addition, fenugreek contains several nutritionally valuable flavonoids such as quercetin, luteolin, vitexin, 7, 4-dimethoxy flavanones, kaempferol, tricin, and naringenin (Petropoulos 2002). Important amino acids including aspartic acid, glutamic acid, leucine, tyrosine, phenylalanine and free amino acid (2S, 3 R, 4S)-4-hydroxyisoleusine are abundantly present in fenugreek (Syed et al. 2020). In a study fenugreek seeds have been found to contain greater amounts of protein with better amino acid profile than soybean protein isolate (Feyzi et al. 2002).

Karyotyping is the process of classifying the chromosomal makeup of a cell by examining the number, size, and structure of each chromosome, which can provide insights into the relationship between different species (Levin 2002). It is a commonly used technique in crop plant research for various purposes, such as characterizing cultivars, linking genetic and physical maps, and studying the evolutionary relationships among different species (de Moraes et al. 2007). Despite its utility, karyotyping is often hindered by the scarcity of chromosome markers, which makes it challenging to identify individual chromosomes (She and Jiang 2015). The utilization of traditional staining techniques can assist in examining the shape, size, and number of chromosomes, but it falls short of being able to differentiate between chromosomes that have similar physical characteristics (Shabir et al. 2017). In order to address the difficulty in distinguishing morphologically similar chromosomes, a number of chromosome banding techniques have been developed which offer a significant advantage for the identification of chromosomes and karyotyping (Andras et al. 2000). Chromosome staining with the combination of both chromomycin A3 (CMA) and 4',6-diamidino-2-phenylindole (DAPI) fluorochromes has been widely used as a method to distinguish chromosome bands (Guerra 2000). CMA and DAPI, due to their proclivity for binding to GC- and AT-rich sequences, respectively, allow for the discernment of various forms of heterochromatin as GC-abundant ($DAPI^{-ve}/CMA^{+ve}$), AT-abundant ($DAPI^{+ve}/CMA^{-ve}$), or AT/GC-balanced (DAPI neutral/CMA neutral) bands (Barros e Silva and Guerra 2010). Nucleolar organizer regions (NORs) are another excellent chromosome landmark effective in chromosomal characterization. The localization of NORs serves as a valuable marker for identifying chromosomes, offering a precise and dependable method of characterizing them (Maragheh et al. 2019). The presence and number of NORs in a cell can help distinguish between different types of chromosomes and provide important information for karyotyping.

Cytological studies using karyotype analysis have been conducted for an extended period in different species and cultivars of fenugreek, having somatic chromosome number $2n = 16$ (Table 1). The karyotype reports concludes that any of the available species of the Foenum-graecum section cannot be considered as the wild progenitor of fenugreek (Ladizinsky and Vosa 1986). The previous studies have been primarily limited to conventional karyotype analysis, with little emphasis placed on documenting and disseminating the findings (Table 1) (Agarwal and Gupta 1983; Bairiganjan and Patnaik 1989; Martin et al. 2011; Najafi et al. 2013). As far as our knowledge extends, the application of advanced differential chromosome banding techniques such as CMA and DAPI has not been previously employed in the study of *T. foenum-graecum*. In light of this deficiency, the present study aims to fill this gap by utilizing these advanced techniques, in conjunction with silver staining (AgNOR), to perform a comprehensive characterization of the chromosomal structure of this species. The comprehensive characterization of chromosomes plays a crucial role in breeding programs. This process provides important information that enables breeders to make informed mating decisions, leading to the production of offspring that possess both desirable traits and optimal health.

MATERIAL AND METHODS

Somatic chromosome preparation

Seeds of *T. foenum-graecum* have been collected from the cultivated fields of Sainthia, Birbhum (24°00'55.9"N 87°44'09.4"E) West Bengal. The growing roots from germinated seeds of *T. foenum-graecum* were taken for

Table 1. Previous chromosome reports in *Trigonella foenum-graecum.*

Sl. No.	Chromosome counts		Karyotype	Symmetry/Asymmetry	Reference
	Gametophytic (*n*) cells	Sporophytic (2*n*) cells			
1.	8	16	$1scA^{sm}+5A^{sm}+1B^{m}+1C^{sm}$	Asymmetrical	Agarwal and Gupta (1983)
2.	8	16	–	–	Laxmi et al. (1983)
3.	–	16	–	Asymmetrical	Ladizinsky and Vosa (1986)
4.	8	16	–	–	Arya et al. (1988)
5.	–	16	1m+5sm+2st	Asymmetrical	Bairiganjan and Patnaik (1989)
6.	–	16	$A_2B_{12}D_2$	–	Kar and Sen (1991)
7.	–	16	–	–	Jahan et al. (1994)
8.	–	16	–	–	Ahmed et al. (1999)
9.	–	16	–	–	Das et al. (2000)
10.	–	16	–	Symmetrical	Das et al. (2001)
11.	–	16	–	Symmetrical	Das et al. (2002)
12.	–	16	2m+6sm	–	Martin et al. (2011)
13.	–	16	$10sm + 4sm^{sat} + 2m$	–	Najafi et al. (2013)
14.	–	16	–	–	Ranjbar and Zahra (2016)

chromosome preparation. Chromosomes were prepared following Santra et al. (2020) with minor modifications. Roots were pretreated with 0.5 g L^{-1} 8-hydroxyquinoline solution at 16 °C for 6 h and then fixed in acetic acid:methanol solution (1:3) overnight. Digestion of the cell wall was performed with an enzyme mixture containing 1% cellulase (Onozuka-RS, Sigma, USA), 0.5% pectolyase (Sigma, USA), and 0.75% macerozyme (Serva, Germany) in a sodium citrate buffer (pH 4.6) at 37 °C for 90 mins. After washing with the same buffer twice, the root tip was broken down into small pieces on a clean slide with the addition of freshly prepared fixative. The slide was air-dried for at least 24 h before staining.

Giemsa staining

The chromosomes on the air-dried slide were firstly stained with 2% giemsa solution in phosphate buffer, with a ratio of 1:15 (pH 6.8), followed by rinsing with distilled water and analyzed under a microscope. Photomicrographs were taken with an AxioCam ICc 5 camera and ZEN application suite. Individual chromosomes were measured with AxioVision 4.9.1 and categorized based on the arm ratio following Levan et al. (1964).

CMA and DAPI double staining

Prior to simultaneous fluorochrome staining, with CMA and DAPI, the giemsa stained slides were destained with 70% methanol for 15 mins and air-dried. After preincubation of the slides in McIlvaine buffer (pH 7.0) for 10 mins, chromosomes were stained with 0.2 µg mL^{-1} DAPI solution for another 10 mins in the dark. After DAPI staining, slides were preincubated in McIlvaine buffer (pH 7.0) supplemented with 5 mM $MgCl_2$ and air dried. CMA staining was done with 0.25 mg mL^{-1} CMA solution for 60 min in the dark. After a short rinse in the same buffer, slides were mounted with 50% glycerol containing 5 mM $MgCl_2$ and kept at 4 °C for 72 hrs before further analysis. Chromosomes were analyzed under the fluorescent microscope Zeiss Axio Scope A1 equipped with CMA and DAPI-specific filter cassettes. AxioCam ICc 5 and ZEN application suite were used to take the suitable photomicrographs. The karyogram has been carried out using Adobe Photoshop CS6.

Silver staining

In this study, the AgNOR staining was performed using the Ag-I procedure by Bloom and Goodpasture (1976), with a modification introduced by Kodama et al. (1980) of using nylon cloth instead of coverslips. Silver nitrate solution was added to slides, placed in moisture-proof plastic containers and covered with nylon mesh. To keep the environment moist, distilled deionized water is placed at the bottom of the containers, away from the slides. The slides are left to incubate in the water bath for 48 h at 45 °C. The NOR region appeared as dark brown color bands over light brown chromosome arms.

RESULTS

In this analysis with *Trigonella foenum-graecum*, more than 40 root tips were initially studied through giemsa staining, which confirmed that the somatic cells of the present cultivar contain $2n$ =16 chromosomes (Fig. 1a). Additionally, differential chromosome banding with CMA, DAPI and AgNOR have also been performed in metaphase as well as in prometaphase chromosomes (Fig. 1b-f). The somatic chromosomes are small to medium in size and range between 4.70 to 5.92 µm. Individual chromosome sizes, arm ratio, and the centromeric index has been mentioned in Table 2. Analysis through detailed karyomorphological studies revealed two pairs with median (m) to nearly median primary constriction and six pairs of chromosomes having submedian (sm) primary constriction (Fig. 2a-d). Thus, the karyotype formula is 2m+6sm (Fig. 2d). Secondary constrictions are also present in the long arm of one pair of metacentric chromosomes (pair 1) and in the short arm of one pair of submetacentric chromosomes (pair 4) (Fig. 2b,c). The secondary constrictions are intercalary in position. The karyotype is symmetric and falls into 3A category of Stebbins's (1971) classification. Later, fluorochrome staining with CMA and DAPI, revealed all eight pairs of chromosomes with bright, distinct and scorable CMA^{+ve} bands, in their primary constriction (Fig. 2c). DAPI mostly stained the somatic metaphase chromosomes uniformly, however a single $DAPI^{+ve}$ band has been found in the chromosome pair 4 (Fig. 2b), in the intercalary position of short arm, colocalized with a CMA^{-ve} band. $DAPI^{-ve}$ bands have been detected to be colocalized with the CMA^{+ve} bands (Fig. 2b,c). Besides the single $DAPI^{+ve}$ band found in chromosome 4, several DAPI-brilliant regions were found in the prometaphase chromosomes (Fig. 1f), which also showed corresponding CMA^{-ve} bands (Fig. 1e). However, in condensed meta-

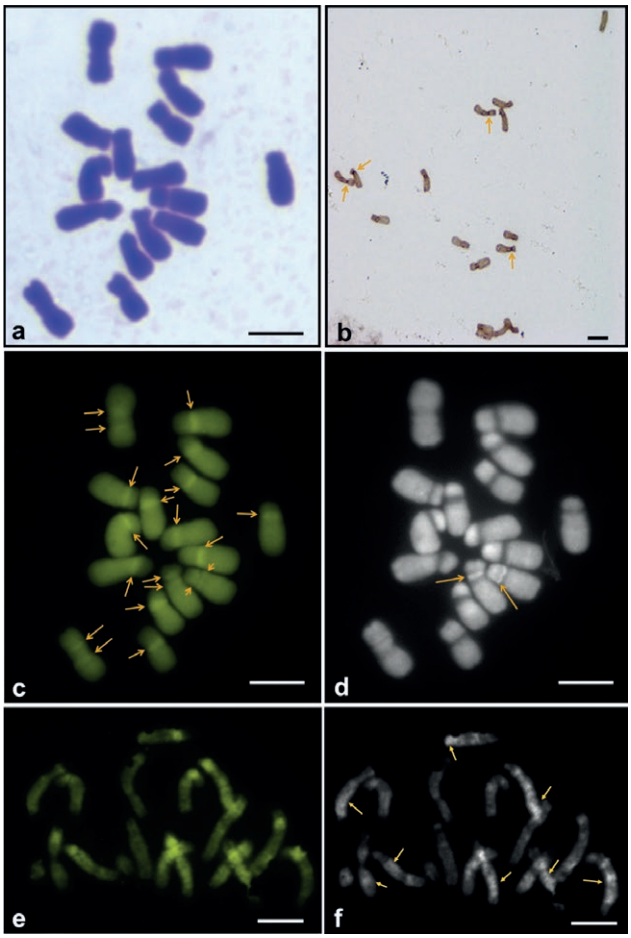

Figure 1. Differential chromosome banding in the somatic cells of *Trigonella foenum-graecum*. (a) giemsa stained metaphase plate; (b) silver staining (arrows indicate AgNOR bands); (c) CMA stained metaphase plate (arrows indicate CMA bands); (d) DAPI stained metaphase plate (arrow indicates DAPI bands); (e-f) CMA and DAPI stained prometaphase chromosomes. Scale bars of 5 µm.

Table 2. Chromosome parameters and banding patterns in *Trigonella foenum-graceum*.

Chromosome number	S (µm)	L (µm)	Total (µm)	Arm ratio	Centromeric index	Chromosome type*	CMA bands (+/-)	DAPI bands (+/-)	AgNOR bands (+/-)
1	2.575 ± 0.019	3.350 ± 0.043	5.925 ± 0.053	1.301	0.434599	m	+	-	+
2	1.789 ± 0.005	4.041 ± 0.005	5.830 ± 0.007	2.259	0.306872	sm	+	-	-
3	1.527 ± 0.016	3.961 ± 0.010	5.487 ± 0.008	2.595	0.278186	sm	+	-	-
4	1.886 ± 0.024	3.587 ± 0.007	5.473 ± 0.018	1.902	0.344541	sm	+/-	+/-	+
5	1.388 ± 0.014	3.526 ± 0.012	4.914 ± 0.003	2.542	0.282366	sm	+	-	-
6	1.231 ± 0.015	3.552 ± 0.018	4.783 ± 0.032	2.885	0.315542	sm	+	-	-
7	1.5 ± 0.002	3.253 ± 0.004	4.753 ± 0.005	2.169	0.406730	sm	+	-	-
8	1.912 ± 0.004	2.789 ± 0.002	4.701 ± 0.003	1.459	0.257422	m	+	-	-

*m = metacentric, sm = submetacentric. Total Chromatin Length (TCL) = 41.866 µm.

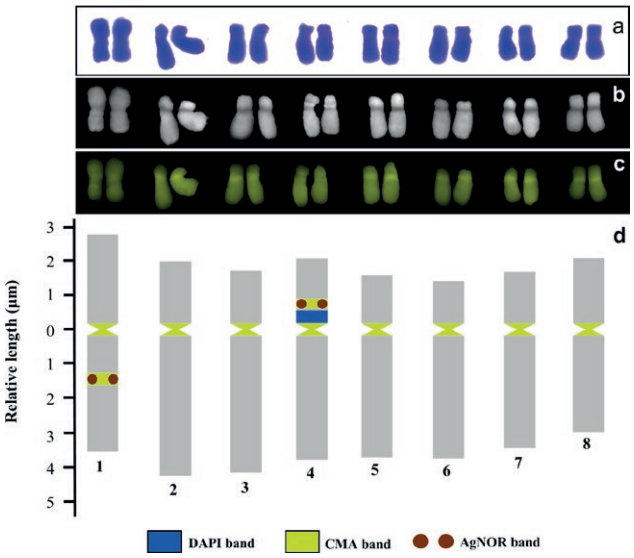

Figure 2. Karyogram and Idiogram representation of the somatic chromosomes of *Trigonella foenum-graecum.* (a) Stained with giemsa; (b) Stained with DAPI; (c) Stained with CMA; (d) Idiogram of the chromosomes along with the localization of different bands.

phase chromosomes, these regions are found to be either dispersed or not clearly visible. Lastly, AgNOR staining specifically stained intercalary positions of chromosomes 1 and 4 (Fig. 1b). Thus, *T. foenum-graecum* chromosomes can be identified and characterized based on the number and position of the CMA^{+ve}/ $DAPI^{-ve}$/ AgNOR bands (Fig. 2d).

DISCUSSION

According to Hutchinson (1964), the genus *Trigonella* is one of the six genera of the tribe Trifoliae and subtribe Trigonellinae. The genus *Trigonella* consists of approximately 134 species, which are found all over the world. These species can be diploid or polyploid, and there is evidence to suggest that their basic chromosome number could be x = 7, 8, or 9, as reported by different studies over the years. (Biddak 1996; Martin et al. 2011; Sharghi et al. 2020). The species *T. foenum-graecum* L. with basic chromosome number 8 ($2n$ = 16) comes under the section Foenum-graecum along with eight other species (Basu 2023). Karyotype studies, chromosome banding and Fluorescent In Situ Hybridization techniques have depicted finer variation in species and cultivars of *T. foenum-graecum* L. (Agarwal and Gupta 1983; Ahmed et al. 1999; Das et al. 2000). *T. foenum-graecum,* in the present study shows $2n$ = 16 chromosomes in the somatic cell with the basic chromosome number x = 8 (Fig. 2d). The present study revealed the size of the somatic chromosomes was within a moderate range, ranging from 4.70-5.92 µm (Table 2). The karyotype formula, which is used to describe the number and appearance of chromosomes in a cell, was determined to be 2m+6sm. These findings were consistent with previous studies, indicating a similarity in the chromosome size and formula between the present investigation and prior research (Martin et al. 2011). The process of enzymatic maceration of plant cells helps to prepare the chromosomes in a way that enables clear and unobstructed visualization during cytological analysis. The use of fluorescent banding techniques with CMA and DAPI, has significantly advanced the field of plant cytogenetics by identifying GC- and AT-rich constitutive heterochromatin regions on chromosomes, leading to increased knowledge and advancements in plant chromosome research (Schweizer 1976; Yamamoto 2012). The current study represents the first documented use of a double staining approach combining CMA and DAPI on chromosomes in *T. foenum-graecum* to date, producing a clear and easily distinguishable banding pattern, marking the first recorded instance of fluorochrome banding in this species based on our current knowledge. The centromeres, along with secondary constrictions, were reliably designated as CMA^{+ve} and were also correlated with $DAPI^{-ve}$ bands. This establishes that the centromere region has a high concentration of GC nucleotides. A thorough examination of several species unveiled that the DNA found in centromeres can possess a substantial richness of GC nucleotides. While some animal species exhibit, a predilection for AT-rich tandem repeats, no such tendency was apparent in the plant kingdom (Melters et al. 2013). The detection of CMA^{+ve} centromeric heterochromatin in *Crotalaria*, a member of the Fabaceae family, implies the existence of GC-rich DNA repeat units at the centromere (Mondin and Aguiar-Perecin 2011). In most species, the rDNA sites exhibit a positive stain, when subjected to CMA staining and a negative stain when treated with DAPI. These sites are frequently the sole regions displaying positive CMA staining (de Melo and Guerra 2003). A common characteristic of plants is the association of GC-rich regions with 35S rDNA sites, resulting in the generation of CMA^{+ve} bands in the NOR (Marcon et al. 2005; Dydak et al. 2009; Kolano et al. 2013). The rDNA sites are generally positively stained with CMA and negatively stained with DAPI. In many species, the rDNA sites are the only regions that are positively stained with CMA. In one pair of chromosomes, positive bands detected through DAPI staining have been identified in the region between the primary and secondary constrictions (Fig. 2b). During prometaphase, when the chromatins are less compact,

distinct signals were observed through DAPI staining. This has been documented in several plant species, and the observation that the DAPI signal is only present during prometaphase and disappears during metaphase suggests that it is not a manifestation of heterochromatin, but instead an early stage of chromatin condensation (Berjano et al. 2009; Santra et al. 2021). The use of silver nitrate staining enables the recognition of ribosomal DNA (rDNA) sites that were transcribing during the preceding interphase of the cell cycle, as visualized in the metaphase stage (Jiménez et al. 1988). In *T. foenum-graecum*, two pairs of chromosomes have been observed with AgNOR bands at secondary constrictions corresponding to the CMA^{+ve} bands. In this species, previous studies have documented information about the count and placement of the AgNOR bands, which are in agreement with the results of the current research (Ahmad et al. 1999). The authors also hypothesized that the origin of the two satellite chromosome pairs in fenugreek remains unclear, but it may stem from the hybridization of two distinct species or cytotypes. The localization of AgNOR, CMA, and DAPI bands appear to be valuable cytological markers, which have enabled us to distinguish and identify the chromosomes in *T. foenum-graecum*. The standardized techniques of EMA, Giemsa staining, silver staining and fluorochrome banding are considered to be reliable and reproducible. The results of this study hold great significance in understanding the genetic makeup of fenugreek. The study offers critical knowledge on the characterization and preservation of this neglected crop and its diversity, leading to an enrichment of its improvement program. This is vital for maintaining the sustainability of food production and the environment's well-being.

ACKNOWLEDGEMENT

Authors are thankful to Swami Kamalasthananda, Principal, Ramakrishna Mission Vivekananda Centenary College, Rahara, Kolkata (India), for the facilities provided for the present study. DB acknowledges, Council of Scientific & Industrial Research (CSIR-HRDG) for providing CSIR – Senior Research Fellowship.

REFERENCES

Acharya SN, Thomas JE, Basu SK. 2008. Fenugreek, an alternative crop for semiarid regions of North America. Crop Sci 48:841–853. https://doi.org/10.2135/cropsci2007.09.0519

Agarwal K, Gupta PK. 1983. Cytological studies in the genus *Trigonella* Linn. Cytologia 48:771–779. https://doi.org/10.1508/cytologia.48.771

Ahmad F, Acharya SN, Mir Z, Mir PS. 1999. Localization and activity of rRNA genes on fenugreek (*Trigonella foenum-graecum* L.) chromosomes by fluorescent *in situ* hybridization and silver staining. Theor Appl Genet 98:179–185. https://doi.org/10.1007/s001220051056

Al-Jasass FM, Al-Jasser MS. 2012. Chemical Composition and Fatty Acid Content of Some Spices and Herbs under Saudi Arabia Conditions. Sci World J. 2012:1–5. https://doi.org/10.1100/2012/859892

Andras SC, Hartman TPV, Alexander J et al. 2000. Combined PI–DAPI staining (CPD) reveals NOR asymmetry and facilitates karyotyping of plant chromosomes. Chromosome Res. 8:387–391. https://doi.org/10.1023/A:1009258719052

Arya ID, Rao SR, Raina SN. 1988. Cytomorphological studies of *Trigonella foenum-graecum* autotetraploids in three (C1, C2, C3) generation. Cytologia 53:525–534. https://doi.org/10.1508/cytologia.53.525

Bairiganjan GC, Patnaik SN. 1989. Chromosomal evolution in Fabaceae. Cytologia 54:51–64.

Barros e Silva AE, Guerra M. 2010. The meaning of DAPI bands observed after C-banding and FISH procedures. Biotech Histochem 85:115–125. https://doi.org/10.3109/10520290903149596

Basu S. 2023. Elucidating karyotype structure and affinity through application of karyomorphological parameters and multivariate analysis, as discerned from the study of four important legumes. Nucleus 66:39–46. https://doi.org/10.1007/s13237-023-00416-8

Berjano R, Roa F, Talavera S, Guerra M. 2009. Cytotaxonomy of diploid and polyploid *Aristolochia* (Aristolochiaceae) species based on the distribution of CMA/DAPI bands and 5S and 45S rDNA sites. Plant Syst Evol 280:219–227. https://doi.org/10.1007/s00606-009-0184-6

Biddak L. 1996. Inter-and intraspecific chromosomal variations in four species of *Trigonella* L. J Union Arab Biol, Cairo 3:203–215.

Bloom SE, Goodpasture C. 1976. An improved technique for selective silver staining of nucleolar organizer regions in human chromosomes. Hum Genet 34:199–206. https://doi.org/10.1007/BF00278889

Das AB, Mohanty S, Das P. 2001. Cytophotometric estimation of 4C DNA content and karyotype analysis in ten cultivars of *Trigonella foenum-graecum*. Iran J Bot 9:1–9.

Das AB, Mohanty S, Das P. 2002. Cytophotometric estimation of 4C DNA content and karyotype analysis in ten cultivars of *Trigonella foenum-graecum*-II. Iran J Bot 9:151–159.

Das AB, Mohanty S, Thangaraj T, Das P. 2000. Variation of 4C DNA content and karyotype in nine cultivars of fenugreek (*Trigonella foenum-graecum* L.). J Herbs Spices Med Plants 7:25–32. https://doi.org/10.1300/J044v07n01_04

de Melo NF, Guerra M. 2003. Variability of the 5S and 45S rDNA sites in *Passiflora* L. species with distinct base chromosome numbers. Ann Bot 92:309–316. https://doi.org/10.1093/aob/mcg138

de Moraes AP, dos Santos Soares Filho W, Guerra M. 2007. Karyotype diversity and the origin of grapefruit. Chromosome Res 15:115–121. https://doi.org/10.1007/s10577-006-1101-2

Dydak M, Kolano B, Nowak T, Siwinska D, Maluszynska J. 2009. Cytogenetic studies of three European species of *Centaurea* L. (Asteraceae). Hereditas 146:152–161. https://doi.org/10.1111/j.1601-5223.2009.02113.x

Feyzi S, Varidi M, Zare F, Varidi MJ. 2015. Fenugreek (*Trigonella Foenum Graecum*) Seed Protein Isolate: Extraction Optimization, Amino Acid Composition, Thermo and Functional Properties. J Sci Food Agric. 95:3165–3176. https://doi.org/10.1002/jsfa.7056

Guerra M. 2000. Patterns of heterochromatin distribution in plant chromosomes. Genet Mol Biol. 23:1029–1041. https://doi.org/10.1590/S1415-47572000000400049

Jahan B, Vahidy AA, Ali SI. 1994. Chromosome numbers in some taxa of Fabaceae mostly native to Pakistan. Ann Mo Bot Gard 792–799. https://doi.org/10.1508/cytologia.54.51

Jiménez R, Burgos M, de La Guardia RD. 1988. A study of the Ag-staining significance in mitotic NOR's. Heredity 60:125–127. https://doi.org/10.1038/hdy.1988.18

Kar K, Sen S. 1991. A comparative karyological study of root and embryo tissue of a few genera of Leguminosae. Cytologia 56:403–408. https://doi.org/10.1508/cytologia.56.403

Kodama Y, Yoshida MC, Sasaki M. 1980. An improved silver staining technique for nucleolus organizer regions by using nylon cloth. Jpn J Hum Genet 25:229–233. https://doi.org/10.1007/BF01997700

Kolano B, Saracka K, Broda-Cnota A, Maluszynska J. 2013. Localization of ribosomal DNA and CMA3/DAPI heterochromatin in cultivated and wild *Amaranthus* species. Sci Hortic 164:249–255. https://doi.org/10.1016/j.scienta.2013.09.016

Ladizinsky G, Vosa CG. 1986. Karyotype and C-banding in *Trigonella* section Foenumgraecum (Fabaceae). Plant Syst Evol 153:1–5. https://doi.org/10.1007/BF00989412

Laxmi V, Gupta MN, Datta SK. 1983. Investigations on an induced green seed coat colour mutant of *Trigonella foenum-graecum* L. Cytologia 48:373–378. https://doi.org/10.1508/cytologia.48.373

Levan A, Fredga K, Sandberg AA. 1964. Nomenclature for centromeric position on chromosomes. Hereditas 52:201–220. https://doi.org/10.1111/j.1601-5223.1964.tb01953.x

Levin DA. 2002. The role of chromosomal change in plant evolution. Oxford University Press, New York, USA.

Maragheh FP, Janus D, Senderowicz M, Haliloglu K, Kolano, B. 2019. Karyotype analysis of eight cultivated *Allium* species. J Appl Genet 60:1–11. https://doi.org/10.1007/s13353-018-0474-1

Marcon AB, Barros ICL, Guerra M. 2005. Variation in chromosome numbers, CMA bands and 45S rDNA sites in species of *Selaginella* (Pteridophyta). Ann Bot 95:271–276. https://doi.org/10.1093/aob/mci022

Martin E, Akan H, Ekici M, Aytac Z. 2011. Karyotype analyses of ten sections of *Trigonella* (Fabaceae). Comp Cytogenet 5:105–121. https://doi.org/10.3897/compcytogen.v5i2.969

Melters DP, Bradnam KR, Young HA et al. 2013. Comparative analysis of tandem repeats from hundreds of species reveals unique insights into centromere evolution. Genome Biol 14:1–20. https://doi.org/10.1186/gb-2013-14-1-r10

Mikić A. 2015. Brief but alarming reminder about the need for reintroducing 'Greek hay' (*Trigonella foenum-graecum* L.) in Mediterranean agricultures. Genet Resour Crop Evol 62:951–958. https://doi.org/10.1007/s10722-015-0260-4

Mondin M, Aguiar-Perecin ML. 2011. Heterochromatin patterns and ribosomal DNA loci distribution in diploid and polyploid *Crotalaria* species (Leguminosae, Papilionoideae), and inferences on karyotype evolution. Genome 54:718–726. https://doi.org/10.1139/g11-034

Najafi S, Anakhatoon EZ, Birsin MA. 2013. Karyotype Characterisation of Reputed Variety of Fenugreek (*Trigonella foenum-graecum*) in West Azerbaijan-Iran. J Appl Biol Sci 7:23–26.

Petropoulos GA. 2002. Fenugreek: The Genus *Trigonella*. CRC Press, Boca Raton, Florida, USA.

Ranjbar M, Zahra H. 2016. Chromosome numbers and biogeography of the genus *Trigonella* (Fabaceae). Caryologia 69:223–234. https://doi.org/10.1080/00087114.2016.1169090

Rasheed MSAA, Wankhade MV, Saifuddin MSSK, Sudarshan MAR. 2015. Physico-chemical properties of fenugreek (*Trigonella foenum-graceum* L.) seeds. Int J Eng Res 4:68–70.

Santra I, Halder T, Ghosh B. 2021. Somatic and gametic chromosomal characterization with fluorescence

banding of Giloy (*Tinospora cordifolia*): A berberine synthesizing important medicinal plant of India. Caryologia. 74:63–73. https://doi.org/10.36253/caryologia-1014

Santra I, Haque SM, Ghosh B. 2020. Giemsa C-banding Karyotype and Detection of Polymorphic Constitutive Heterochromatin in *Nigella sativa* L. Cytologia. 85:85–90. https://doi.org/10.1508/cytologia.85.85

Schweizer D. 1976. Reverse fluorescent chromosome banding with chromomycin and DAPI. Chromosoma. 58:307–324. https://doi.org/10.1007/BF00292840

Shabir PA, Wani AA, Nawchoo IA. 2017. Banding Techniques in Chromosome Analysis. In: Bhat T, Wani A (eds) Chromosome Structure and Aberrations. Springer, New Delhi, pp 167–180 https://doi.org/10.1007/978-81-322-3673-3_8

Sharghi H, Azizi M, Moazzeni H. 2020. A karyological study of some endemic *Trigonella* species (Fabaceae) in Iran. Caryologia. 73:155–161. https://doi.org/10.13128/caryologia-184

She CW, Jiang XH. 2015. Karyotype analysis of *Lablab purpureus* (L.) sweet using fluorochrome banding and fluorescence in situ hybridization with rDNA probes. Czech J Genet Plant Breed. 51:110–116. https://doi.org/10.17221/32/2015-CJGPB

Stebbins GL. 1971. Chromosomal Evolution in Higher Plants. Edward Arnold Ltd., London.

Syed QA, Rashid Z, Ahmad MH, Shukat R, Ishaq A, Muhammad N, Rahman HUU. 2020. Nutritional and therapeutic properties of fenugreek (*Trigonella foenum-graecum*): a review. Int J Food Prop. 23:1777–1791. https://doi.org/10.1080/10942912.2020.1825482

Wani SA, Kumar P. 2018. Fenugreek: A Review on Its Nutraceutical Properties and Utilization in Various Food Products. J Saudi Soc Agri Sci. 17:97–106. https://doi.org/10.1016/j.jssas.2016.01.007

Yamamoto M. 2012. Recent progress on studies of chromosome observation in deciduous fruit trees. J Jpn Soc Hortic Sci. 81:305–313. https://doi.org/10.2503/jjshs1.81.305

Caryologia
International Journal of Cytology, Cytosystematics and Cytogenetics

Firenze University Press
www.fupress.com/caryologia

OPEN ACCESS

Citation: Serafini, S., & Turova, T.S. (2023). "Searching for order at all levels". Antonio Lima-de-Faria (July 4, 1921 – December 27, 2023). *Caryologia* 76(3): 71-73. doi: 10.36253/caryologia-2465

Data Availability Statement: All relevant data are within the paper and its Supporting Information files.

Competing Interests: The Author(s) declare(s) no conflict of interest.

"Searching for order at all levels". Antonio Lima-de-Faria (July 4, 1921 – December 27, 2023)

Stefano Serafini[1], Tatyana S. Turova[2]

[1] *International Society of Biourbanism, Italy*
[2] *Centre for Mathematical Sciences, Lund University, Sweden*
E-mail: tatyana.turova@matstat.lu.se

Professor Antonio Lima-de-Faria was our friend and, in a sense, a teacher. Despite our different fields of study, this master of scientific thought has deeply influenced both of us.

Dr. Stefano Serafini came to know the work of Antonio Lima-de-Faria when he was just a teenager thanks to a disseminative article by the late Italian geneticist, Giuseppe Sermonti. Lima-de-Faria's elegant vision of a universal order at all levels of nature opened his eyes to the consistency of patterns, forms, and function throughout the mineral, vegetable, and animal realms – a concept that has influenced his work in urban studies.

Prof. Tatyana Turova met Antonio Lima-de-Faria on a museum tour of the Royal Physiographic Society (Lund). He was 95. When Antonio came to know that she is a mathematician working in probability, the discussion went straight to a critical analysis of the concept of randomness. That conversation kept going over the years.

Professor Emeritus of Molecular Cytogenetics at Lund University (Sweden), Antonio Lima-de-Faria was a scientist of rare character. He had the innate gift of courage and the ability to tackle big problems despite dominant opinions. He was rigorous and tenacious in his method, and he had an immense knowledge and a sharp rationality.

Antonio Lima-de-Faria defined himself as "a surviving dinosaur" to both of us. He was a magnificent old man – but that "dinosaur" had been ahead of his time since the beginning of his career. This was a constant. In the early 1960s, a multinational company discreetly requested him to develop a futuristic agrifood bioengineering program. This is the current reality of the genetically modified organism.

Known to the scientific world as a pioneer and one of the most relevant exponents of molecular cytogenetics (his 1969 *Handbook of Molecular Cytology* is a classic) – not to mention author of over 200 research articles and influencing monographs – Lima-de-Faria became a member of some of the world's top scientific societies. He also taught in some of the most prestigious universities. He received awards and recognition for his extraordinary activity. These included the appointment as Knight of the Order of the North Star

by the Swedish King and as Great Official of the Order of Santiago by the President of Portugal. He held scientific consultancy positions for governments and institutions, including the European Space Agency, the United Nations Educational, Scientific and Cultural Organization, and the World Bank Group. He never stopped working and studying. In fact, he focused on the molecular organization of the chromosome until the end of his long life.

Despite all of this, his endeavor was not always understood. His famous book, *Evolution without Selection: Form and Function by Autoevolution* (Elsevier, 1988, translated into Russian, Japanese, and Italian) is not only fundamental and revolutionary but also a case of sociology of science. This book, which advanced the current trend in molecular biology, even branded him as anti-evolutionist. Such a tag limited the essence of his work to a mere attack against natural selection – "a parlor game to explain life," as Giuseppe Sermonti would say.

Rather, this treatise, based on his vast physical, chemical, crystallographic, botanical, and zoological expertise, proposed to overcome the concept of natural selection. It downsized the role of genes and chromosomes in the architecture of living things through a plethora of biological forms that came directly from physical constraints. His self-evolutionism united the biological and inorganic worlds. This echoed Aristotelian and Goethean intuitions of morphofunctional homologies, that is, a sort of "non-genic kinship" between the spin of the ultramicroscopic electron, the shell of a *Limnaea*, and the spirals of immense galaxies.

Indeed, selectionism (identifying natural selection not as a contributing cause but as the main engine of biological development) is the major methodological obstacle to the recognition and explanation of Lima-de-Faria's morphofunctional homology. This is the true protagonist of his book. An order crosses and defines the subatomic, chemical, and physical worlds on all of their scales through progressive and deterministic channels. The form of *Chitoniscus feedjeanus*, traditionally explained as a classic example of the mimetic imitation of leaves, has a precedent in the arrangement of the crystals of pure bismuth. The same structure appears in the patterns of chlorite crystals, several vegetal hooks, the shells of ancient ammonites, or goat horns. The bird's-eye-view of an estuary, the branches of a tree, and the vascularization of a mammal follow a single dendritic development pattern – so much so that their images, once reduced to the same size, are difficult to distinguish. Constant chemical commonalities actually underlie these and countless, more apparent natural oddities. Now, selection is not only powerless to account for them but also logically incompatible with any attempt to explain them. Like all strong theoretical systems faced with a fact that is refractory to integration, selectionism ignores homology. And when it cannot help but deal with it, it defines it as mere analogy. This then relegates it to that metaphor of annihilation, which is accidentality.

Therefore, demolishing selectionism in biology was the necessary premise for developing a theory of self-evolution, towards which Lima-de-Faria has led us with a firm, methodical hand. Indeed, he deploys a set of images and observations that are rarely rivalled in modern scientific literature.

Beyond classic studies on the subject, from D'Arcy Thompson (*On Growth and Form*, 1917) onwards, there is no doubt that recent molecular biology has continued to confirm with ever greater evidence the importance of elements that are complementary to classical theoretical genetics in the formation of living organisms. Lima-de-Faria had already begun to indicate and systematize these elements 40 years ago in *Molecular Evolution and Organization of the Chromosome* (1983). In fact, as the author himself recalled, *Evolution without Selection* is the consequence of those premises once applied to evolutionism.

The last writing of Antonio Lima-de-Faria, printed in this very issue of *Caryologia*, develops and complements his marvelous treatise *Praise of Chromosome "Folly": Confessions of an Untamed Molecular Structure* (2008). This masterpiece continues the great tradition of scientific giants such as Schrödinger and Feynman (authors that Antonio Lima-de-Faria highly regarded) talking to the public about the most advanced theories in a clear way. It is written with such wit and humor and such an elegant reference to art that any reader with a natural sciences or mathematics background, having read the first sentence, will not stop until the last. The book summarizes results on chromosome research and offers directions and ideas for further studies. It clearly confirms that understanding evolution requires a deep knowledge in not only chemistry and physics, but also mathematics – especially when it comes to the atomic level.

Long discussions with Antonio Lima-de-Faria of one the authors began soon after *Molecular Origins of Brain and Body Geometry: Plato's Concept of Reality is Reversed* (2014) was published. In an intriguing manner, this work unveils and explains the emergence of body patterns in animals by tracing them to the origin of the brain. For Antonio Lima-de-Faria, "geometry" manifests an "utter simplicity coupled to rigorous order that underlines the phenomenon." He does not use the language of mathematics, as he was not trained in it. However – even if this may sound paradoxical for a non-mathematician – his search for order, for "a common denominator", for a unifying theory, make them akin to fundamental mathematics.

Remarkably, already in his early nineties, Antonio Lima-de-Faria completed an extensive analysis of the structures and functions of living organisms on a molecular level. He then created a new book, *Periodic Tables Unifying Living Organisms at the Molecular Level: The Predictive Power of the Law of Periodicity* (2017). This truly fascinating work provides a new perspective on the relations between matter and energy. Its logical systematic approach links different levels, from atoms to macromolecules to organisms.

As Lima-de-Faria stated, his books do not give ultimate answers and immediate solutions to the posed questions. On the other hand, readers are invited to use the tools, methods, and ideas that he generously expressed in his late works. "Order allows variation but imposes in the same time a canalization that is patent in what we call evolution, being that of galaxies or of living organisms."

Antonio Lima-de-Faria was almost 100 years old when he released his last book, *Science and Art are Based on the Same Principles and Values* (2020) – something he had thought about "for 30 years." It was his scientific testament, encompassing his life-long love for art, beauty, and truth. There, as a "lonely wolf howling in the immensity of the night," he launched a straightforward warning:

"At present a wave of obscurantism is spreading over Western countries affecting both science and art in a deadly way. (…) Modern technology has been most successful in transforming our daily lives and in allowing us to conquer outer space. These impressive achievements have, to a large extent, made us dumb, making it difficult to perceive the danger that lies ahead. Hence, there is a pressing need to bring forward the original sources in which, leading scientists and renowned artists, explained the principles that they followed in their discovery of novel phenomena and in the creation of unique works of art. It turns out that both types of minds speak the same language. There is a basic denominator that unites the human endeavor."

Lima-de-Faria's works are jewels for scientific and aesthetic minds. The beauty of Nature absorbed him completely, and he devoted himself passionately to it. He was an admirer and a true connoisseur of the arts, music, and ballet. He was a passionate gardener and loved roses and the fragrance of flowers. Antonio Lima-de-Faria was a man of enlightenment, dedication, will, and truth. With his gentle and generous attitude towards anyone around him, Antonio Lima-de-Faria radiated love. He knew what happiness is ("What is Happiness?", *Journal of Biourbanism*, IX, 2021).

Antonio Lima-de-Faria is an endless source of inspiration and admiration for us.

Finito di stampare da
Logo s.r.l. – Borgoricco (PD) – Italia

OPEN ACCESS POLICY

Caryologia provides immediate open access to its content. Our publisher, Firenze University Press at the University of Florence, complies with the Budapest Open Access Initiative definition of Open Access: By "open access" , we mean the free availability on the public internet, the permission for all users to read, download, copy, distribute, print, search, or link to the full text of the articles, crawl them for indexing, pass them as data to software, or use them for any other lawful purpose, without financial, legal, or technical barriers other than those inseparable from gaining access to the internet itself. The only constraint on reproduction and distribution, and the only role for copyright in this domain is to guarantee the original authors with control over the integrity of their work and the right to be properly acknowledged and cited. We support a greater global exchange of knowledge by making the research published in our journal open to the public and reusable under the terms of a Creative Commons Attribution 4.0 International Public License (CC-BY-4.0). Furthermore, we encourage authors to post their pre-publication manuscript in institutional repositories or on their websites prior to and during the submission process and to post the Publisher's final formatted PDF version after publication without embargo. These practices benefit authors with productive exchanges as well as earlier and greater citation of published work.

PUBLICATION FREQUENCY

Papers will be published online as soon as they are accepted, and tagged with a DOI code. The final full bibliographic record for each article (initial-final page) will be released with the hard copies of *Caryologia*. Manuscripts are accepted at any time through the online submission system.

COPYRIGHT NOTICE

Authors who publish with *Caryologia* agree to the following terms:

- Authors retain the copyright and grant the journal right of first publication with the work simultaneously licensed under a Creative Commons Attribution 4.0 International Public License (CC-BY-4.0) that allows others to share the work with an acknowledgment of the work's authorship and initial publication in Caryologia.
- Authors are able to enter into separate, additional contractual arrangements for the non-exclusive distribution of the journal's published version of the work (e.g., post it to an institutional repository or publish it in a book), with an acknowledgment of its initial publication in this journal.
- Authors are permitted and encouraged to post their work online (e.g., in institutional repositories or on their website) prior to and during the submission process, as it can lead to productive exchanges, as well as earlier and greater citation of published work (See The Effect of Open Access).

PUBLICATION FEES

Open access publishing is not without costs. *Caryologia* therefore levies an article-processing charge of € 150.00 for each article accepted for publication, plus VAT or local taxes where applicable.

We routinely waive charges for authors from low-income countries. For other countries, article-processing charge waivers or discounts are granted on a case-by-case basis to authors with insufficient funds. Authors can request a waiver or discount during the submission process.

PUBLICATION ETHICS

Responsibilities of *Caryologia*'s editors, reviewers, and authors concerning publication ethics and publication malpractice are described in *Caryologia*'s Guidelines on Publication Ethics.

CORRECTIONS AND RETRACTIONS

In accordance with the generally accepted standards of scholarly publishing, *Caryologia* does not alter articles after publication: "Articles that have been published should remain extant, exact and unaltered to the maximum extent possible".

In cases of serious errors or (suspected) misconduct *Caryologia* publishes corrections and retractions (expressions of concern).

Corrections

In cases of serious errors that affect or significantly impair the reader's understanding or evaluation of the article, *Caryologia* publishes a correction note that is linked to the published article. The published article will be left unchanged.

Retractions

In accordance with the "Retraction Guidelines" by the Committee on Publication Ethics (COPE) *Caryologia* will retract a published article if:

- there is clear evidence that the findings are unreliable, either as a result of misconduct (e.g. data fabrication) or honest error (e.g. miscalculation)
- the findings have previously been published elsewhere without proper crossreferencing, permission or justification (i.e. cases of redundant publication)
- it turns out to be an act of plagiarism
- it reports unethical research.

An article is retracted by publishing a retraction notice that is linked to or replaces the retracted article. *Caryologia* will make any effort to clearly identify a retracted article as such.

If an investigation is underway that might result in the retraction of an article *Caryologia* may choose to alert readers by publishing an expression of concern.

COMPLYNG WITH ETHICS OF EXPERIMENTATION

Please ensure that all research reported in submitted papers has been conducted in an ethical and responsible manner, and is in full compliance with all relevant codes of experimentation and legislation. All papers which report in vivo experiments or clinical trials on humans or animals must include a written statement in the Methods section. This should explain that all work was conducted with the formal approval of the local human subject or animal care committees (institutional and national), and that clinical trials have been registered as legislation requires. Authors who do not have formal ethics review committees should include a statement that their study follows the principles of the Declaration of Helsinki

ARCHIVING

Caryologia and Firenze University Press are experimenting a National legal deposition and long-term digital preservation service.

ARTICLE PROCESSING CHARGES

All articles published in *Caryologia* are open access and freely available online, immediately upon publication. This is made possible by an article-processing charge (APC) that covers the range of publishing services we provide. This includes provision of online tools for editors and authors, article production and hosting, liaison with abstracting and indexing services, and customer services. The APC, payable when your manuscript is editorially accepted and before publication, is charged to either you, or your funder, institution or employer.

Open access publishing is not without costs. *Caryologia* therefore levies an article-processing charge of € 150.00 for each article accepted for publication, plus VAT or local taxes where applicable.

FREQUENTLY-ASKED QUESTIONS (FAQ)

Who is responsible for making or arranging the payment?

As the corresponding author of the manuscript you are responsible for making or arranging the payment (for instance, via your institution) upon editorial acceptance of the manuscript.

At which stage is the amount I will need to pay fixed?

The APC payable for an article is agreed as part of the manuscript submission process. The agreed charge will not change, regardless of any change to the journal's APC.

When and how do I pay?

Upon editorial acceptance of an article, the corresponding author (you) will be notified that payment is due.

We advise prompt payment as we are unable to publish accepted articles until payment has been received. Payment can be made by Invoice. Payment is due within 30 days of the manuscript receiving editorial acceptance. Receipts are available on request.

No taxes are included in this charge. If you are resident in any European Union country you have to add Value-Added Tax (VAT) at the rate applicable in the respective country. Institutions that are not based in the EU and are paying your fee on your behalf can have the VAT charge recorded under the EU reverse charge method, this means VAT does not need to be added to the invoice. Such institutions are required to supply us with their VAT registration number. If you are resident in Japan you have to add Japanese Consumption Tax (JCT) at the rate set by the Japanese government.

Can charges be waived if I lack funds?

We consider individual waiver requests for articles in Caryologia on a case-by-case basis and they may be granted in cases of lack of funds. To apply for a waiver please request one during the submission process. A decision on the waiver will normally be made within two working days. Requests made during the review process or after acceptance will not be considered.

I am from a low-income country, do I have to pay an APC?

We will provide a waiver or discount if you are based in a country which is classified by the World Bank as a low-income or a lower-middle-income economy with a gross domestic product (GDP) of less than $200bn. Please request this waiver of discount during submission.

What funding sources are available?

Many funding agencies allow the use of grants to cover APCs. An increasing number of funders and agencies strongly encourage open access publication. For more detailed information and to learn about our support service for authors.

APC waivers for substantial critiques of articles published in OA journals

Where authors are submitting a manuscript that represents a substantial critique of an article previously published in the same fully open access journal, they may apply for a waiver of the article processing charge (APC).

In order to apply for an APC waiver on these grounds, please contact the journal editorial team at the point of submission. Requests will not be considered until a manuscript has been submitted, and will be awarded at the discretion of the editor. Contact details for the journal editorial offices may be found on the journal website.

What is your APC refund policy?

Firenze University Press will refund an article processing charge (APC) if an error on our part has resulted in a failure to publish an article under the open access terms selected by the authors. This may include the failure to make an article openly available on the journal platform, or publication of an article under a different Creative Commons licence from that selected by the author(s). A refund will only be offered if these errors have not been corrected within 30 days of publication.

2023
Vol. 76 – n. 3

Caryologia

International Journal of Cytology, Cytosystematics and Cytogenetics

Table of contents